

The human body as sensor for thermal comfort control

Student: D.R. (Derek) Vissers
ID number: 0677399
d.r.vissers@student.tue.nl

Supervisors: prof.ir. W. (Wim) Zeiler
ir. G. (Gert) Boxem
dr.ir. M.G.L.C. (Marcel) Loomans

Program: Master track Building Services
Unit Building Physics and Services
Department of the built environment
Eindhoven University of Technology

Project: 7YY40 – Graduation Project

Date: May 2012

Preface

The master thesis that is lying in front of you is the final result of my study Building Services at the University of Technology in Eindhoven. Over the last year, I worked with a lot of pleasure and enthusiasm on this thesis. The measurements were a real challenge and have gone through ups and downs. Especially working with human subjects and their unpredictability was a great learning process. In addition, I did a lot of literature research in human thermoregulation, what opened a total new world for me. Finally, the measurements brought new insights, which could be of great value for future HVAC control strategies. In my opinion I succeeded in answering the research questions, and I hope this thesis will contribute to a future with both comfortable and energy-efficient buildings.

I would like to thank several people for their support and commitment during my graduation period. A first word of thanks goes to my first supervisor prof.ir. W. (Wim) Zeiler. I would like to thank him for his advice, actually thinking 'out of the box', reading my report and for giving remarks on the both the content and structure of my thesis.

My second word of thanks goes to ir. G. (Gert) Boxem. I would like to thank him for helping me defining my research questions, introducing me in the world of (comfort) control theory, his positive coaching, his critical look at the results and at the structure of the thesis. Third, I would like to thank dr.ir. M. (Marcel) Loomans for his advice, help and substantive criticism during my graduation project. Furthermore, I would like to thank all my supervisors for keeping the overall planning in mind.

Fourth, I would like to say a word of thanks to ir. Lisje Schellen. Her expertise in the field of thermal comfort and human subject measurement helped me enormously in defining my experiments. In addition, she introduced me at the University of Maastricht to discuss my research results with PhD students of the department of Human biology.

A fifth word of thanks goes to the staff of the BPS laboratory. In particular, Wout van Bommel gets a special mention in this thesis for his help during the experimental phase. The sixth word of thanks goes to the subjects, Rik and Daphne, who participated several times in this research and spending their time in the test room. Last, but definitely not least, I would like to thank my parents, my girlfriend and friends for the motivational support. They were always there to support me and to keep me positive, even when I got stuck with my research.

Derek Vissers
Eindhoven, May 2012

Summary

One of the primary objectives of a heating, ventilation and air-conditioning system is to provide a thermally comfortable environment. The satisfaction of the occupants with their thermal environment determines the success of the application of HVAC systems. A lot of effort has been taken to design energy efficient HVAC systems. However, in practice the intended comfort level of these HVAC systems is not achieved, resulting in more sickness absence and lower productivity of the building occupants. This is mainly due to the fact that the control paradigm for HVAC systems has remained relatively unchanged, namely regulating indoor environmental variables such as air temperature without including the thermal state of the individual occupant in the control loop.

Recently, individual controlled (HVAC) comfort systems were proposed, which can cope with the individual differences (e.g. clothing behaviour, body fat) between office workers. In addition, these systems focus on the body parts (hands, feet and head) which mainly dictate thermal discomfort in mild cool/warm office environments.

This thesis presented a new control strategy, for automatic control of personalized radiant heating in mild cool office environments, by including the human body as sensor in the control loop. The upper-extremity and facial skin temperature, both remotely sensed by infrared (IR) thermography, were proposed as feedback control signals. The objective of this control strategy is to save energy, while maintaining thermal comfort of the individual building occupant.

Theory

The specific roles of the hands and face in thermoregulation and thermal sensation were explained in Chapter 2. The human body can regulate heat flow to the environment by increasing or decreasing the skin blood flow. During mild cool exposure vasoconstriction is the most important thermoregulatory effector, which can be clearly observed in the upper-extremity region. In addition, the variations in facial skin temperature may also indicate if a person is getting warmer or cooler.

The challenge for automatic control of radiant heating is to detect the turning point from a neutral thermal state to a cooler thermal state before the user perceives any cool thermal sensation. The fact that the skin temperature can fluctuate within a range of temperatures without producing any temperature sensation (i.e. the neutral zone) is highly useful in this.

Experiments I: User-control

A number of user-controlled experiments were performed, in mild cool conditions ($T_a=19\sim 20^\circ\text{C}$), in order to determine if a decreasing trend in skin temperature of the hands or face was observed, before the user performed any heating control action (Chapter 3). Two human subjects participated in this research. The results 'proof-of-principle' demonstrated that the finger skin temperature was a critical performance indicator of the body thermal state in the cooling region. To test whether the finger temperature was actually useful as control signal, the experiments were reversed: from user-control to automatic control.

Experiments II: Automatic comfort control

The finger temperature, measured by IR thermography, was tested as feedback control signal for automatic regulation of a radiant hand-heating system by applying different set-points: the small, medium and large bandwidth (Chapter 4). The bandwidth is defined as a range of skin temperatures in which the finger temperature was controlled. By controlling the finger temperature in a small bandwidth ($T_{sk}=29\sim 31.5^\circ\text{C}$), it was possible to feed-forward respond to user thermal preferences (i.e. before cool discomfort occurred), while the basic room air temperature was

lowered from 22 to 19.5°C (Figure 0.1). The local- and overall thermal sensation of the subjects were maintained at neutral or slightly higher level, and the subjects (n=2) did not prefer any environmental control action. A correlation between the finger temperature and overall sensation was found ($r^2=0.45$, $P<0.05$). By modeling the preference that arises from the interactions with the user, this small bandwidth might be applicable to other individuals.

Energy savings

The energy saving potential of this control strategy results from the fact that the basic room air set-point temperature can be lowered from 22 to 19.5°C, so that less energy is needed to condition the entire space. A simulation, using a whole-building model programmed in the MATLAB HAMBBase environment, was performed to calculate the energy saving potential (Chapter 5). The 4th floor of an office building in Rotterdam the Netherlands was chosen as case study, because real-occupancy profiles were available. The case study showed an energy saving potential of 17% for heating by decreasing the set point of the indoor air temperature from 22°C to 19.5°C, and taking into account local radiant heating of 98W per occupied workplace.

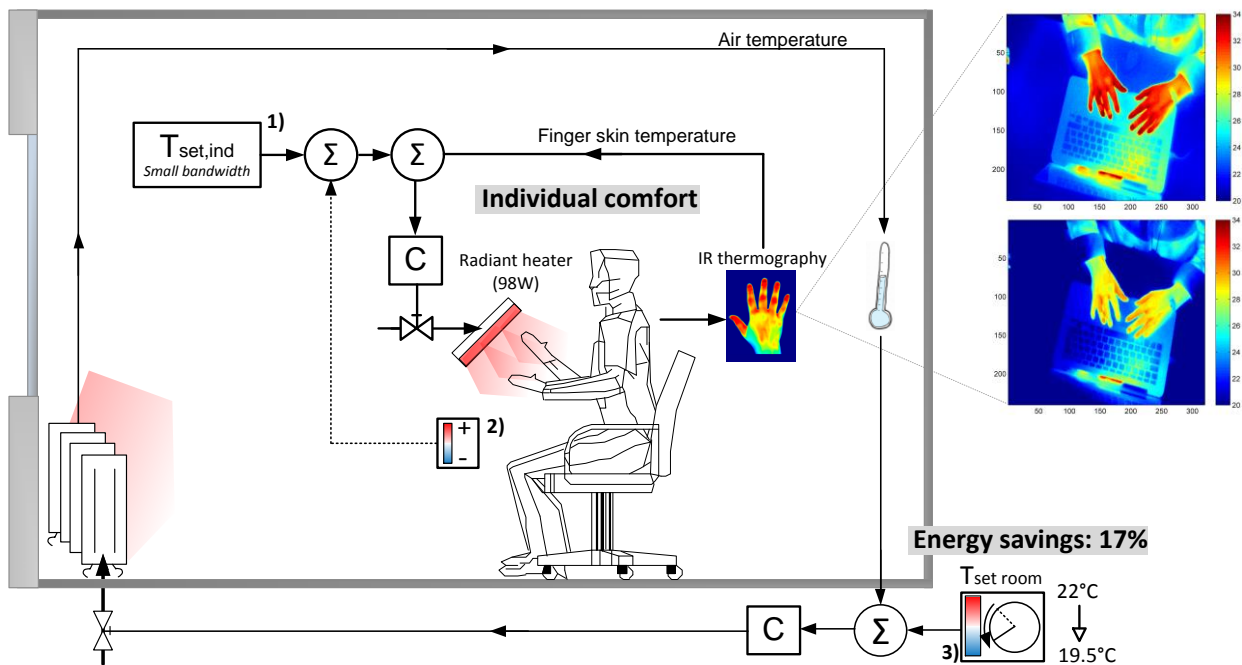


Figure 0.1 Overview of the human-in-the-loop control strategy for a typical winter situation as developed in this graduation project: a local control loop controlled by occupant's upper-extremity skin temperature and a global control loop for controlling the room conditions. 1) The small bandwidth (finger temperature) as individual set-point for automatic comfort control. 2) An individual control unit for optional fine-tuning by the user. 3) The room temperature set-point which can be lowered when local heating is applied.

Content

PREFACE	2
SUMMARY	3
1. INTRODUCTION	7
1.1 BACKGROUND.....	7
1.1.1 <i>Limitations of traditional (HVAC) comfort control</i>	7
1.1.2 <i>Individual controlled (HVAC) comfort systems</i>	7
1.1.3 <i>The human in the loop approach</i>	8
1.2 OBJECTIVE.....	10
1.3 RESEARCH QUESTIONS.....	10
1.4 RESEARCH METHOD.....	10
2. SKIN'S ROLE IN HUMAN THERMOREGULATION AND SENSATION	12
2.1 HUMAN THERMOREGULATION.....	12
2.1.1 <i>Thermoreception</i>	13
2.1.2 <i>Thermoregulatory response</i>	15
2.1.3 <i>Thermo-neutral zone</i>	17
2.2 THE ROLE OF THE UPPER-EXTREMITIES AND FACE IN THERMAL SENSATION.....	18
2.2.1 <i>Upper-extremities</i>	18
2.2.2 <i>Face</i>	20
2.3 RADIATION HEAT EXCHANGE AT THE SKIN SURFACE.....	21
2.4 APPLICATION OF THEORY TO EXPERIMENTS.....	23
3. EXPERIMENTS I: USER-CONTROL	25
3.1 EXPERIMENTS.....	25
3.2 MEASUREMENT SET-UP.....	27
3.2.1 <i>Test-room</i>	27
3.2.2 <i>Experimental workplace: physiological and physical measurements</i>	27
3.2.3 <i>Data-analysis</i>	29
3.3 RADIANT HEATING SYSTEM.....	29
3.4 RESULTS.....	31
3.4.1 <i>General observations in facial- and upper-extremity skin temperature</i>	31
3.4.2 <i>Experiment 1: no control, cool conditions</i>	33
3.4.3 <i>Experiment 2: no control, neutral conditions</i>	34
3.4.4 <i>Experiment 3: user-control, mild cool conditions</i>	34
3.5 DISCUSSION AND EVALUATION.....	36
4. EXPERIMENTS II: AUTOMATIC COMFORT CONTROL	38
4.1 IMPROVED HEATING SYSTEM.....	38
4.2 EXPERIMENTS.....	38
4.3 MEASUREMENT SET-UP: ADJUSTMENTS.....	40
4.4 RESULTS.....	42
4.4.1 <i>Experiment 1: Small bandwidth, male subject</i>	42
4.4.2 <i>Experiment 1: Small bandwidth, female subject</i>	43
4.4.3 <i>Experiment 2: Medium bandwidth, male subject</i>	45
4.4.4 <i>Experiment 3: Large bandwidth, male subject</i>	46

4.4.5	<i>Statistic results of all experiments</i>	47
4.5	DISCUSSION ON MEASUREMENT RESULTS.....	49
5.	ENERGY SAVING POTENTIAL	51
5.1	INTRODUCTION	51
5.2	CASE STUDY.....	51
5.2.1	<i>Building description</i>	51
5.2.2	<i>Internal heat gains</i>	52
5.2.3	<i>Room conditioning</i>	53
5.2.4	<i>Local heating</i>	53
5.3	SIMULATION MODEL	53
5.4	RESULTS.....	55
6.	CONCLUSION, DISCUSSION AND FUTURE DIRECTIONS	57
6.1	CONCLUSIONS.....	57
6.2	GENERAL DISCUSSION.....	58
6.3	FUTURE DIRECTIONS.....	59
6.3.1	<i>Recommendations</i>	59
6.3.2	<i>Future control of the thermal environment</i>	60
	LIST OF SYMBOLS	61
	REFERENCES	63
APPENDIX A:	BACKGROUND ON THERMAL RADIATION	68
APPENDIX B:	MEASUREMENT SET-UP AND EQUIPMENT	71
APPENDIX C:	LABVIEW CONTROL SCHEME	79
APPENDIX D:	MODELING RADIANT PANEL HEAT TRANSFER	81
APPENDIX E:	RADIANT PANELS	86
APPENDIX F:	USER-CONTROLLED EXPERIMENTS	89
APPENDIX G:	HEATING LAMP CHARACTERISTICS	92
APPENDIX H:	QUESTIONNAIRE	93
APPENDIX I:	AUTOMATIC CONTROLLED EXPERIMENTS	94
APPENDIX J:	SIMULATION MODEL MATLAB/SIMULINK	107

1. Introduction

1.1 Background

The energy use in the built environment accounts for nearly 40% of the total energy use in the Netherlands. Most of this energy (nearly 87% for non-residential) is used for building systems with the goal of providing comfort for the building occupants [Opstelten et al., 2007]. This emphasizes the importance of reducing the energy use for comfort systems.

The satisfaction of the occupants with their thermal environment mainly determines the success of the application of HVAC systems. A lot of effort has been taken to design energy efficient HVAC systems. However, in practice the intended comfort level of these HVAC systems is not achieved, resulting in more sickness absence and lower productivity of the building occupants. To achieve comfortable indoor environmental conditions in the future, in an energy-efficient way, it is necessary to implement knowledge on the interaction between thermal comfort systems, and the human body in comfort control strategies. This paragraph gives an introduction on traditional HVAC control and its limitations, individual controlled systems and the proposed human in the loop approach.

1.1.1 Limitations of traditional (HVAC) comfort control

Well-being, health and productivity of office workers are highly related to the indoor thermal conditions. Traditional HVAC comfort control has been focused on temperature regulation of the indoor environment. This control objective often fails in achieving the primary goal of HVAC systems: a thermally comfortable environment.

The main reason is that the body thermal state not only depends on indoor air temperature, but also on other environmental variables (e.g. mean radiant temperature, air velocity, relative humidity) and personal factors such as clothing resistance and activity level. These parameters are combined in the well-known Predicted Mean Vote (PMV) comfort index developed by [Fanger, 1970]. Although this thermal comfort index has been widely used for analysis of indoor climates and the design of HVAC systems, application for real-time control purposes has only achieved limited success [Zhou, 1998]. The PMV-index is based on the statistical average of a certain population; however the average office worker (due to individual differences) does not exist.

Additionally, effective control of thermal comfort is a highly non-trivial task as for example holistic factors (expectations, home situation etc.) may also influence the mental condition which expresses the satisfaction with the thermal environment. Thermal comfort for all can thus only be achieved when occupants have effective control over their own thermal environment [Hoof van, 2008].

1.1.2 Individual controlled (HVAC) comfort systems

If no individual control actions (including adjustments in clothing and metabolism) are allowed, it is not possible to satisfy all office workers with the same indoor thermal conditions [Zeiler et al., 2010]. Recent studies on human thermal comfort demonstrated that in 'mild cool' conditions the hands and feet dictates overall discomfort, while under 'mild warm' conditions the head and hands dictates a person's overall discomfort [Arens et al., 2006] [Zhang et al., 2010a].

These results suggest that a personally controlled HVAC system, which focuses directly on these body parts, may efficiently improve thermal comfort in office environments. In addition these systems create an asymmetrical thermal environment (i.e. spatially non-uniform) which might even produce higher levels of thermal comfort than a uniform neutral condition [Zhang et al., 2010a]. Recently, individual controlled HVAC systems for direct conditioning of these body parts were

developed by [Filippini, 2009] [Watanabe et al., 2010] [Zhang et al., 2010b]. An example of a task-ambient conditioning system is shown in Figure 1.1.

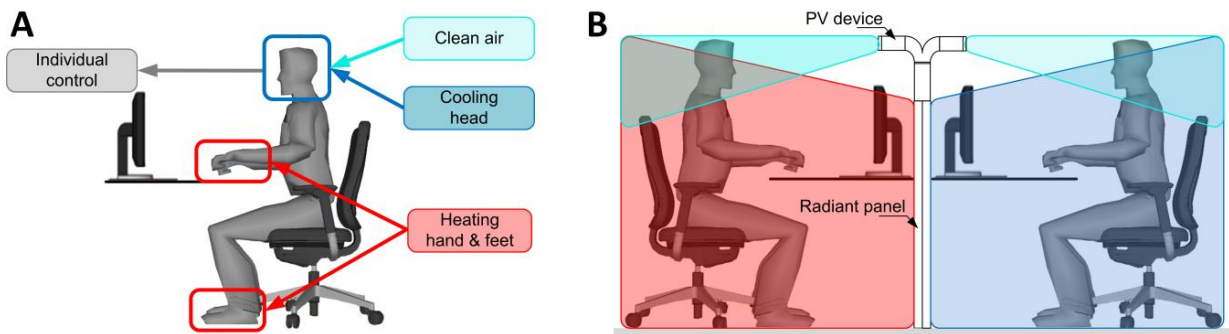


Figure 1.1 (A) Set up for individual thermal environmental control, and (B) a task-ambient conditioning system consisting of individual controlled radiant panels and a personalized ventilation (PV) device. Modified from [Filippini, 2009].

By conditioning the head, hands and feet with a relatively small energy input, the room temperature may be controlled in a relatively wide range (i.e. expanded dead-band). A numerical study showed that this expanded dead-band can result in energy savings up to 35% [Zhang et al., 2009]. The benefits of an individually controlled system are however only fully achieved when the user understands the system behaviour and can interact correctly with it. Incorrect use of individual temperature control (e.g. over-adjusting or misconceptions) may result in energy wasting behaviour and thermal discomfort [Vastamäki et al., 2005] [Karjalainen et al., 2007].

To avoid energy wasting behaviour and to maintain thermal comfort, it is more convenient if the local HVAC set points automatically adapt to the individual needs. This requires a method to include the human body as a sensor in the control loop of thermal comfort systems. Within this research the method is called the '*human in the loop approach*'.

1.1.3 The human in the loop approach

A control strategy for personalized radiant heating based on actual thermo-physiology of the human body is proposed. According to thermoreception of the human body, the ideal sensing point is the central nervous system where the temperature information is processed. It is however unrealistic to measure this part of the body. Physiological responses are measured more straightforward by the human skin temperature, as it reflects the balance between thermo-physiological behaviour of the body and the environmental conditions.

Literature shows that the hands are the most sensitive body parts for the human thermoregulatory system [Zhang, 2003]. In addition, upper-extremity skin temperature is a sensitive indicator of the body thermal state in the cooling region [Wang et al., 2007]. Studies in the automotive field have shown that facial skin temperature is a measure for overall thermal sensation [Taniguchi et al., 1992] [De Oliveira et al., 2009]. Both the hands and face are directly exposed to the environment and show potential to be remotely sensed.

The hypothesis is that hand- and facial skin temperature can be used as control parameters for automatic regulation of radiant heating in mild cold office environments (Figure 1.2). Thereby, the control objective is to regulate the local heating system so that minimum effort is required for the human thermoregulatory system to maintain a neutral body thermal state. This strategy intends to make it possible to save energy, while maintaining individual comfort level. Infrared thermography

is proposed as measurement method, because of its non-contact measurement (no disturbance for office worker), and presumed fast development of low-cost sensors.

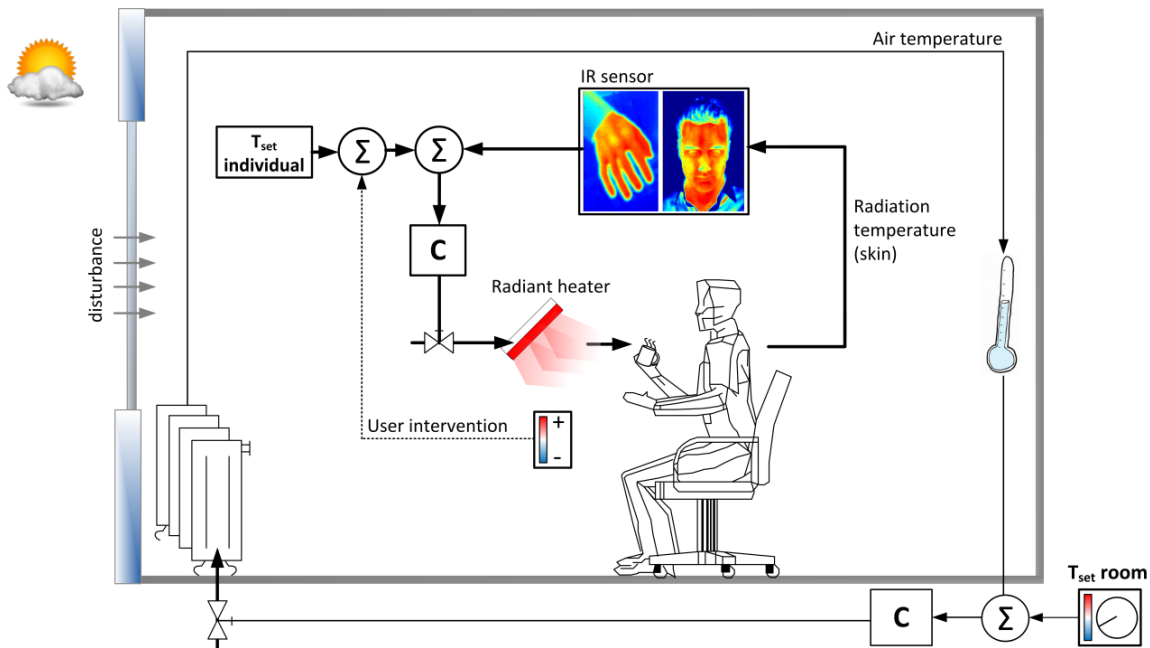


Figure 1.2 The proposed human in the loop control strategy based on actual thermo-physiology of the upper-extremities and face (at local level), and basic room temperature control (global level). C=controller, Σ=error fraction.

In contrary to the traditional control strategies, which are mainly focused on control of environmental variables such as air temperature, the 'human in the loop approach' focuses on the thermoregulatory response of the individual. The energy will only be transferred to those positions where it is actually needed. An overview of the different control strategies is shown in Figure 1.3: in part A, the room air temperature is used as feedback control signal, in part B an individual controlled system is shown using the panel temperature as feedback control signal, and in part C the automatic comfort control is proposed, using the skin temperature as feedback control signal.

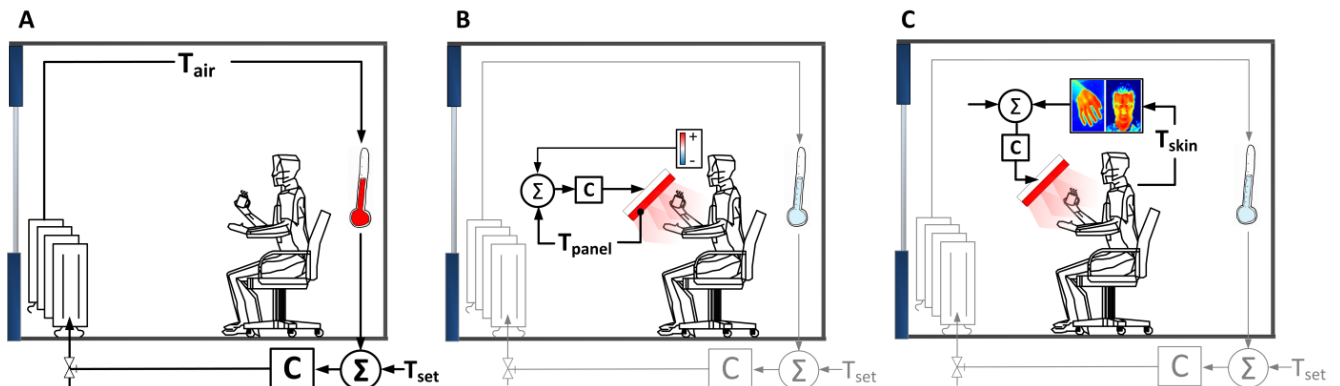


Figure 1.3 Comfort control strategies as introduced. A) Traditional room HVAC control using indoor air temperature as feedback control signal, B) individual controlled HVAC system u, and C) the proposed human-in-the-loop control strategy using the facial / upper-extremity skin temperature as feedback control signal.

1.2 Objective

The research objectives are defined at three levels of abstraction:

1. To save energy, while maintaining thermal comfort of the individual building occupant;
2. To achieve this by individual automatic comfort control, and;
3. To use the upper-extremity and facial skin temperature, measured by infrared thermography, as feedback control signal to include the human body in the comfort control loop.

Thereby, the energy savings can be obtained in two ways, namely 1) the dead-band in which the room air temperature is controlled can be expanded, and 2) energy wasting behaviour caused by incorrect use of individual controlled systems can be avoided by the automatic regulation.

1.3 Research questions

The background description and the research objective resulted in a research question (RQ), which can be subdivided into a couple of sub questions.

RQ: Is it possible to save energy and maintain individual thermal comfort, by using the upper-extremity or facial skin temperature as control parameter for automatic regulation of personalized radiant heating in a mild cold office environment?

1. What is the role of the skin in human thermoregulation?
2. What are the specific properties of the upper-extremities and face with respect to the human thermoregulatory system and how do they correlate with thermal sensation?
3. Which of these body parts shows the highest potential to be used as control parameter, and can be defined as the critical performance indicator (CPI)?
 - How sensitive are the body parts for mild cold office environments?
 - Is a transition in skin temperature detectable before cool discomfort becomes a possibility?
4. Is the radiant heating system able to feed-forward respond to user thermal preferences by using this 'critical performance indicator' as control signal?
5. What is the energy saving potential of the proposed control strategy?

1.4 Research method

The methodology applied during this graduation project is schematically shown in Figure 1.4. The positions of the research questions are also indicated. Below, the different phases are shortly explained and the report outline is given.

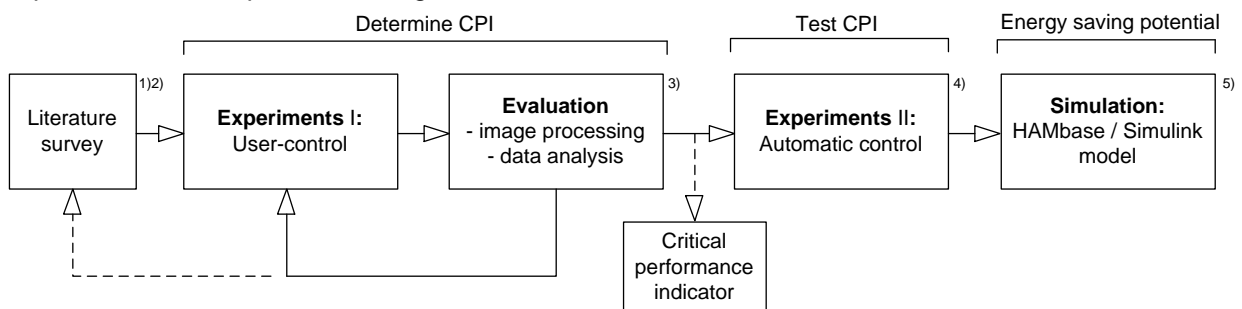


Figure 1.4 Schematic overview of the graduation project.

Literature survey

In the literature survey, the role of the hands and face in human thermoregulation and thermal sensation were the central point of interest. Before the role of the hands and face in human thermal sensation is clarified (§2.2), the basic principles of the human thermoregulatory system (§2.1) are discussed. Radiant heat exchange at the skin surface (§2.3) is also topic of interest as local radiant heating was applied in the experimental phase. Application of the theory to the experiments is summarized in §2.4.

Determine the critical performance indicator

A number of human subject experiments (§3.1) were performed to test whether the facial- and upper-extremity skin temperatures show potential to include the human body in the control loop. Therefore a measurement set-up (§3.2) was built in the BPS laboratory of the Eindhoven, University of Technology. The specific performance of the radiant heating system applied during the experiments is discussed in §3.3. This phase in the graduation project was a repeating process of measurements and evaluation, with the objective of determining the critical performance indicator (CPI). The results are presented in §3.4 and are discussed in §3.5.

Test the critical performance indicator

This phase concerns the second series of experiments. The critical performance indicator (the finger temperature) was tested as control signal for automatic regulation of the radiant heating system. First an improved radiant heating system is introduced (§4.1), where after the experiments are defined (§4.2), and the adjustments in the measurement set-up are discussed (§4.3). Finally, the measurement results of the experiments are presented in §4.4 and they are discussed in §4.5.

Energy saving potential

To determine the energy saving potential of the proposed strategy, a simulation was performed using a whole building model programmed in the MATLAB HAMBBase environment. A state-of-the-art office building in the Netherlands was chosen as a reference case to make the results more realistic (§5.2). The simulation model and results are presented in respectively §5.3 and 5.4.

2. Skin's role in human thermoregulation and sensation

This chapter explains the basic principles of human thermal physiology to make a better understanding in the interaction between comfort systems, the indoor environmental conditions and the human body. The hypothesis is that upper-extremity and facial skin temperature are useful as control parameter, for automatic regulation of radiant heating, in mild cool office conditions.

Before the role of the hands and face in human thermal sensation are clarified, the basic principles of the human thermoregulatory system are discussed. In particular attention has been paid to thermal reception (§2.1.1), the thermoregulatory response by skin blood flow regulation (§2.1.2), and the thermo-neutral zone (§2.1.3). The role of the hand- and facial skin temperatures in thermal sensation are explained in §2.2. The application of this theory within the experiments is discussed in §2.4.

2.1 Human thermoregulation

"Thermoregulation is the ability of an organism to keep its body temperature within certain boundaries, under different surrounding temperatures" [Arens et al., 2006]. The normal core temperature of the human being is about 37°C and varies with a daily pattern in between 36-38°C. By various physiological mechanisms (i.e. the autonomic thermoregulation), this core temperature is held between a narrow range. The human skin is the major organ that controls heat and moisture flow to and from the surrounding environment [Arens et al., 2006].

Thermoregulation itself consists of three major components namely: 1) thermal reception by temperature sensitive neurons, 2) integration through neural pathways, and 3) the effective thermoregulatory response [Kingma, 2011]. The effective thermoregulatory response consists of heat production, heat loss and heat transport. The structure of the human thermoregulatory control system is schematically shown in Figure 2.1.

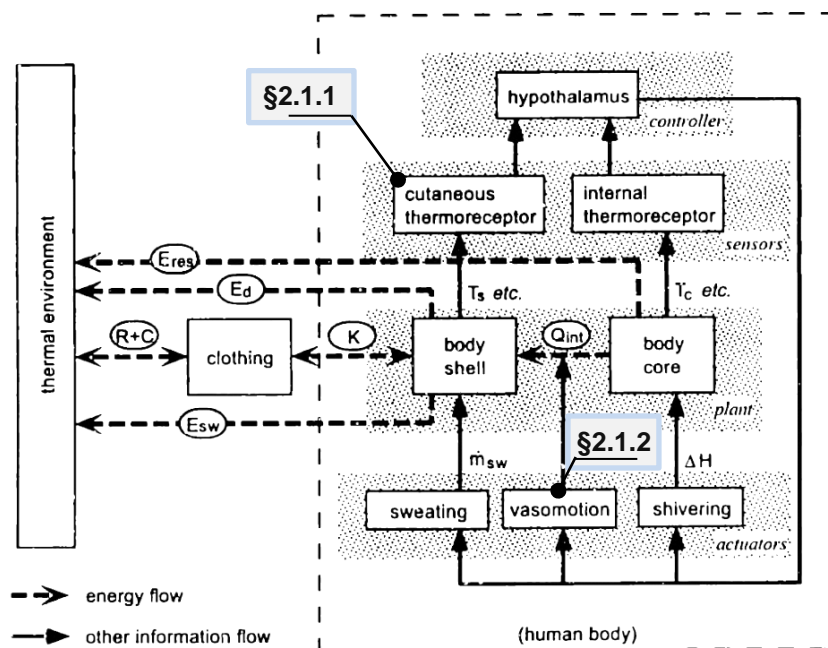


Figure 2.1 Human thermoregulatory control system. The major components are the thermoreceptors (sensors), thermoregulatory effectors (actuators), and the central nervous system (the controller). Figure modified from [Zhou, 1998].

2.1.1 Thermoreception

Thermoreception can be defined as “a process where at different levels heat energy is perceived by living organisms” [Hensel, 1981]. The main issue is that humans do not sense temperature directly. Temperature information is coded into the firing rate of temperature sensitive neurons (thermoreceptors) [Kingma, 2011]. These neurons are found all over the body. Via the sympathetic nerve system, the temperature information is passed to the hypothalamus in the brains. In this part of the brains the autonomic thermoregulation is activated when the temperature becomes lower or higher than the desired reference temperature [Stolwijk, 1971].

The human skin contains two types of thermoreceptors, namely “cold” and “warm” sensitive receptors. The skin consists of two different layers, the epidermis and the dermis. A cross-sectional view of the skin is shown in Figure 2.2. The cold sensitive receptors are mostly located in the epidermis, and the warm sensitive receptors are located in the dermis layer, direct below the epidermis [Arens et al., 2006].

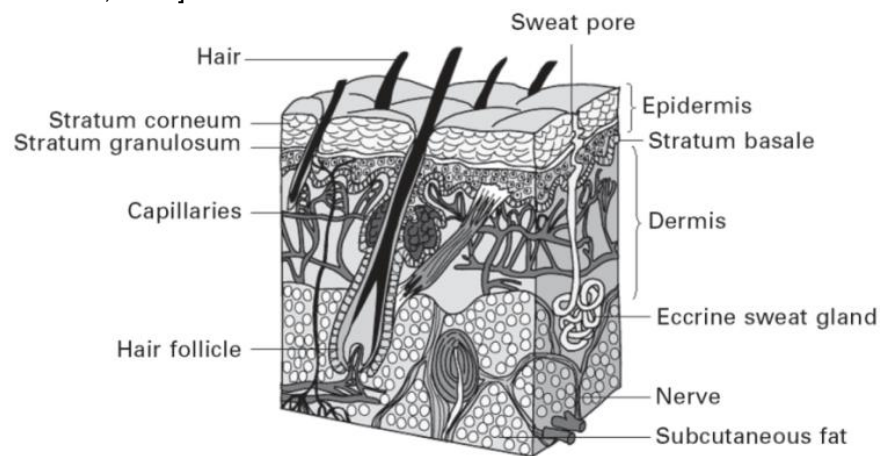


Figure 2.2 Cross-sectional view of the human skin [Arens et al., 2006].

Static and dynamic response

Each receptor is activated in a specific range. Zotterman reported thermoreceptor fire rates for steady-state temperature experiments on cat tongue [Zotterman, 1953]. The maximum steady state discharge rate for cold sensitive receptors lies around 25°C (11 imp/sec) and for warm sensitive receptors around 38°C (4 imp/sec), see Figure 2.3-A.

Most of the thermoreceptor data is derived from experiments with anesthetized animals. However in literature the thermoreceptor data differs considerably. Experiments by Hensel and Kenshalo on cat nose showed totally different results [Hensel et al., 1969]. In addition, the static profile as found in the textbook of medical physiology [Guyton and Hall, 2000] differs from the data as found by Zotterman (Figure 2.3-B). Guyton reported that there are three types of thermoreceptors, namely cold receptors, warm receptors and pain receptors. The maximum steady-state discharge rate for the cold sensitive receptors lies at 25°C (7 imp/sec) and for the warm sensitive receptors at 44°C (10 imp/sec) [Guyton and Hall, 2000].

In addition to the steady state discharge rate, time dependent changes in skin temperature also influence the discharge rate. When a receptor is subjected to an abrupt change in temperature, it is strongly stimulated at first, sending impulses at a high frequency (Figure 2.3-C). For this reason a person feels much colder or warmer when the temperature of the skin is actively falling or rising than when the temperature remains at the same level. The overreaction during transient exposures is called ‘overshoot’ [Arens et al., 2006].

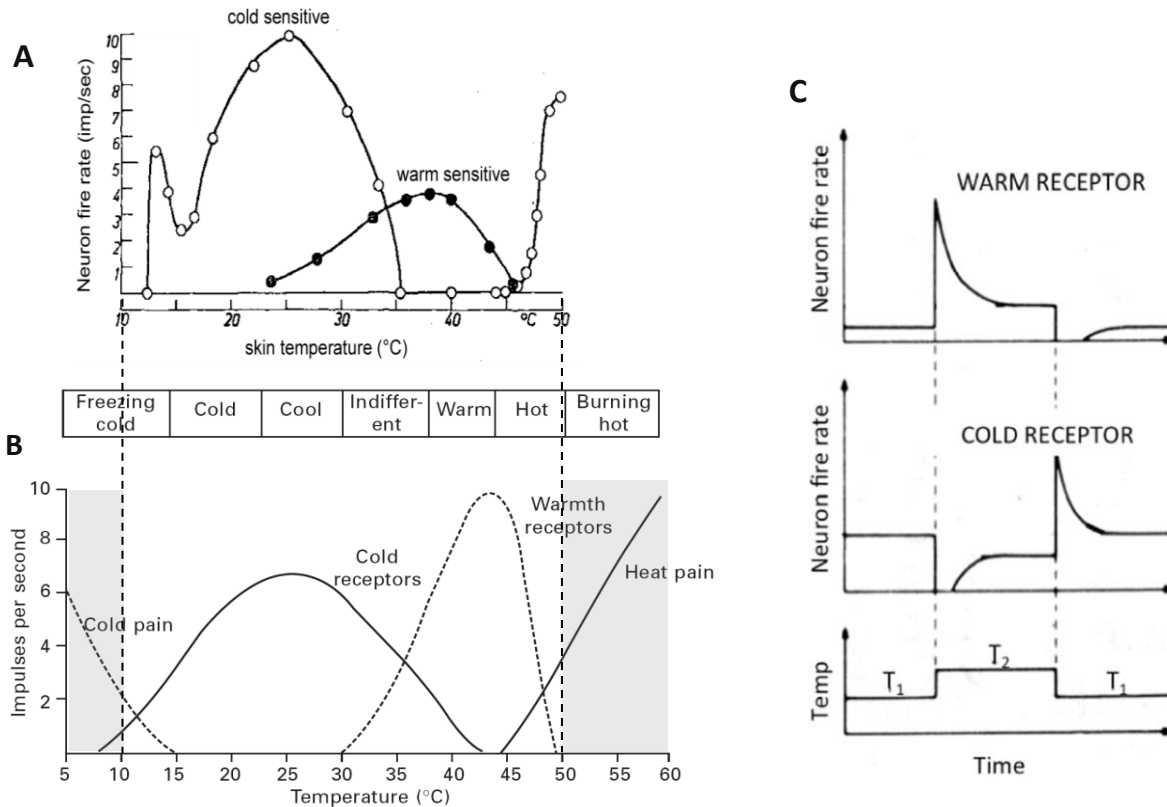


Figure 2.3 A) Steady-state neuron fire rate versus skin temperature for cold- and warm sensitive neurons for data obtained by [Zotterman, 1953]. B) Steady-state neuron fire rate for data obtained by [Guyton, 1981]. Clearly visible is the difference in neuron fire rates, in particular for the warm sensitive neurons, between A and B. C) Dynamic neuron fire rate of the temperature sensitive neurons [Kingma, 2011]. Original adapted from [Hensel, 1982].

Skin adaption to temperature

Skin adaptation to temperature is an aspect of human physiology similar to other sensory adaptations, e.g. eyes to darkness, tongue to taste, and ears to noise [Zhang, 2003]. Using noise as an example: most of the time human beings are unaware of the noise level in the environment; only when this level exceeds a certain threshold human beings become aware of it. The same is applicable for the reference set-point skin temperature, at which no warm or cold sensation is felt. When a local area of the skin has adapted to a temperature, the *skin temperature can fluctuate* within a range of temperatures *without producing any temperature sensation* [Kenshalo, 1970]. In this range the set point for sensation adapts to the current skin temperature.

The results of Kenshalo's study are presented in Figure 2.4-A. It shows the adapting temperature (horizontal axis) and thermal stimulus (vertical axis), and the perception of a change in skin temperature (dotted line). There is a neutral zone (31-36°C) in which the skin temperature can be changed without influencing thermal sensation. Above and below the neutral zone, a persisting warm or cool sensation was felt. However this is only valid for small changes in skin temperature. Based on these results, an adaptation model was proposed by Zhang, see Figure 2.4-B [Zhang, 2003]. This theory is important for the proposed control strategy, because it indicates the possibility to detect a transition in skin temperature *before* the user perceives a persisting cool or warm thermal sensation.

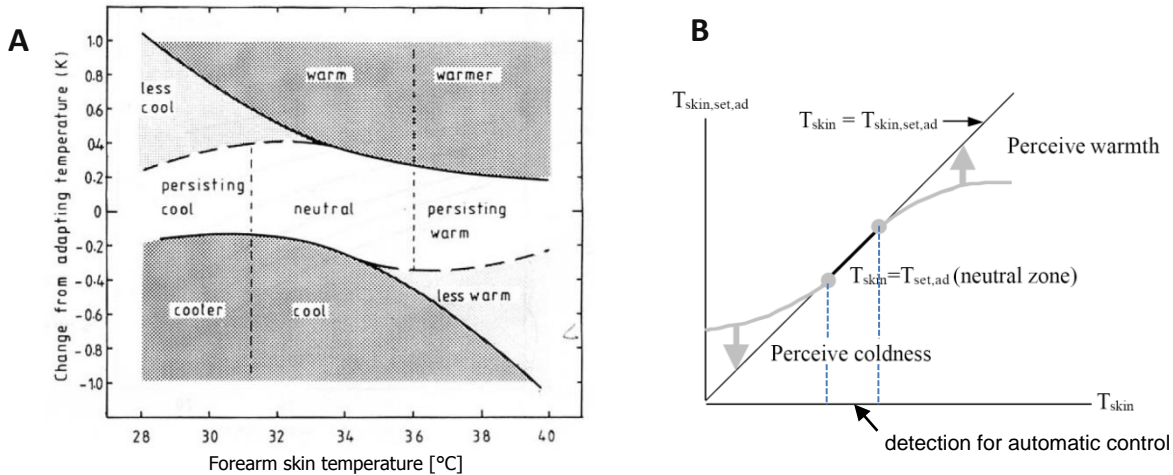


Figure 2.4 Skin adaption to temperature A) Just noticeable changes in forearm skin temperature as a function of the adapting temperature. Thresholds for a change in sensation are shown by the dotted curve [Zhang, 2003]. Original figure adapted from Kenshalo (1970). B) Adaptation model as proposed by Zhang: skin temperature versus the adapting set-point temperature [Zhang, 2003].

2.1.2 Thermoregulatory response

The effector mechanisms of the human thermoregulatory system are vasoconstriction, vasodilation, sweating and shivering (Figure 2.1). The most important effector during mild cool exposure is vasoconstriction. For this reason skin blood flow regulation is discussed in more detail.

Skin blood flow regulation

The primary function of blood circulation is to deliver nutrients and oxygen to tissues and organs. In addition, skin blood flow regulation is a major thermoregulatory mechanism to control the body heat loss. It keeps the heat within the body when it is cold by reducing blood circulation (vasoconstriction) to the extremities. To prevent the core temperature rises too much, the body can release heat to its surroundings by increasing blood flow to the extremities. In that case the blood vessels dilate so that more heat can be delivered to the tissue (vasodilatation). As a result, cold extremities indicate that the body is acting to retain heat and warm extremities indicate the body is acting to lose heat [Zhang, 2003]. Vasomotion occurs primary in the large arteries and small arterioles (Figure 2.5).

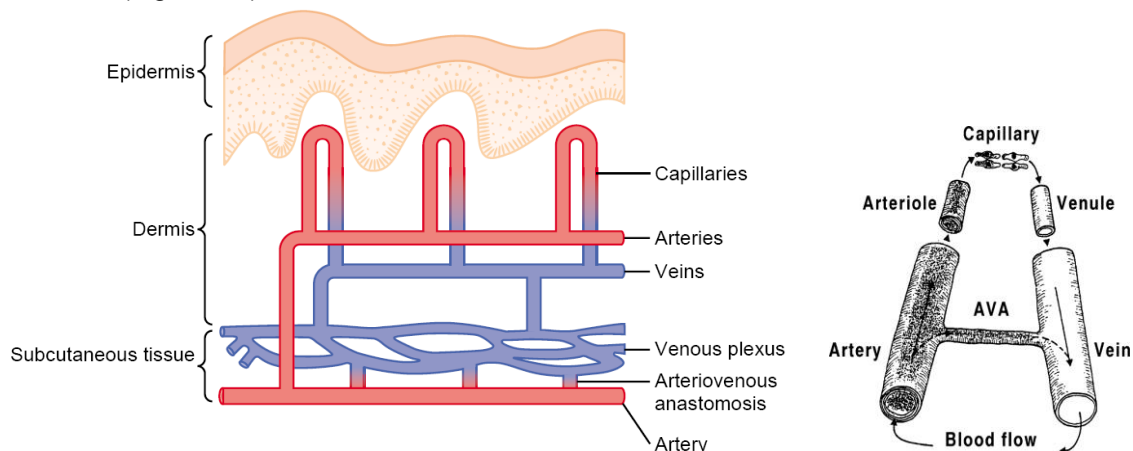


Figure 2.5 Vascular system in the human skin [Guyton and Hall, 2000]. The AVAs (arteriovenous anastomoses) are valves that control vasoconstriction and vasodilation by shortcut the route of normal blood flow. They can be mainly found in glabrous skin area such as palms, fingers, soles, and the forehead.

The human extremities have an additional vascular control mechanism that can vary the temperature and heat loss across a wide range: the arteriovenous anastomoses (AVAs), valves that control vasoconstriction and vasodilatation. These valves shortcut the route of normal blood flow and can increase (when opened) heat loss by conduction through overlying tissues. The AVAs are primarily controlled by signals from the hypothalamus, so their actions represent overall thermal state [Wang et al., 2007]. The AVAs are mostly found in glabrous skin such as palms, fingers, soles, and the forehead. In a thermo-neutral condition (§2.1.3), vasoconstriction and vasodilatation alternate continuously. In such a situation the skin blood flow has a characteristic fluctuation of 2 to 3 vasoconstrictions per minute [Bergersen, 1993]. Under these thermo-neutral conditions, the finger skin temperature fluctuates with 1-2K [Huizenga et al., 2004].

Central versus local regulation

During cold stress, reduced temperatures lead to cutaneous vasoconstriction through combined neural and local mechanisms [Kellogg, 2006]. In other words, the reduction in skin blood flow during cold exposure is partly due to the reflex vasoconstrictor response from whole body cooling, and partly to the direct effect of local cooling [Alvarez et al., 2005].

A decrease in the local temperature of cutaneous blood vessels reduces skin blood flow through mechanisms that require intact sympathetic noradrenergic innervation. Effects of local temperature decreases are independent of a change in core temperature. As mentioned before are reductions in local skin temperature sensed by cold sensitive neurons. These neurons effect the release of norepinephrine (i.e. neurotransmitter) from sympathetic active vasoconstrictor nerves. Norepinephrine acts through alpha- and beta-receptors to produce an initial vasoconstriction.

The local effects can be described by (1) the cold-induced translocation of α_{2c} -adrenergic receptors¹ which enhance vasoconstrictor activity of cutaneous vessel, and (2) non-neural local mechanism such as the rho-kinase pathway, which enhances the calcium sensitivity to stimulate smooth muscle contraction [Kellogg, 2006]. Wissler argued that the combined effect of reflex and local vasoconstriction is multiplicative, rather than additive [Wissler, 2008]. The early phase of vasoconstriction to local cooling is mainly dependent on neural regulation and the late phase vasoconstriction relies more on non-neural mechanisms. The local cooling responses and vasoconstrictor mechanism in the human skin are schematically shown in Figure 2.6.

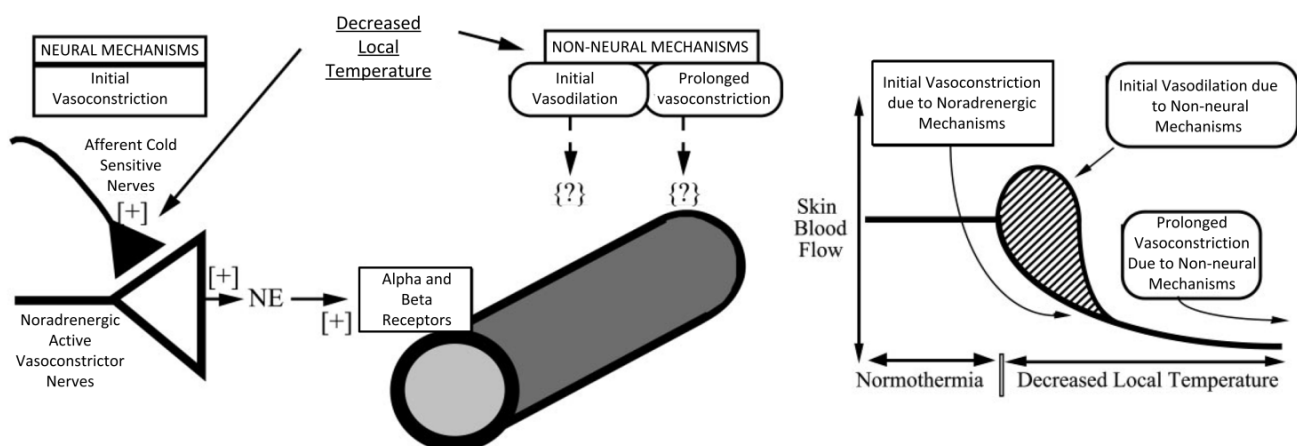


Figure 2.6 Local cooling responses and vasoconstrictor mechanisms in human skin. Figure modified from [Kellogg, 2006]. The reduction in skin blood flow (and thus skin temperature) during cold exposure is partly due to reflex response from whole-body cooling and partly due to the direct effect of local cooling.

¹ These receptors have a critical role in regulating neurotransmitter release from sympathetic nerves and from adrenergic neurons in the central nervous system.

2.1.3 Thermo-neutral zone

The thermo-neutral zone (TNZ) is defined as “the range of ambient temperatures at which temperature regulation is achieved only by control of sensible (dry) heat loss, without regulatory changes in metabolic heat production or evaporative heat loss” [Kingma, 2011]. The regulation of skin blood flow is thus the main thermoregulatory mechanism through which core temperature is regulated.

Below the lower critical temperature (LCT) extra metabolic heat production is required. Above the upper critical limit (UCT) the heat loss is mainly increased by evaporation. In office buildings, the indoor temperature is generally controlled in a dead-band so that the average office worker is within the thermo-neutral zone. The average office worker does however not exist. Due to individual differences such as clothing resistance, metabolic heat production, the percentage body fat, the energy expenditure etc., the TNZ strongly varies among individuals. See Figure 2.7.

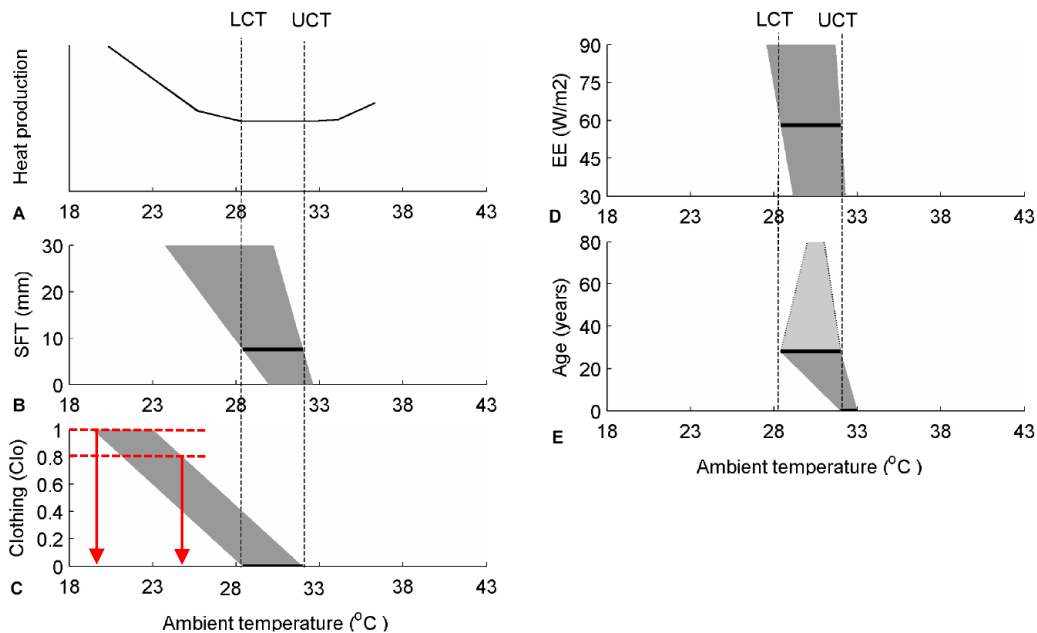


Figure 2.7 A) Standard thermo-neutral zone with the lower critical temperature (LCT=28.6°C) and the upper critical temperature (UCT=32°C) for a 28 year old male subject with a standard basal metabolic rate (58W/m²). B) Subcutaneous fat thickness (SFT). C) Clothing resistance. D) Energy expenditure. E) Age. Figure modified from [Kingma, 2011].

From Figure 2.7 it can be concluded that the clothing resistance and the amount of body fat have a major influence on the ambient temperature at which thermo-neutrality is reached. The clothing resistance varies greatly throughout the year and correlates with the external temperature [De Carli et al., 2007]. Typical clo-values for office workers lie in between 0.8 - 1.0clo for a winter situation. This corresponds to a temperature range of 20-25°C at which thermo-neutrality is reached. This research focusses on mild cool conditions (19~20°C), so that additional heat required is to maintain the occupant thermally neutral.

The amount of body fat is the most important thermo-physiological difference between individuals. It directly influences conduction heat transfer through overlying layers and blood flow [Zhang et al., 2001]. As a result, the ambient temperature at which thermo neutrality will be reached varies significant between for example a lean and an obese person.

2.2 The role of the upper-extremities and face in thermal sensation

2.2.1 Upper-extremities

The hands are probably the most active body parts in responding to the body's thermoregulation [Zhang, 2003]. Vasoconstriction and vasodilation vary blood flow to the hands to control the heat loss from the skin to the environment. In cool conditions, the hand is fully vasoconstricted and the fingertips are the coldest areas of the hand. This pattern is reversed when heating.

The fingertip-forearm skin temperature gradient is an index of thermoregulatory vasoconstriction [Rubinstein et al., 1990] [House et al., 2002]. Since the fingers mainly consist of skin and subcutaneous tissue, the thermoregulatory effect on the circulation system can be well observed by measuring the blood flow through a finger. Another reason that makes the finger blood flow very sensitive is the large amount of AVAs present in the fingers (see §2.1.2).

Thermal sensation

Wang et al. reported that the fingertip skin temperature and the fingertip-forearm temperature gradient are sensitive indicators of body thermal state in the cooling region [Wang et al., 2007]:

- A fingertip skin temperature of 30°C (measured at the 4th finger) is a significant threshold for overall thermal sensation (Figure 2.8). Above this threshold of 30°C, the overall thermal sensation was above -0.5 (at the 9-point ASHRAE scale) and there was no possibility of cool discomfort. Below this threshold, cool discomfort becomes a possibility.
- A fingertip-forearm skin temperature gradient of 0K had the same effect of separating warm from cool sensations as with the finger temperature of 30°C.

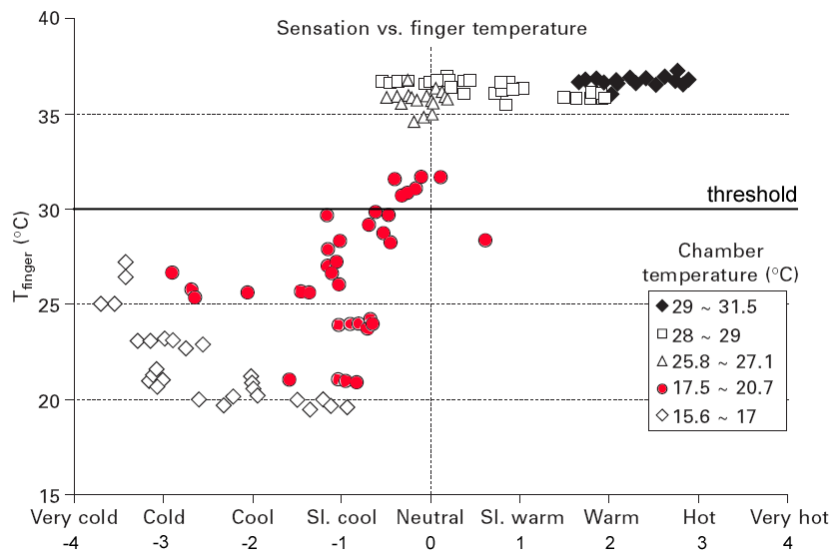


Figure 2.8 Fingertip skin temperature versus whole-body thermal sensations for different chamber temperatures. Thermal sensation scale from -4 to 4 was applied according to the ASHRAE standard 9-point scale. Figure modified from [Arens et al., 2006]. Original adapted from [Wang et al., 2007]. The data-points covering this research are marked red.

Interpreting the results obtained by Wang, it seems to be possible to recognize cool body thermal sensations by a transition of the finger skin temperature out of the neutral range.

The results obtained for the chamber temperature of 17.5 to 20.7°C cover the area of this research, focusing on mild cool office environments. For this area a trend can be recognized (see red marked results in Figure 2.8), however the dispersion is quite large. In addition, a 3.2K temperature difference in room temperature is very large for office environments.

It can be concluded that in the neutral zone (TS=0), the fingertip skin temperature and the fingertip-forearm temperature gradient may not be good indicators for body thermal state due to

large fluctuations (28-36°C). However, environmental control actions are not needed within this range. The challenge is to detect a transition out of this range, before cool discomfort becomes a possibility. Measuring the finger temperature in the experiments (Chapter 3 and 4) is therefore recommended.

Typing vs. holding mouse

A significant difference between the 4th fingertip of the left and right hand has been observed in mild cold office conditions by Huizenga (Table 2.1). This variation is caused by the difference in muscular exertion between typing and holding the computer mouse [Huizenga et al, 2004]. For an ambient temperature of 19°C, the observed difference was about 1.8K. When using the hands as control parameter it is important to know which of the hands gives the most reliable results.

Table 2.1 Effect of using a computer mouse on the 4th finger skin temperature for a cold, mild cold, neutral and warm environment after a 2-hour test [Huizenga et al, 2004]. Neutral refers to conditions at which thermo-neutrality was reached.

	$T_a = 15.6^\circ\text{C}$	$T_a = 19^\circ\text{C}$	neutral	$T_a = 30^\circ\text{C}$
Left	21.1	21.1	35.4	36.4
Right (using mouse)	17.8	19.3	34.7	36.2

Hand warming

The effect of hand-warming and hand recovering on overall thermal sensations and comfort was also investigated by [Wang et al., 2007], see Figure 2.9. The chamber air temperature was 19°C and the left hand was locally *convectively* heated by supply air of 36°C. The results are summarized as follows:

- Improvements in whole-body thermal sensation (± 1.6 scale units) and comfort (± 2 scale units) were obtained by warming the left hand. However warming this hand was not sufficient enough to bring overall comfort to a positive level because the body itself was cold. The hands are relatively small and when vasoconstricted they cannot transfer a large amount of heat to the body.
- After removal of the hand-warming an 'undershoot' in overall thermal sensation occurred. The comfort votes showed an 'overshoot' after removal of the hand-warming due to relief from the high supply air temperature (36°C).

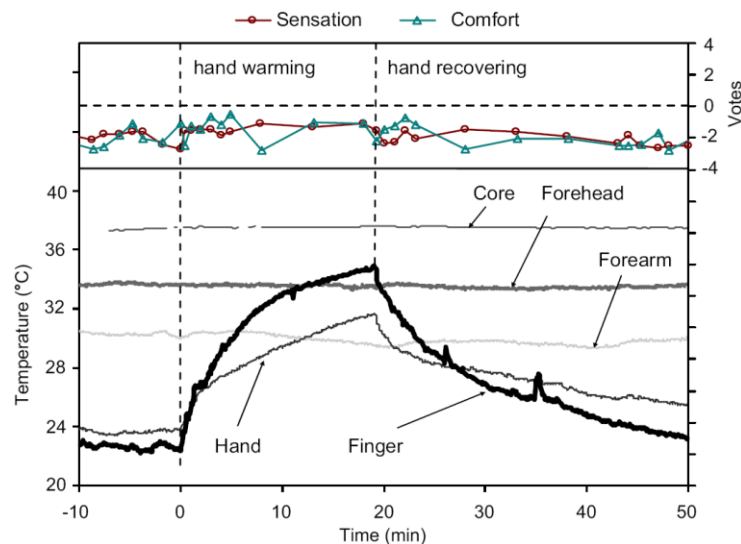


Figure 2.9 The influence of hand heating and recovery on thermal sensations and comfort votes. The chamber temperature was set to 19°C and hand heating was performed by local supply air of 36°C [Wang et al., 2007].

The experiments focused on conditions which can be found in automobiles. In the experiments the body was perceived as cold. However in an office environment, the level of body cooling is often quite small that only the extremities will become cold. So the hands (and feet) may be the only source of discomfort. In this situation, local hand-heating could directly remove the only source of discomfort and may therefore have a strong effect on overall sensation and comfort. This requires further investigation [Wang et al., 2007].

Individual differences in upper-extremity skin temperature

Individual differences such as body fat percentage can have an influence on respectively the upper-extremity skin temperature and the degree of vasoconstriction. Savastano et al. studied the fingernail-bed and abdominal skin temperature of 23 obese and 13 normal weight adults under thermo-neutral conditions [Savastano et al., 2009]. The objective of his research was to test the hypothesis that the skin temperature in a heat-dissipating region of the hand is increased in obese adults. The results are presented in Figure 2.10: the fingernail-bed temperature was significantly higher in obese subjects than in normal weight subjects ($33.9 \pm 0.7^\circ\text{C}$ compared with $28.6 \pm 0.9^\circ\text{C}$; $P < 0.001$). This is mainly caused by the decreased heat loss in the abdominal region.

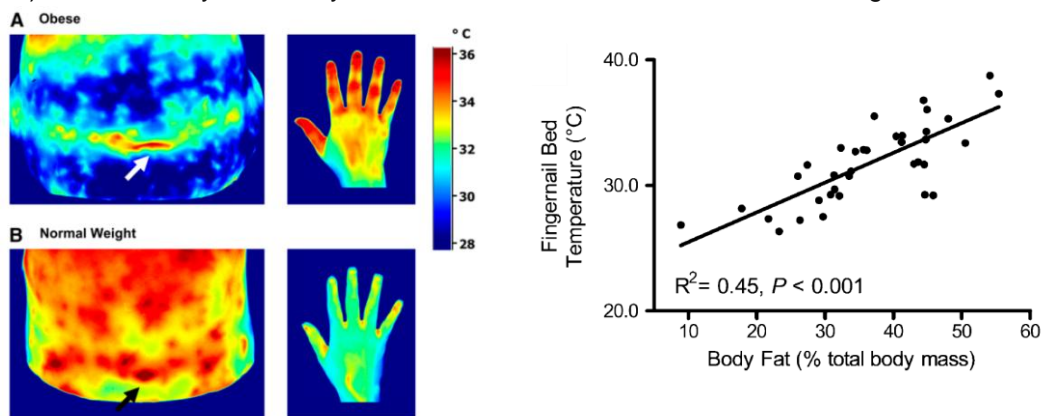


Figure 2.10 The abdominal and right-hand skin thermographs of an obese female (A), and a normal-weight female (B). In (C) the fingernail-bed relative to the percentage of body fat is shown [Savastano et al., 2009].

2.2.2 Face

The facial skin temperature variability can give information on many physiological functions [De Oliveira et al., 2007]. A state-of-the-art application is the measurement of human heart rate by detecting small changes in the color of facial skin by a low-cost camera integrated in modern tablets [Philips Vital Signs, 2012].

From the viewpoint of thermal discomfort, the human head is the most sensitive body part for warm ambient conditions. The head region is perceived as most comfortable when it is slightly cooler than the rest of the body [Zhang et al., 2010a]. In neutral conditions the skin temperature of the face is quite uniform distributed. The face shows a greater variation in skin temperature when it is cold. The nose and cheeks (i.e. the extremities of the head) are then the coldest parts. When a person is very warm, the cheek is warmer than the forehead. Evaporation of sweat on the forehead reduces the forehead skin temperature, while the cheek can be dilated and does not sweat much [Zhang, 2003].

Automobile environment

In automobile environment the forehead skin temperature has been shown to correlate with the overall thermal sensation [Taniguchi et al., 1992]. De Oliveira (2009) also found a correlation between thermal sensation and facial skin temperature measured at the forehead, cheek, nose and

periorbital region [De Oliveira et al., 2009]. In both studies facial skin temperature was directly influenced by a local controlled airflow.

As a result of Taniguchi's study an air-conditioning system controlled by car occupant's facial skin temperature was developed, where skin temperature is measured by a passive remote infrared sensor [Taniguchi et al., 1992]. Nowadays, more and more applications of automatic climate control by infrared measurements of occupants' body surface temperature can be found in automobile environment [Katoaka et al., 2008]. Next to facial skin temperature, the body clothing temperature is also measured. The results from automotive field are promising, however they are not directly applicable to office environments, because:

- The conditions in automobile environment are much more extreme than in office buildings and car passengers have to deal with rapidly changing thermal conditions (i.e. direct solar radiation on their body). In office buildings the conditions are generally less extreme and thermal conditions do not change as fast as in automobiles.
- The correlations between facial skin temperature and overall thermal sensation as found in literature were obtained by directly blowing air in the facial region. This is more closely to the concept of personalized ventilation² instead of personalized radiant heating. Nevertheless, it is expected that the facial skin temperature distributions can indicate if a person is getting warmer or colder.

2.3 Radiation heat exchange at the skin surface

The basic principles of the human thermoregulatory system and the specific roles of the upper-extremities and face in thermal sensation were explained in §2.1 and §2.2. In the experiments (Chapter 3), long-wave radiant heating was applied to compensate for the extra heat loss in mild cool office conditions. For this reason, it is important to know how radiant heat exchange at the skin surface actually takes place. Is the radiation heat transfer, for example, equal for a dark- or light-skinned body; and what is the influence of the radiation wavelength on the penetration depth in the skin? These questions are answered in this paragraph.

The fundamental heat transfer mechanisms at the skin surface are conduction, convection, radiation and evaporation, see Figure 2.11. Radiation heat transfer between the human body and the environment depends on the skin temperature (result of thermoregulatory response) and the mean radiant temperature.

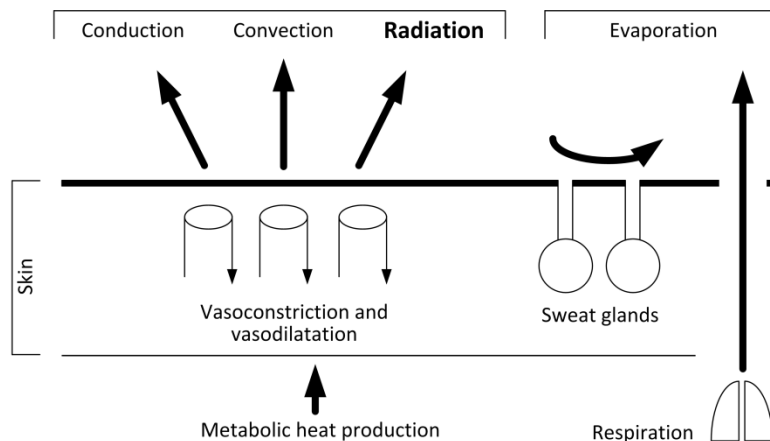


Figure 2.11 Heat transfer mechanism at the skin surface. Modified from [Arens et al., 2006].

² Personalized ventilation (PV) aims to provide clean air to the breathing zone of occupants. Due to air motion over the facial skin surface the convective heat transfer is directly influenced.

Heat transfer equations

The radiation emitted from the human body is proportional to the fourth power of absolute temperature according to the Stefan-Boltzmann law. The basic laws of radiation heat transfer (Planck's law, Wien's displacement and the Stefan-Boltzmann law) are included in Appendix A.

A common method is to calculate the radiant heat exchange by a linear coefficient when temperatures are within a limited range. See equation 2.1.

$$R = h_r(T_{sk} - \bar{T}_r) \left[\frac{W}{m^2} \right] \quad (2.1)$$

The linearized radiation heat transfer coefficient (h_r) can be derived from equation 2.2. In this equation, ε is the skin emissivity, σ the Stefan-Boltzmann constant, A_r is the effective radiation area of the body and A_D is the total area of the body (i.e. Dubois area). For a seated person this ratio $A_r/A_D=0.70$. For typical indoor temperatures the radiation heat transfer coefficient (h_r) is about $4.7 \text{ Wm}^{-2}\text{K}^{-1}$.

$$h_r = 4\varepsilon\sigma \frac{A_r}{A_D} \left(\frac{T_{sk} + \bar{T}_r}{2} \right)^3 \left[\frac{W}{m^2K} \right] \quad (2.2)$$

Commonly, the heat transfer coefficients for radiation (h_r) and convection (h_c) are combined to describe the sensible heat loss ($R+C$) in terms of the operative temperature³. See equation 2.3.

$$R + C = h(T_{sk} - T_o) \left[\frac{W}{m^2} \right], \quad \text{where } h = h_r + h_c \left[\frac{W}{m^2K} \right] \text{ and } T_o = \frac{h_r \bar{T}_r + h_c T_a}{h_r + h_c} \text{ [K]} \quad (2.3)$$

Thermal emissivity of the skin

The emissivity (ε) of the human skin is approximately 0.98, which is close to that of a black body. By using Wien's displacement law (Appendix A), the human skin at 35°C emits a maximum of energy at a wavelength of $9.4\mu\text{m}$ [De Oliveira et al., 2007]. Under equilibrium conditions, the skin absorptivity (i.e. emissivity) is independent of skin color. However in the visible and near-infrared spectrum, the absorptivity of the skin varies with the skin color. In Figure 2.12 the spectral reflectance for a light and dark pigmented human skin is shown. Notice that the skin reflectance equals 1 minus the skin absorptivity.

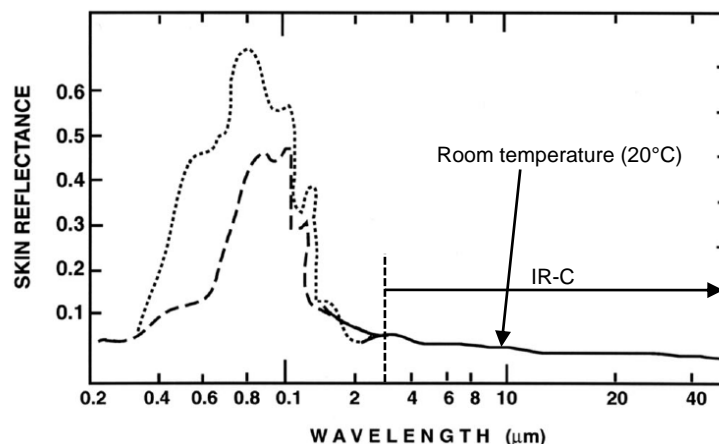


Figure 2.12 Spectral reflectance of lightly (dotted line) and darkly (dashed line) pigmented human skin [ICNIRP, 2006]. For low-temperature radiant heating systems (IR-C), the skin reflectance is the same for both the light and dark skin.

³ The operative temperature (T_o) is defined as a uniform temperature of a radiantly black enclosure in which an occupant would exchange the same amount of heat by radiation plus convection as in the actual non-uniform environment [ASHRAE, 2009].

For visible wavelengths (0.4–0.7 μm), the white skinned body is about 0.5 absorptive, while the black skinned body is about 0.74 absorptive [Houdas et al., 1982]. In the near infrared spectrum (0.8–1.4 μm), the white skin and dark skin are respectively 0.6 and 0.7 absorptive. For wavelengths above 3 μm , the absorptivity is for both the light 9.4 μm and dark pigmented skin the same, which is applicable to the heating system as applied in this graduation project.

Radiation penetration depth

The sensitivity of the human skin is not equal for all wavelengths of radiation. As mentioned before consists the skin of different layers such as the epidermis and the dermis. All these layers have different light-absorbing characteristics. The human skin is more sensitive to visible (0.3–0.7 μm) and middle infrared (1.7–2.3 μm) wavelengths then to near-infrared (0.8-1.35 μm) [Arens et al., 2006]. This difference results from the wavelengths' variable depth of penetration into the skin, relative to where the thermoreceptors are located. See Figure 2.13.

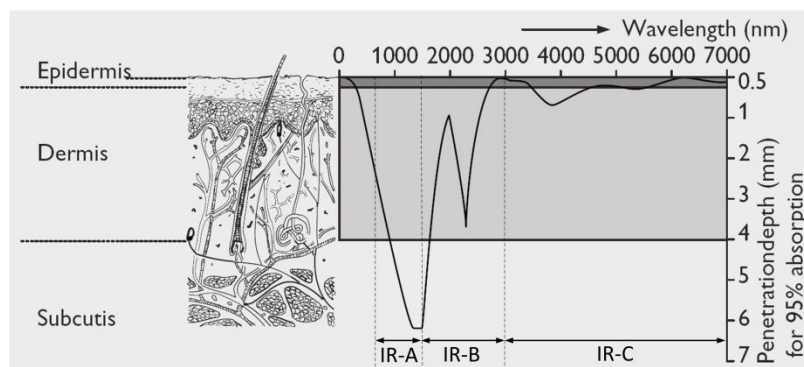


Figure 2.13 The variable penetration depth of infrared radiation versus the wavelength (1000nm=1 μm). Figure modified from [Philips, 2011]. The IR-A: 780-1400nm, IR-B: 1400-3000nm, and IR-C >3000nm spectral regions are indicated.

It can be seen that infrared radiation in the IR-B and IR-C ranges is absorbed in the top layers (i.e. epidermis and dermis) of the skin. Due to the low thickness of these layers a relatively strong heating effect can be achieved. As stated earlier in §2.1.1, the thermoreceptors are also located in these top layers. The IR-A wavelengths have a greater penetration power. This means that the heat is dissipated in a larger skin volume. Application of radiant heating as found in office environments emit generally in the IR-C wavelengths in between 8-10 μm .

2.4 Application of theory to experiments

This paragraph shortly summarizes the most important conclusions as found in literature (§2.1-2.3), and discusses what the theory actually means for the experiments.

- From §2.1.1 it was concluded that the skin temperature can fluctuate within a range of temperatures without producing any temperature sensation [Kenshalo, 1970]. The range in which the skin temperature may fluctuate is considerably greater for the extremities than the torso. Neutral ranges of respectively 32-36.2°C and 30-36°C were found for the face and hands by [Zhang, 2003].

The hypothesis for the experiments is that a decreasing trend in skin temperature of the hands or face can be observed, before the user perceives a cool sensation and performs any heating control action. See §3.1.

- The human skin behaves almost as a black-body radiator with an absorption factor of 0.98 within the 3-20 μm spectral range. In this range the skin reflectance is independent of skin color. The skin emissivity of 0.98 is an important parameter for the infrared measurements. In addition, the spectral range of the IR camera should cover the wavelength of 9.4 μm , at which maximum energy is emitted by the human skin at 35°C.
- Long-wave radiant heat (>3 μm) is already absorbed in the top layers of the skin, where the thermoreceptors are located. The thermoreceptor data as reported in §2.1.1 may be beneficial in order to explain the dynamic behaviour of thermal sensation. By transducing the skin temperatures of the experiments to their equivalent neuron discharge rate these dynamics can be explained [Kingma, 2011]. In §4.4.2 this theory is applied to the measured skin temperatures.
- The upper-extremities are probably the most active body parts in responding to body thermoregulatory system [Zhang, 2003]. The AVAs (arteriovenous anastomoses) can vary the temperature and heat loss across a wide range, by shortcutting the route of normal blood flow. These AVAs are primarily controlled by signals from the hypothalamus, so their actions represent overall thermal state [Wang et al., 2007]. *The challenge for the experiments is to detect the turning point from a neutral thermal state to a cooler thermal state.* The following information with regard to the finger temperature is useful:
 - a) In a thermo-neutral condition (§2.1.3), vasoconstriction and vasodilatation alternate continuously. As a result fluctuations of 1-2K can be observed in the finger temperature;
 - b) A finger temperature of 30°C is a clear threshold separating warm from cool body thermal sensations, according to [Wang et al., 2007];
 - c) Individual differences (for example body fat) may significantly influence the neutral temperature of upper-extremity skin;
 - d) Using a computer mouse or typing may result in variations in the 4th finger temperature up to 1.8K in mild cool conditions. In the experiments it is important to determine which hand is representative for occupant's thermal state.
- The facial skin temperature show also potential as control parameter, because the variations in skin temperature can indicate if a person is getting warmer or colder. The face shows a greater variation in skin temperature when it is cold: The nose (i.e. the extremity of the face) is the region of interest in mild cool conditions.

3. Experiments I: User-control

The control scheme as proposed in the introduction (Figure 1.2) consists of a global- and a local closed-control loop. The objective of the global control loop is controlling the room air temperature, and the objective of the local control loop is maintaining the individual occupant thermally comfortable. The upper-extremity and facial skin temperature were proposed as feedback control signals for the local control loop. As discussed in §2.3, these skin temperatures show high potential in monitoring occupant's thermal state. The hypothesis that hand- and facial skin temperature can be used as control parameter for automatic regulation of radiant heating in mild cold office environments ($T_o=19\sim 20^\circ\text{C}$) was tested. Therefore some experiments were defined (§3.1), and a measurement set-up was built (§3.2).

3.1 Experiments

To test the hypothesis, that it is possible to control the human comfort with the human as sensor in a mild cool environment, an individual controlled radiant heating system (§3.3) was applied. This system focused on the most sensitive body part in mild cold conditions, namely the hands and feet. The user was able to control the surface temperature of both the radiant panels to influence the local thermal environment (exp.3). Skin temperatures of both the hands and face were measured by IR thermography (§3.2) in order to determine whether a trend in skin temperature was recognizable *before* the user performed a control action. Two experiments, without user-control (exp.1, exp.2), were performed to determine the bandwidth in which the skin temperature fluctuates. An overview of the experiments is shown in Table 3.1.

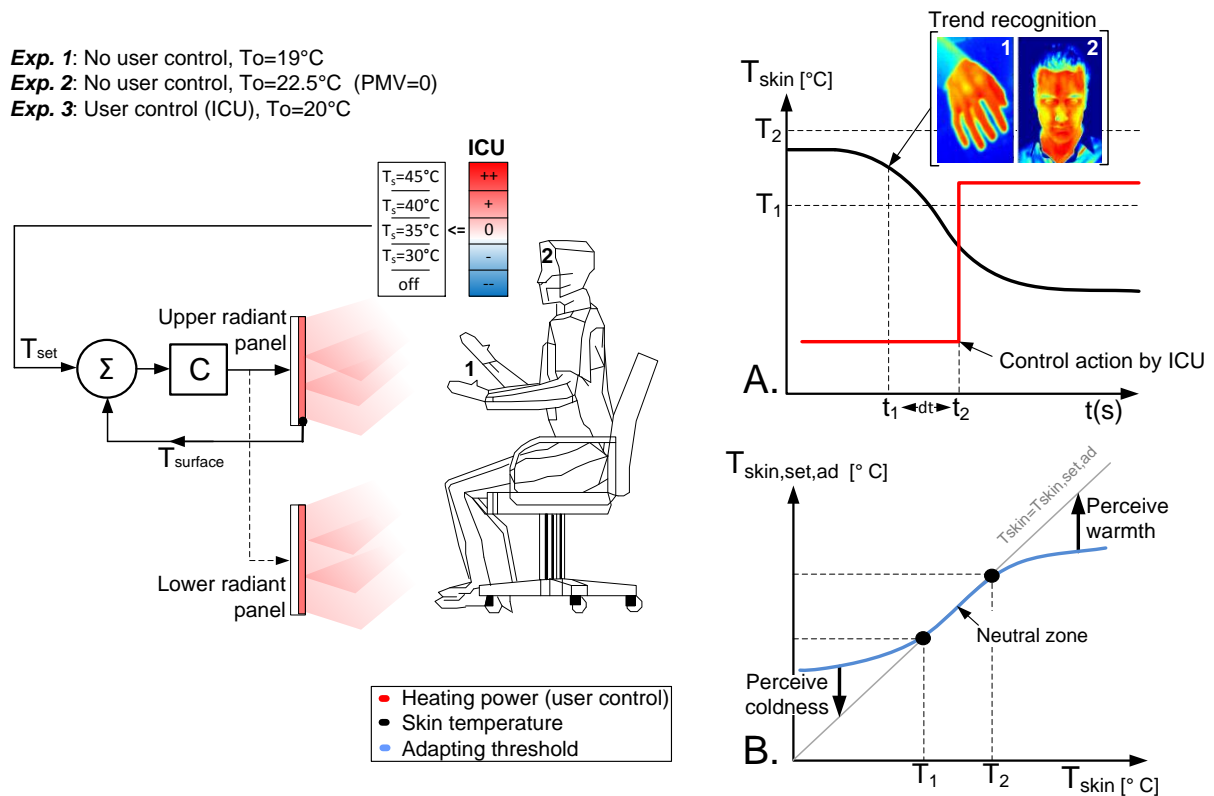


Figure 3.1 Schematic overview of the experiments: the room operative temperature was controlled at $T=19^\circ\text{C}$ for exp.1, at $T=22.5^\circ\text{C}$ for exp.2, and at $T=20^\circ\text{C}$ for exp.3. In experiment 3 the user had the ability to influence the local thermal environment by controlling the radiant panels with an individual control unit (ICU). The skin temperatures of the face and hands were measured to determine whether a trend was recognizable *before* the user control action was performed (A). The hypothesis is that this trend is already recognizable within the neutral zone, so that no cool TS is perceived (B).

In Figure 3.1-A, a fictitious skin temperature and user controlled step-change are plotted against the time. The hypothesis is that the trend in skin temperature is recognizable when the temperature is within the neutral zone (T_1 - T_2) in which the skin temperature can fluctuate without producing any thermal sensation (see §2.1.1). This because the set point for sensation adapts to the current skin temperature, as shown in Figure 3.1-B.

When the skin temperature, of a specific body part, drops below the neutral zone ($<T_1$), a cold sensation occurs. This may result in a user preference for more warmth, and probably in a heating control action. The time delay is defined as the difference in time (dt) between the moment (t_1), a trend in skin temperature is detectable; and the moment (t_2), a control action is performed by the user. The time-delay is of high importance for the selection of HVAC systems with the purpose of providing automatic climate control, as the HVAC system must be able to respond within this time.

Table 3.1 Overview of the experiments. The experiments are ranked according to the operative temperature.

	Case	T_o [°C]	PMV [-]	User control [Yes/No]	Questionnaire [Yes/No]	Number of sessions
Exp. 1	Cool	19	-0.9	No	Yes	1
Exp. 2	Neutral	22.5	0	No	Yes	1
Exp. 3	Mild cool	20	-0.6	Yes	No	6

Protocol for the experiments

The time schedule applied during the experiments is shown in Figure 3.2. One male subject participated several times in these experiments. During the sessions, the subject performed office tasks on his own laptop. The metabolic heat production was assessed 1.2 met ($1\text{met}=58\text{Wm}^{-2}$). A thermal acclimatization time of 15min was applied. The total duration of the experiment was 2.45h.

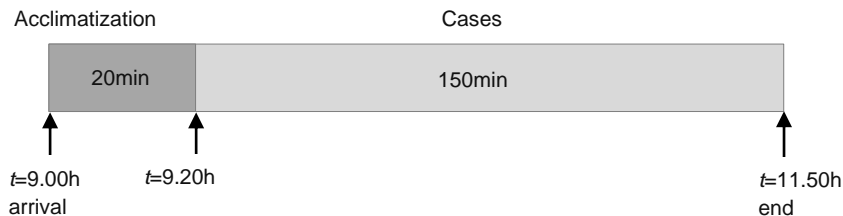


Figure 3.2 Time schedule of the experiments.

The subject wore office clothing consisting of underwear (0.04 clo), ankle-length socks (0.02 clo), shoes (0.02 clo), a pair of trousers (0.24 clo), a shirt with long sleeves (0.25 clo) and a light blouse with long sleeves or equivalent (0.15 clo). Adding 0.1 clo for contact with the chair results in a total clothing resistance of 0.82 clo. These clo-values were obtained from ASHRAE standard 55 (2004). The face and hands were uncovered and directly exposed to the environment.

3.2 Measurement set-up

3.2.1 Test-room

The experimental test room in which the measurement set-up was situated is shown in Figure 3.3-A. The walls of the test room ($V=82\text{m}^3$) are surrounded by a controlled indoor environment with the exception of the west-facing external wall. This external wall contains one window ($1.7\times 1.7\text{m}$). The internal walls consist of hard wood, and the concrete floor is covered with carpet. In order to prevent a major influence of the radiant temperature of the window on the occupant, the desk was placed towards the center of the room. The position of the occupant relative to the walls is indicated in Figure 3.3-B.

The room air temperature was controlled by cool or warm air provided by respectively the ventilation system ($\text{rate}=2\text{h}^{-1}$) or auxiliary heaters. Within most of the experiments, the external air temperature was $<5^\circ\text{C}$, thus no cooling was required in order to achieve the desired set-point room temperature. The auxiliary heater (i.e. radiator, 2kW) was placed below the window. The room air temperature was measured at different positions and height (0.1 , 0.6 and 1.1m) in the test room. The surface temperatures of the walls, the window, ceiling and floor were measured for the calculation of the mean radiant temperature at the position of the occupant. An extensive description of the measurement equipment and sensor positions is included in Appendix B.

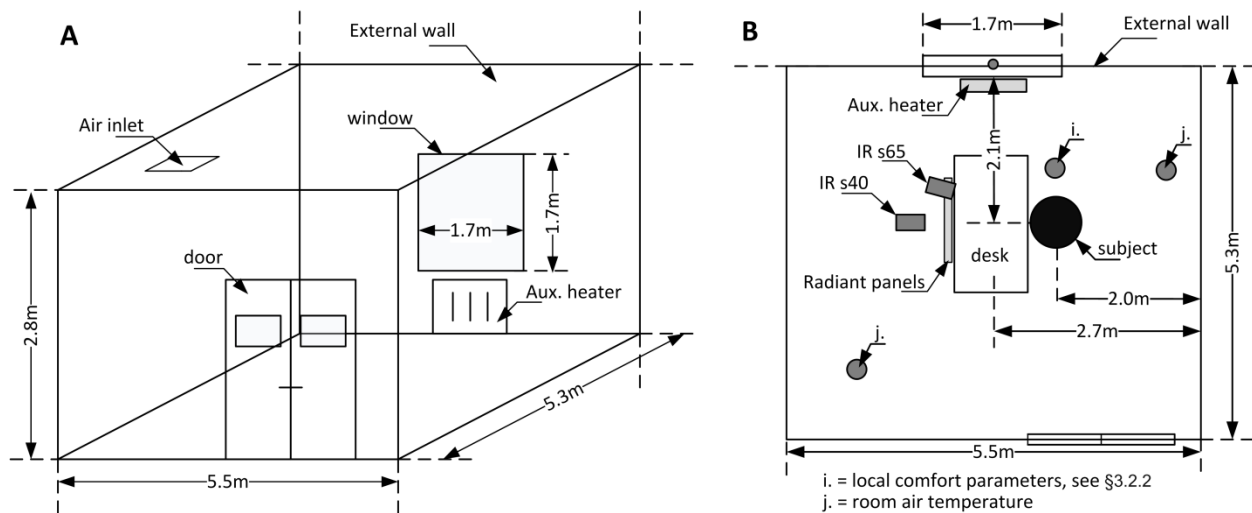


Figure 3.3 Test room in the Building Physics and Services (BPS) laboratory of the TU/e. (A) 3D sketch of the test-room, and (B) position of the desk and occupant relative to the internal- and external walls. The positions of the IR cameras and the comfort measurements at local (i) and room (j) level are also indicated. No scale was applied.

3.2.2 Experimental workplace: physiological and physical measurements

The experimental workplace set-up is shown Figure 3.4 and Figure 3.5. The measurements of the facial- and hand skin temperature (i.e. physiological responses) were performed using two infrared cameras (FLIR ThermoCAM S65-HS / S40), both a thermal sensitivity of 0.08°C at 30°C , and a spatial resolution of 320×240 pixels. An infrared spectral range of $7.5\text{--}13\ \mu\text{m}$ was applied and the object emissivity was set to 0.98 . The cameras were placed in front of the subject.

The physical measurements concern the measurements of the local comfort parameters such as air temperature, radiant temperature, air velocity and relative humidity. These variables were measured according to ISO 7726. The positions of the comfort measurements are indicated by the black circles in Figure 3.4.

At system level, the surface temperatures of both the radiant panels were measured and provided to the control algorithm as programmed in LABview (Appendix C). The energy use of the radiant panels was also measured.

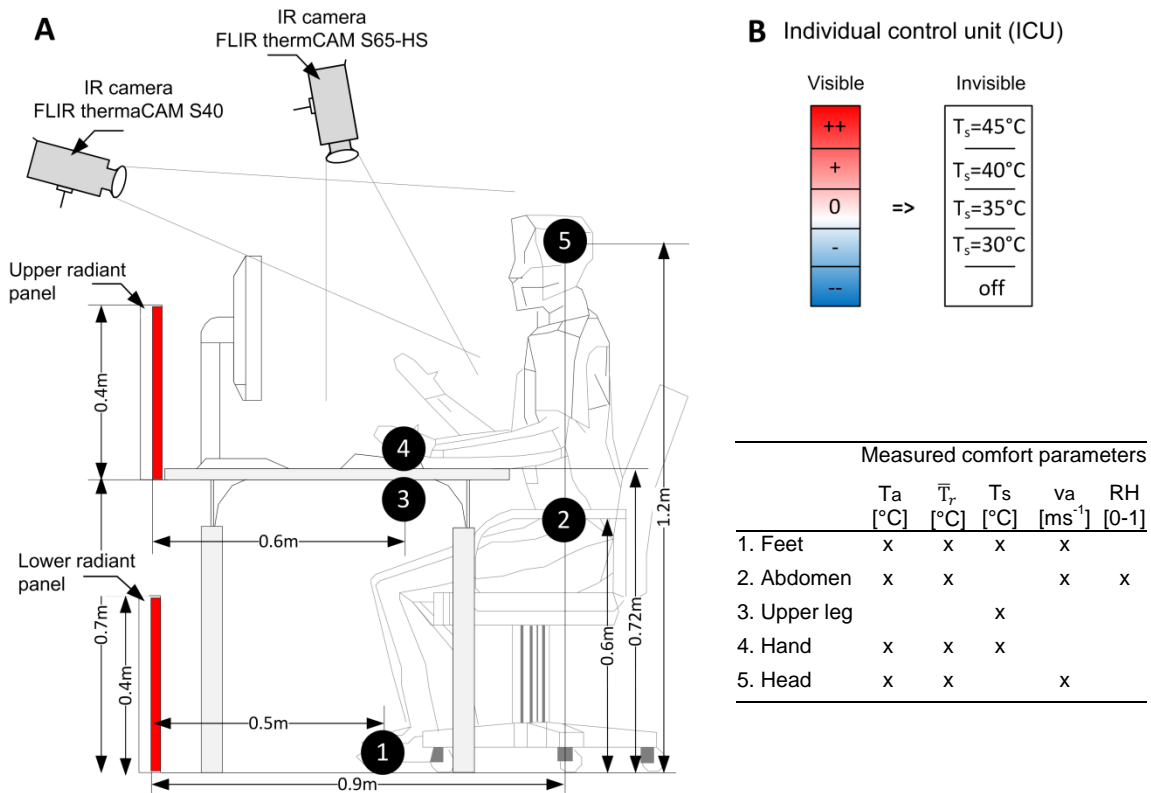


Figure 3.4 Experimental workplace set-up. (A) Two infrared cameras for physiological measurements of the upper extremities and face. The black circles indicate the measurement positions of the local comfort parameters, where 1=feet, 2=abdomen, 3=upper leg, 4=hands and 5=head level. (B) Digital control panel, as programmed in LABview, for regulating the surface temperature of the radiant panels.

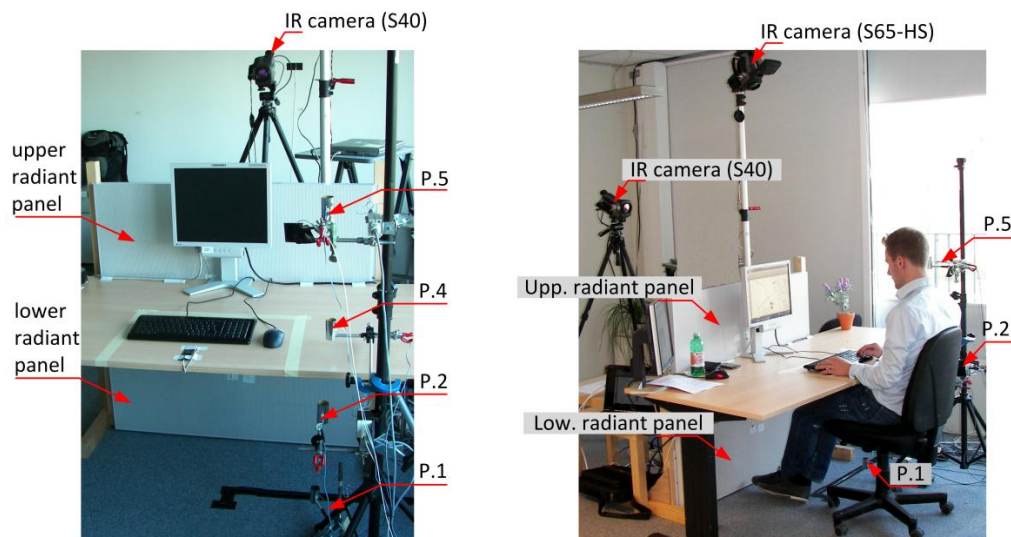


Figure 3.5 Two impressions of the experimental workplace set-up. The positions of the radiant panels, IR cameras and the measurement positions (P.1-P.5) of the local comfort parameters are indicated.

3.2.3 Data-analysis

Infrared measurements

As mentioned before, the upper-extremity and facial skin temperature were measured by IR thermography. ThermaCAM researcher [ThermaCAM, 2004] was used as data processing tool. The infrared images were analyzed using simple matrix operations in MATLAB. The regions of interest (ROI) of the face are the forehead-, and nose skin temperature. The ROI of the upper-extremities are the hand-, and fingertip skin temperature. For the measurement of the finger temperature, the 4th finger was selected. The IR images were analyzed at 5 minute time intervals. See Figure 3.6.

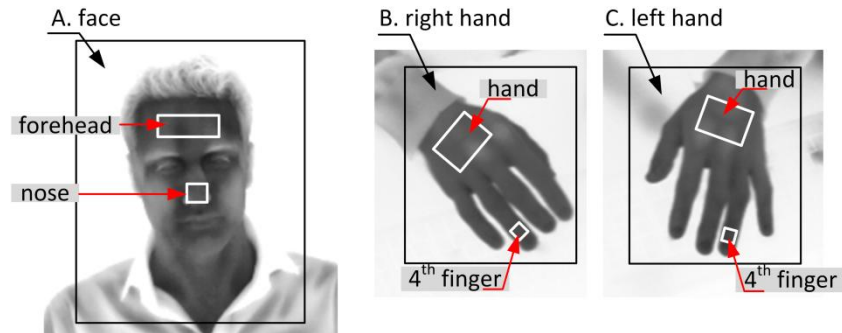


Figure 3.6 Regions of Interest (ROI) for the data analysis. A=facial region with the forehead and nose as ROI. B-C=upper-extremity region with the hand- and finger skin temperature.

Subjective response

In the experiments without user-control (exp.1, exp.2) the thermal sensation votes were asked at 30-min time intervals. The ASHRAE standard 7-point thermal sensation scale was applied. The questionnaire is included in Appendix H. The subjective responses were collected and correlated to the measurement results. Spearman's rank correlation coefficient has been used as a non-parametric measure of statistical dependence between the skin temperature and thermal sensation votes. This is applied to the skin temperature of the upper-extremities and face.

3.3 Radiant heating system

Response time

The radiant heating system consists out of two heating panels which can be individually controlled. Each of the radiant panels consists of a coated aluminum front panel (0.44m^2 , $\epsilon=0.92$), where behind 7 electrical heating foil elements are placed. The back of the panel is thermally insulated. The total electrical input power is 350W, which was transferred as convection and radiation heat towards the environment via the front panel and as heat loss through the back. The power was chosen high enough to ensure a short response time.

The simulated- and measured response times after changing the set-point to 45°C are shown in Figure 3.7-A. The measured response deviates to certain extend from the simulated first-order response. After 4 minutes the panel was almost at final temperature. The temperature distributions over the panel surface are presented by the thermographs in Figure 3.7-B. The positions of the electrical heating foil elements were clearly visible during activation. After a few minutes the temperature was more even distributed over the panel surface (see also Appendix E).

A maximum panel surface temperature (T_s) of 45°C was applied. Otherwise the radiant asymmetry becomes too large, which may results in local discomfort according to the ASHRAE standard 55 (2004). Using a mean radiant temperature (\bar{T}_r) of 20°C , the radiated power towards the

environment equals 150Wm^{-2} according to Stefan Boltzmann law. A small part of the radiated power, depending on the view factor, reaches the human body. To more accurately determine the radiant heat transfer between the heating panels and the human body, some basic view factor calculations were made and a sophisticated radiance simulation was made (Appendix D).

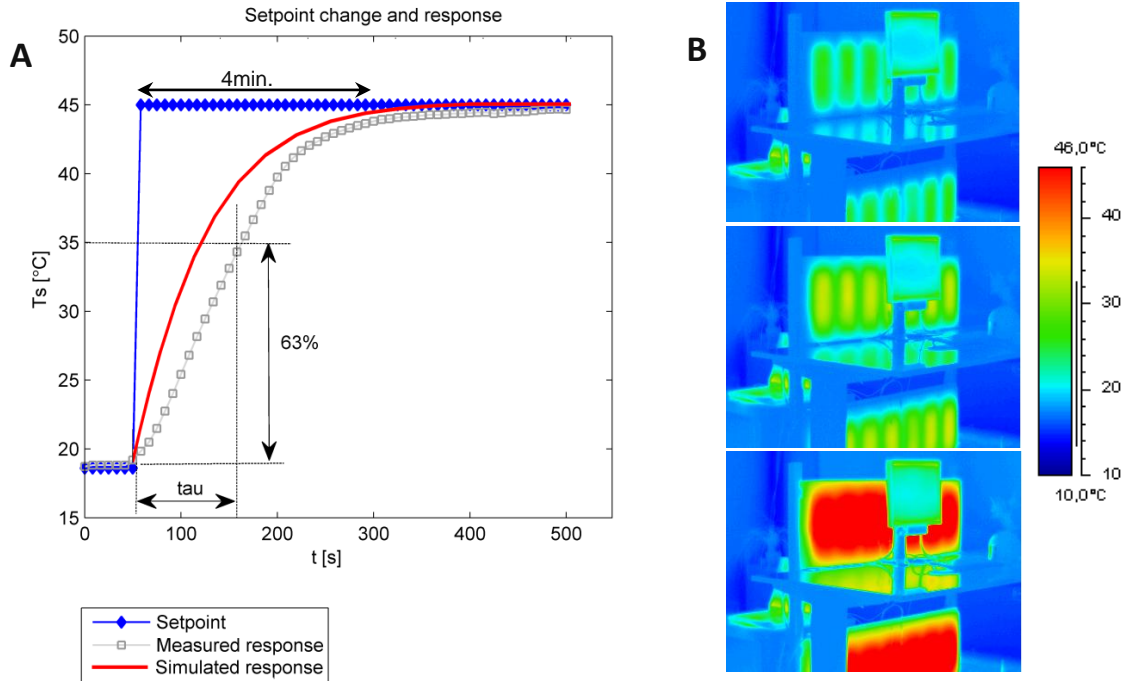


Figure 3.7 (A) Measured- and simulated response time after a set-point change to 45°C, and (B) temperature distribution over the panel surface measured by IR thermography. Session 13-10-2011.

Influence of radiant heating on local physical parameters

Measurements were performed to assess the influence of radiant panel temperature on black globe- and air temperature at the measurement positions as indicated in Figure 3.4 (Appendix E).

The increase in operative- and surface temperature caused by a step change of 25K is shown in Figure 3.8, after reaching a quasi-stationary situation. The operative temperature mostly increased at the positions near to the extremities, which indicates that these body parts can be effectively heated.

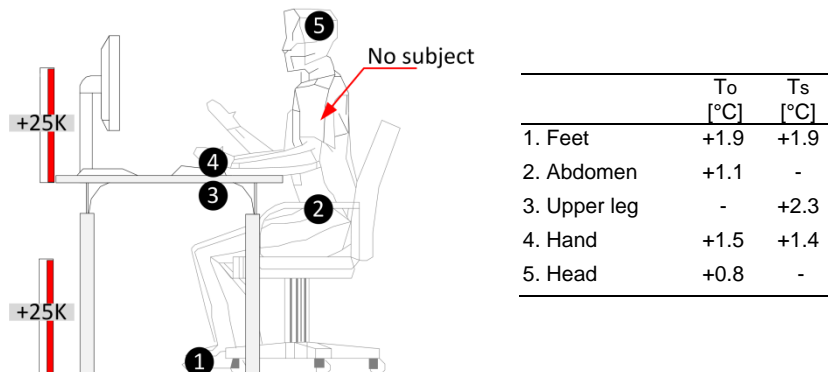


Figure 3.8 Increase in operative- and surface temperature at the positions of the most sensitive body parts, after a step-change of 25K. The measurements were performed without human subject.

3.4 Results

3.4.1 General observations in facial- and upper-extremity skin temperature

A few data-scaled images of the facial region obtained during experiment 1 are presented in Figure 3.9. The mean skin temperature and standard deviation of the regions of interest are also shown. Clearly visible is the decreasing trend in the nose skin temperature, from $32.4 \pm 0.3^\circ\text{C}$ to $28.6 \pm 0.3^\circ\text{C}$, while the forehead skin temperature slightly increases from $32.8 \pm 0.5^\circ\text{C}$ to $33.2 \pm 0.4^\circ\text{C}$. Image A was taken at $t=60\text{min}$, image B at $t=80\text{min}$ and image C at $t=100\text{min}$. The measurement data is presented in §3.4.2.

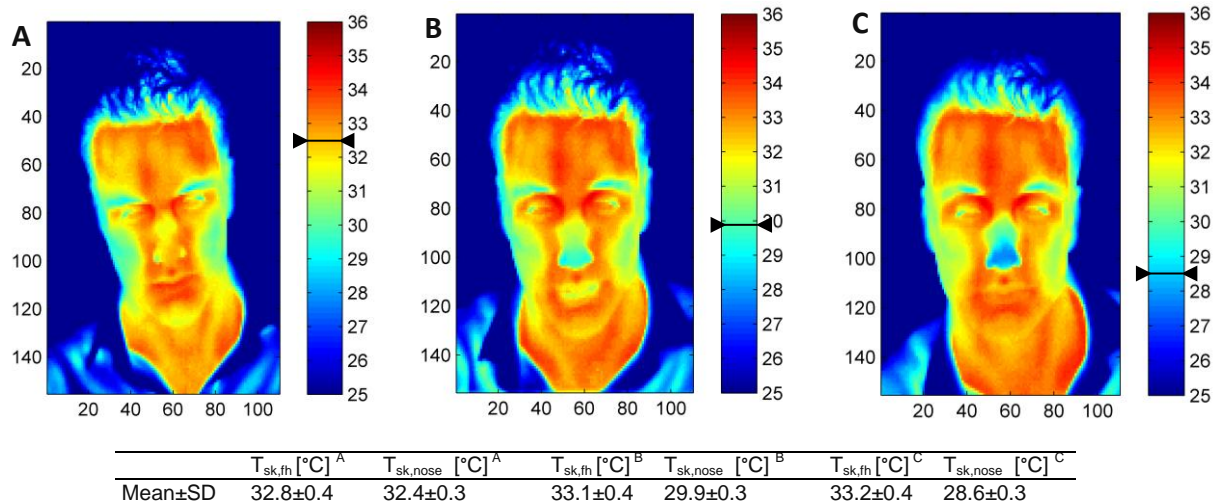
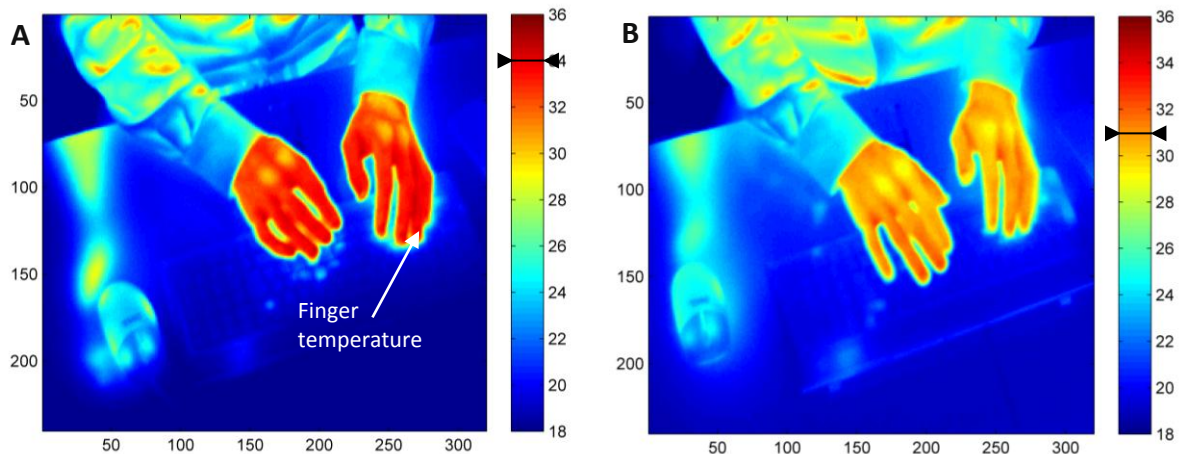


Figure 3.9 Data-scaled images of facial radiant temperature during experiment 1, obtained by IR thermography ($\epsilon=0.98$). Image A was taken at $t=60\text{min}$, B at $t=80\text{min}$, and C at $t=100\text{min}$. The temperature scales are in degrees Celsius, and the nose temperature is indicated by the black arrow. The nose skin temperature decreased by 3.8K.

Some data-scaled images of the upper-extremity region obtained during experiment 3 (session 10-11-2011) are presented in Figure 3.10. The fingertip skin temperature decreased in total 8.2K from $34.0 \pm 0.3^\circ\text{C}$ to $25.8 \pm 0.3^\circ\text{C}$. Notice that the finger temperature was measured at the 4th finger of the left hand. While image C was taken by the infrared camera, the radiant panel was activated by the subject. The influence of the radiant panel temperature on the surface temperature of the desk has been clearly observed in image D.



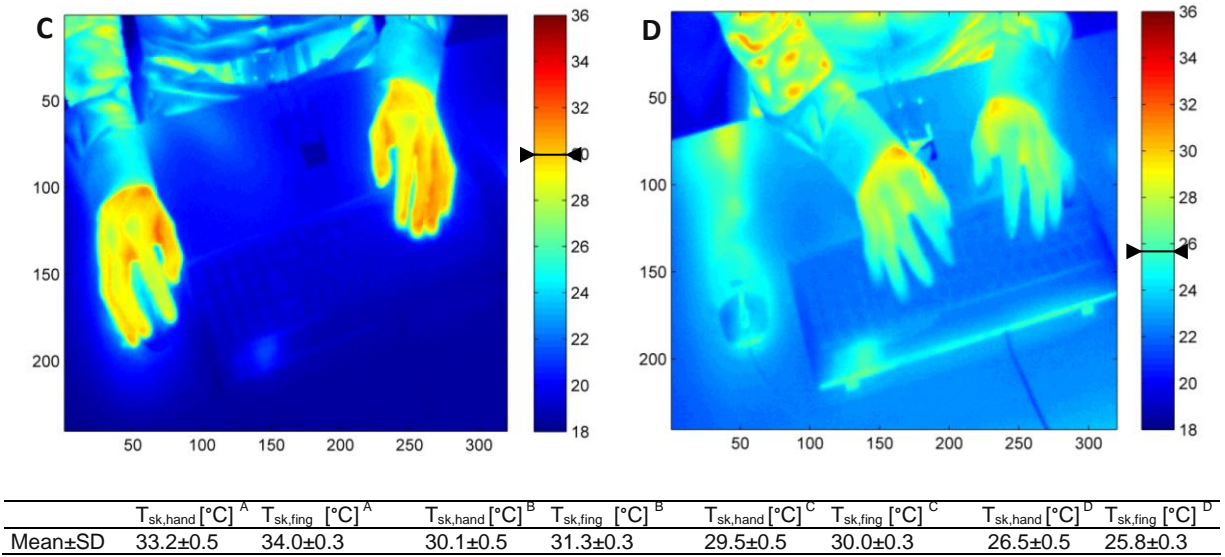


Figure 3.10 Data-scaled images of the upper-extremity radiant temperature during experiment 3, obtained by IR thermography ($\epsilon=0.98$). Image A was taken at $t=15min$, B at $t=45min$, C at $t=55min$, and D at $t=60min$. The temperature scales are in degrees Celsius, and the finger temperature is indicated by the black arrow. The finger temperature decreased by 8.2K.

3.4.2 Experiment 1: no control, cool conditions

The result for the cool conditions test ($T_o=19^\circ\text{C}$) are presented in Figure 3.11. In part A, the primary vertical axis shows the fingertip- and hand skin temperature measured by IR thermography. The 30°C line represents the threshold separating warm from cool sensation as found in literature [Wang et al., 2007].

The secondary vertical axis shows the surface temperature of the radiant heating panels. In part B, the forehead- and nose skin temperature are shown. In part C, the overall thermal sensation (WB-TS) and local thermal sensation of the hands (TS-hands) are shown on the 7-point ASHRAE thermal sensation scale. The mean environmental conditions and corresponding standard deviation (SD) are also included.

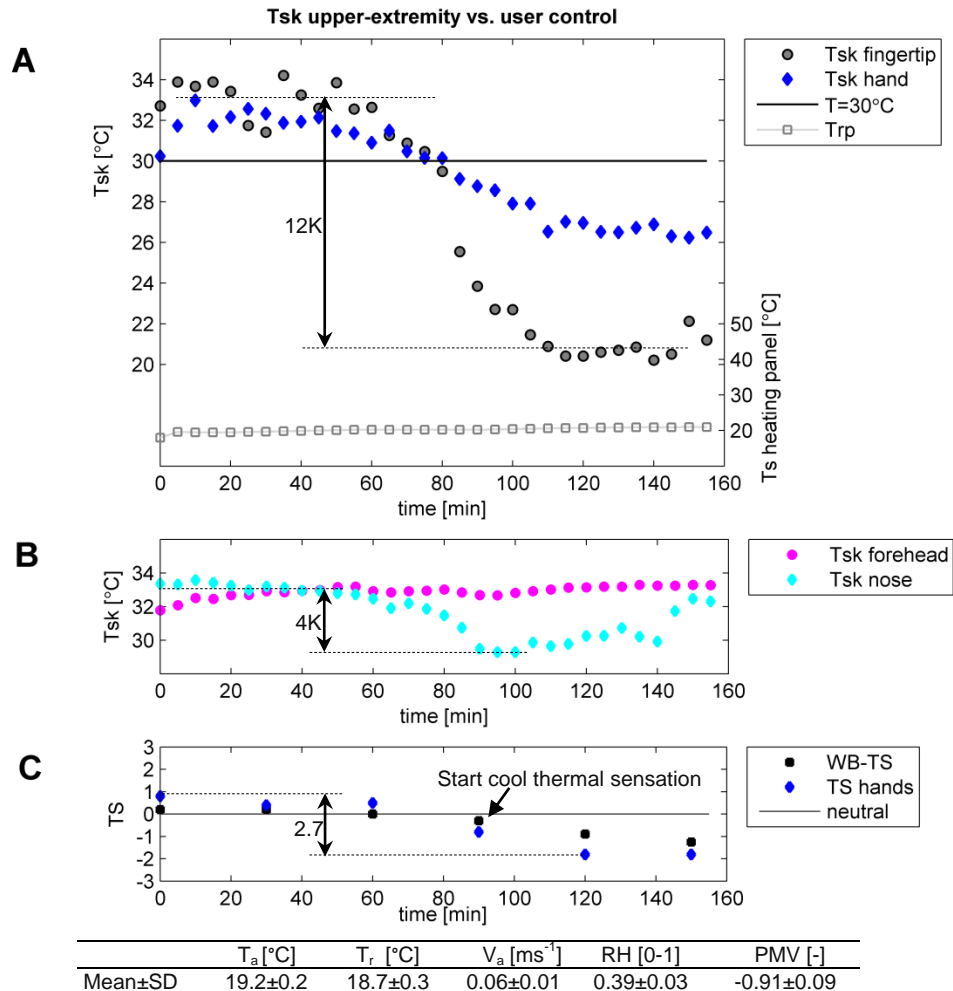


Figure 3.11 Upper-extremity- and facial skin temperature (from IR data) during the cool condition test. (A) Fingertip and hand skin temperatures versus heating panel temperature, (B) forehead and nose skin temperature, and (C) Whole-body and local thermal sensation. Session 09-11-2011: male subject.

After 80min, a strong decrease in the fingertip skin temperature was observed. This effect is also reflected in the local thermal sensation of the hands. A less strong effect can be seen on the overall thermal sensation. The nose skin temperature also showed a decreasing trend, while the mean forehead skin temperature remained relatively constant.

3.4.3 Experiment 2: no control, neutral conditions

In this case, neutral refers to a thermal environment which approaches $PMV=0$. The results are shown in Figure 3.12. Throughout the entire session, the skin temperatures of the hands and fingers remained in the 30-34°C bandwidth. Notice that the radiant panels were again not activated. The overall- and local sensation were assessed above zero.

Both the nose- and forehead skin temperature remained relatively constant. In these environmental conditions ($PMV=0.04\pm 0.07$) it was possible, without applying local heating, to maintain thermal sensation of the subject above zero.

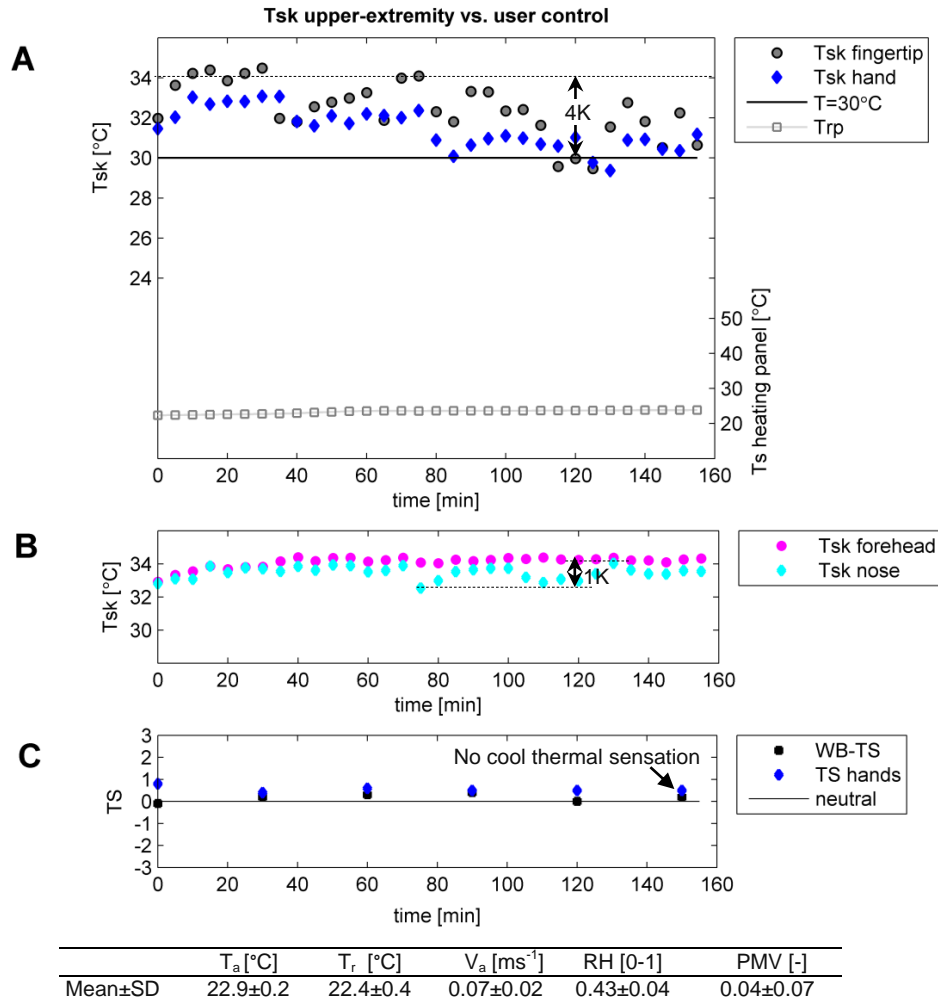


Figure 3.12 Upper-extremity- and facial skin temperature (from IR data) during the neutral condition test. (A) Fingertip and hand skin temperatures versus heating panel temperature, (B) forehead and nose skin temperature, and (C) Whole-body and local thermal sensation. Session 15-11-2011: male subject.

3.4.4 Experiment 3: user-control, mild cool conditions

In the user-controlled experiments the radiant heating system was activated and the subject had the ability to control the panel surface temperature by the individual control unit. The room temperature was controlled at 20°C, which is below the thermo-neutral zone of the subject, and lies in between the 'cool and 'neutral' experiments as presented in §3.4.2. In Figure 3.13 and 3.14 the results are shown for two of the six user-controlled sessions. I refer to Appendix F for the other four

sessions. The heating control action is presented by the surface temperature of the radiant panels, and is shown on the secondary vertical axis. When the skin temperature dropped below the 30°C line, it is called a 'transition'.

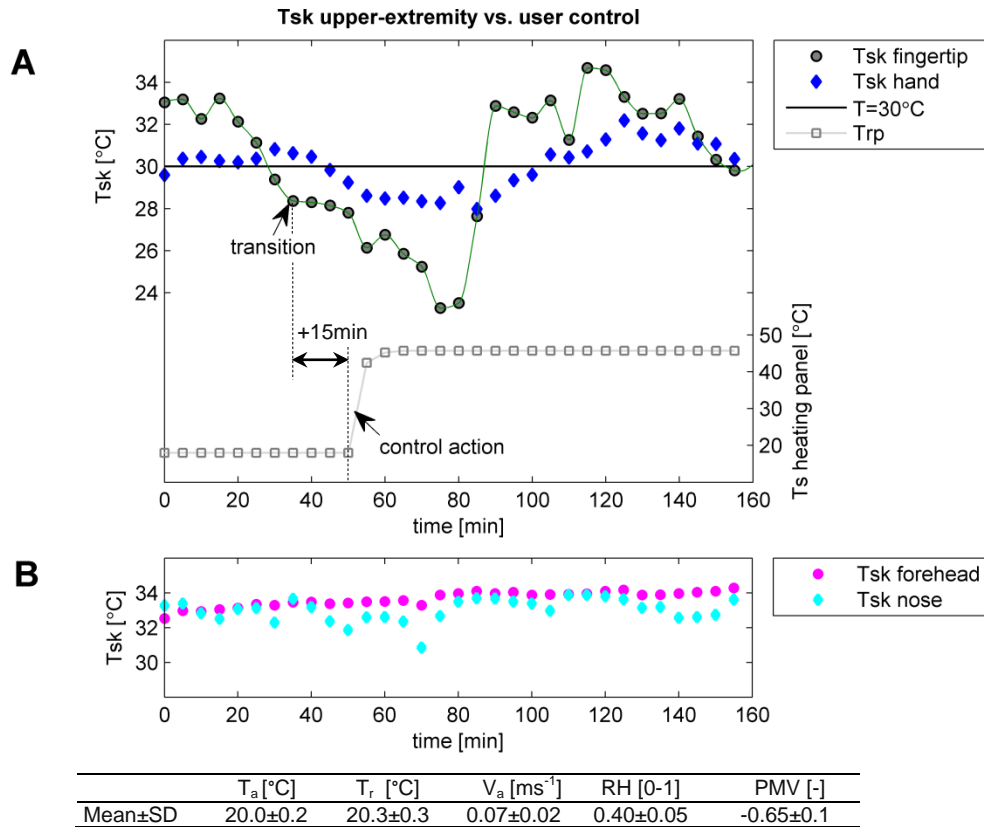


Figure 3.13 Upper-extremity- and facial skin temperature (from IR data) during the user-controlled test. (A) Fingertip and hand skin temperatures versus heating panel temperature, and (B) forehead and nose skin temperature. Session#5 dd. 16-11-2012: male subject.

Figure 3.13 shows a transition in fingertip skin temperature ($t=35\text{min}$), before the subject performed a control action ($t=50\text{min}$), resulting in a time-delay of +15min. This positive time-delay indicates that the fingertip skin temperature might be a useful parameter for automatic comfort control purposes. In addition, it was shown that the user still preferred the maximum radiant panel temperature, also when skin temperatures of the upper-extremities, after 100min, were back in the neutral zone.

In the user-controlled experiment as presented in Figure 3.14, the user performed a first heating control action ($T_s \rightarrow 35^\circ\text{C}$) at $t=50\text{min}$, before a transition in fingertip skin temperature was detectable. The control action was thus feed forward explained by the measured skin temperatures. A second control action ($T_s \rightarrow 45^\circ\text{C}$) was performed, after the transition in fingertip skin temperature. Despite of the maximum radiant panel temperature, the heating system was not able to compensate for the decreasing skin temperature of the upper-extremities. It should be noticed that the operative temperature was 0.5K lower than in the session presented above ($T_o=19.7^\circ\text{C}$ instead of $T_o=20.2^\circ\text{C}$). For this reason, the sensible heat loss by radiation and convection increased, which was likely to be the reason for the remaining cold upper-extremities.

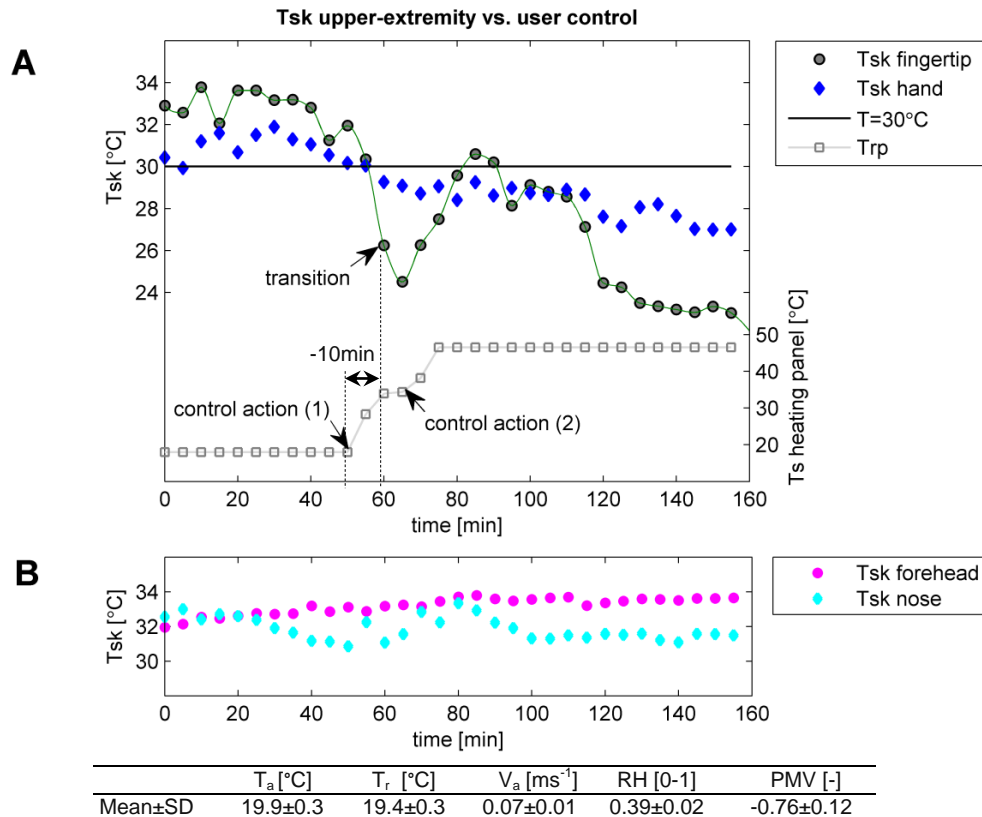


Figure 3.14 Upper-extremity- and facial skin temperature (from IR data) during the user-controlled test. (A) Fingertip and hand skin temperatures versus heating panel temperature, and (B) forehead and nose skin temperature. Session#3 dd. 10-11-2011: male subject.

An overview of the time delays obtained for the different sessions of experiment 3 is shown in Table 3.2. A positive time-delay indicates that a trend in finger temperature was recognized before the control action was performed. A negative time-delay indicates that the trend was recognized after a control action was performed.

Table 3.2 Overview of the time delay between transition in finger temperature and the control action performed by the user for the sessions during experiment 3: user-control.

Exp.3	Ses#1	Ses#2	Ses#3	Ses#4	Ses#5	Ses#6
Time-delay	+10min	-10min	-10min	+15min	+15min	-40min

3.5 Discussion and evaluation

Measurement results

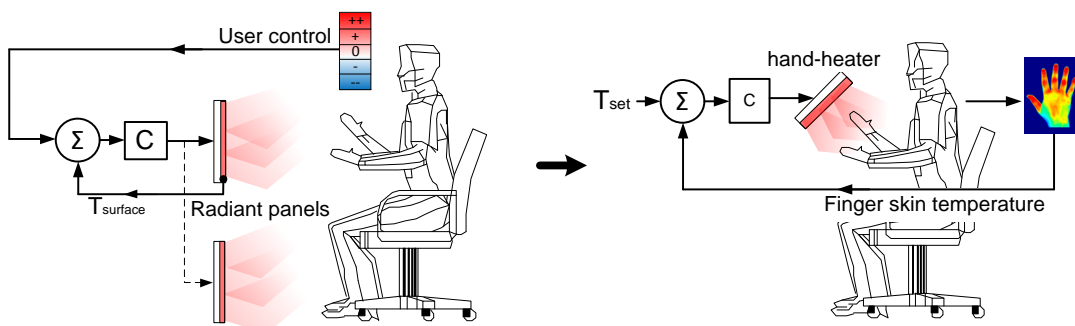
- The 4th finger skin temperature is according to the measurement results a promising indicator to include the human body as a sensor in the control loop of local heating systems. The fingertip skin temperature was highly sensitive for the applied environmental conditions and seems to correlate with local ($r^2=0.74$, $p<0.01$) and overall thermal sensation ($r^2=0.68$, $p<0.05$). In addition, the fingers were highly accessible, and the thermoregulatory effect was clearly visible. These results are consistent to the finding of Wang [Wang et al., 2007], as discussed in §2.2.1.
- Oscillations of the 4th finger skin temperature in the neutral zone of about 1.5K were observed during all the measurements. These oscillations make it more difficult to recognize a clear transition out of the neutral zone, before cool discomfort becomes a

- possibility. Using the moving average is highly recommended when using the finger temperature as control signal. This to eliminate the effect of these oscillations.
- The facial skin temperature shows less potential for automatic regulation of local heating in mild office conditions, because no clear correlations with the control actions of the user were found. Only in the cool environmental condition test (Figure 3.11) the nose temperature correlated with overall thermal sensation ($r^2=0.56$, $p=0.1$).
 - From the measurement results of the user-controlled experiments it was not clear if the time-delay between the transition in 4th finger temperature and the user control action was large enough for automatic control (see Table 3.2). To test whether the fingertip skin temperature is useful as a control signal for local heating, the experiment has to be reversed. This means that the *finger* skin temperature will be used as feedback control signal for regulation of the radiant heater. The heating- preferences and thermal sensation of the user will be surveyed to assess the performance of this control signal.
 - In the experiments 4th finger of the left hand was analyzed. Due to occupant movements and the position of the hands, it was more easily to track the temperature of the 3rd finger instead of the 4th finger. Both the experiments and literature [He et al., 2010] conducted that there is no significant temperature difference between those fingers. Therefore the 3rd finger temperature is used in the next series of experiments.

Shortcomings

- The radiant panels were unable to compensate for the decreasing skin temperature of the hands, under the circumstances of a room air temperature controlled below 20°C. From the black-globe measurements (Figure 3.8) and heat transfer calculations, it was concluded that the radiant temperature near the extremities increased the most. However the black-globes ($D=0.15\text{m}$) have a large frontal area which was directly irradiated by the panels. The view factor with the hands, flat on the table, is much smaller and is probably the reason for the ineffective way of heating. Due to the small view-factor, a large amount of the radiated energy was transferred to the environment without warming the subject. Therefore the heating system was very ineffective. A heating system with an improved view-factor with respect to the upper-extremities is therefore required.
- In addition, it was not clear if the skin temperature of the most influential body parts (chest, back, and pelvis) also decreased, or that only the skin temperature of the extremities decreased. To overcome this shortcoming in the next series of experiments, it is also necessary to measure the mean skin temperature.

	Chapter 3	→	Chapter 4
Type of control	User-control		Automatic control: finger temperature
Heating system	Radiant panels		Local hand heater (improved view-factor)



4. Experiments II: Automatic comfort control

From the first series of experiments (§3.4) it was concluded that the fingertip skin temperature is a critical performance indicator for radiant heating in a mild cold office environment. The question remains: can the radiant heating system feed-forward respond on users' thermal preferences by using this CPI as control signal?

A number of experiments were performed to answer this question. First, the radiant heating system was improved. This chapter describes the improved heating system (§4.1), the experiments (§4.2), and the measurement results. Finally the results are discussed and conclusions are drawn.

4.1 Improved heating system

As mentioned before, the radiant panels were not able to maintain the upper-extremity skin temperature at a neutral or higher thermal state in mild cold conditions. For this reason the heating panels were replaced by a heating system which can transfer the radiation energy more concentrated to the hands, as the view factor was improved.

This so-called hand-heating system consists of two incandescent reflector heating lamps (properties, see Appendix G). At maximum temperature the heating lamps emit mostly in the IR-A and IR-B wavelengths⁴. A dimmer has been used to decrease the temperature level and thus the radiation heating intensity. The total supplied power was 98W.



Figure 4.1 (A) Improved local heating system, consisting of two reflector heating lamps, (B) male subject performing office tasks, and (C) female subject performing office tasks.

4.2 Experiments

The hypothesis that the finger temperature can be used as feedback control signal for automatic regulation of the radiant hand-heating system was tested for different finger temperature bandwidths. Thereby, the objective was to determine whether the system was able to feed-forward respond on user thermal preferences.

Two healthy young subjects (male and female) participated several times in these experiments. A schematic overview of the experiments is shown in Figure 4.2.

⁴ Notice that at lower temperatures the wavelength at which maximum spectral emittance occurs, shifts towards the IR-B, and IR-C spectrum (Planck's law, Appendix A).

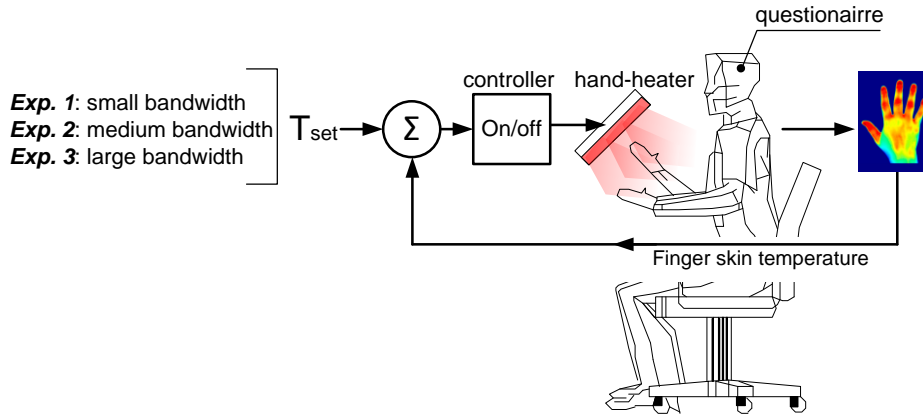


Figure 4.2 Schematic overview of the experiments: the finger skin temperature is used as a feedback control signal for automatic regulation of the radiant hand-heater. The applied set-points differ according to the bandwidth applied. The user thermal-sensation and preferences were assessed by a questionnaire.

Bandwidth in which finger temperature is controlled

During all experiments, the basic room air temperature was controlled between 19.5-20.0°C, which was below the thermo neutral zone of the subjects. For this reason, the upper-extremity skin temperature was presumed to decrease.

When finger skin temperature reached a predefined lower limit, the hand-heating system was switched on. The heating system was switched off when skin temperature reached the upper limit. Skin temperature was then allowed to drop, and used as control signal again. The turn-on and turn-off temperature differs significantly to ensure sufficient influence on thermal sensation. The difference between these skin temperatures is called bandwidth. The cases are ranked according to the size of this bandwidth, namely small, medium and large. In Figure 4.3, the small and medium bandwidths are schematically shown.

	bandwidth	dT [K]	T _{sk,min} [°C]	T _{sk,max} [°C]	Number of sessions	Comfort parameters
Exp.1	small	2.5	29	31.5	4	T _o =19.5-20°C M=1.2met
Exp.2	medium	5.5	26	31.5	2	V _a <0.1 ms ⁻¹ R _{cl} =0.82clo
Exp.3	large	11.5	20	31.5	1	RH=40-60%

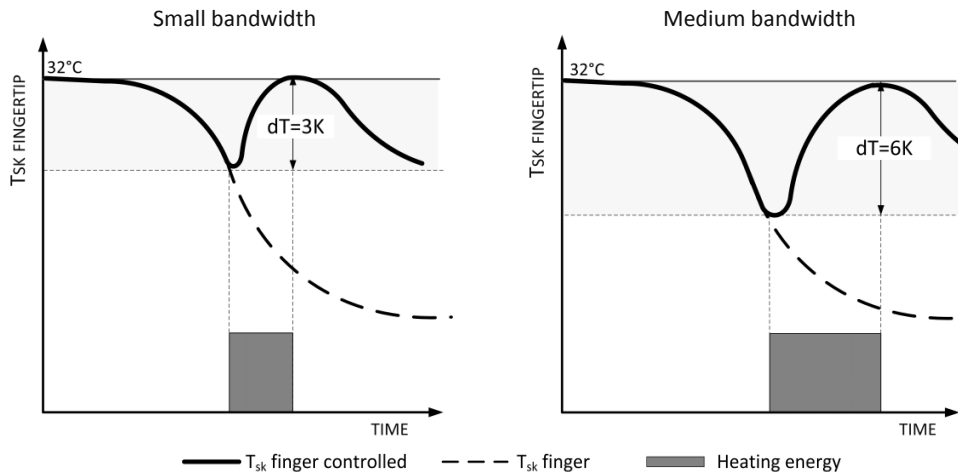


Figure 4.3 Overview of small and medium bandwidths in which the finger skin temperature was controlled.

Time-schedule of the experiments

The time schedule applied during the experiments is shown in Figure 4.4. During the sessions, the subjects performed office tasks on their own laptop. The metabolic heat production was assessed 1.2 met ($1\text{met}=58\text{Wm}^{-2}$). A thermal acclimatization time of 20 minutes was applied to ensure the subject's upper-extremity skin temperature was in the neutral zone at the start of the session. Thereafter skin temperature sensors were attached. The total duration of the experiment was 3.5h. The time differs from the first series of experiments, so that the bandwidth can be tested several times per session. The subjects wore office clothing of 0.82clo as reported in §3.1.



Figure 4.4 Time schedule applied during the experiments.

Questionnaire

In order to investigate whether the proposed control algorithm is able to respond to user thermal preferences a questionnaire was applied. Thermal preferences were asked every 10 minutes during the entire session. The user was able to indicate if a warmer, neither warmer nor cooler, or a cooler environment was preferred. In addition, local- and overall thermal sensation, and thermal acceptability were assessed. The ASHRAE standard 7-point thermal sensation scale has been applied. The questionnaire is included in Appendix H. These subjective responses were collected and correlated to the measurement results.

4.3 Measurement set-up: adjustments

Some adjustments were made in the measurement set-up as proposed in §3.2. The adjustments are as follows:

- The infrared measurement data was real-time used as control signal for regulation of the hand-heater. An $M \times N$ matrix skin surface area was selected at the 3rd finger (instead of the 4th finger, see §3.5) of the left hand of the subject. An example is presented in Figure 4.5, where skin temperatures are shown in a histogram along with the normal density function. The mean local skin temperature (μ) was used as the controlled variable. To avoid large fluctuations in the control signal the moving average signal (over 120s) was used. This resulted in a more smooth controlled profile.

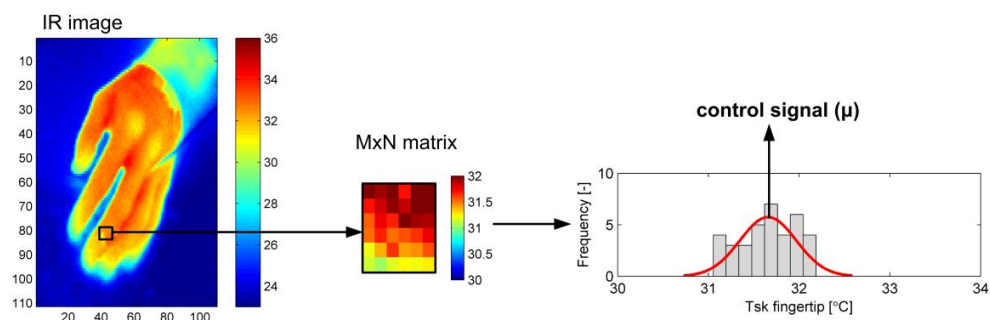


Figure 4.5 Real-time control signal (μ) obtained from IR measurement of upper-extremity skin temperature.

- In order to assess the level of whole body cooling, the mean skin temperature was also measured. The mean skin temperature was measured continuously at 1 min intervals by iButton sensors placed at 14 predefined locations on the body according to ISO 9886 (Figure 4.6). The iButton sensor has recently been evaluated for studies into humans [Van Marken Lichtenbelt et al., 2006]. They reported a mean accuracy of 0.09°C, with a maximum deviation of 0.4°C. The mean skin temperature is calculated according to equation 4.1.

$$T_{sk,mean} = \frac{1}{14} \sum_{i=1}^{14} T_{sk,i} \text{ [}^{\circ}\text{C]} \quad (4.1)$$

The fingertip–forearm gradient (position 15-16) will be used as an index of thermoregulatory vasoconstriction [Rubinstein et al., 1990].

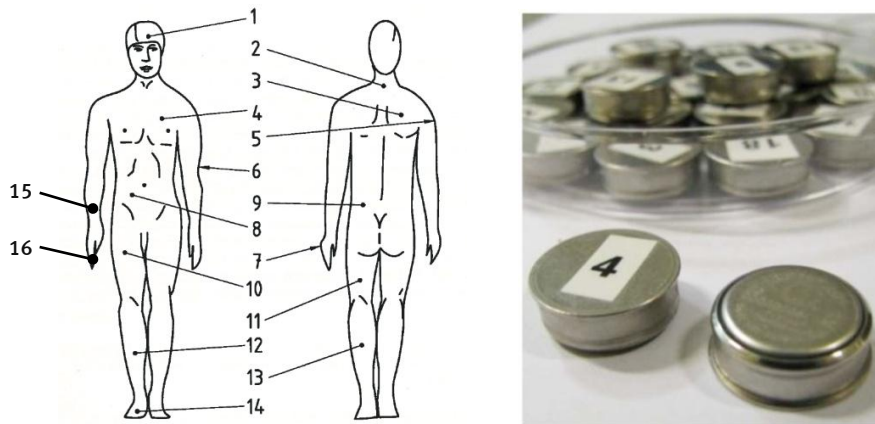


Figure 4.6 Mean skin temperature measurement positions (1-14) [ISO 9886], and fingertip-forearm temperature gradient (15-16) as measure for vasoconstriction.

4.4 Results

The measurement results of the experiments are presented in this paragraph for respectively the small, medium and large bandwidth. An extensive presentation of the results is included in Appendix I. Using the applied bandwidths it should be possible to assess whether the critical performance indicator (CPI) is able to feed-forward respond to the thermal preferences of the user.

4.4.1 Experiment 1: Small bandwidth, male subject

The upper-extremity skin temperature was controlled in a small bandwidth (29-31.5°C). The hypothesis is that within this bandwidth the thermal sensation remains neutral or higher, and that no extra warmth is preferred. Two infrared images of the experiment are shown in Figure 4.7. Image A was obtained during the first half hour of the session, showing that the hand temperature was in the neutral zone. In image B, taken after 1 hour, the decreasing skin temperature in the fingertips was clearly observed.

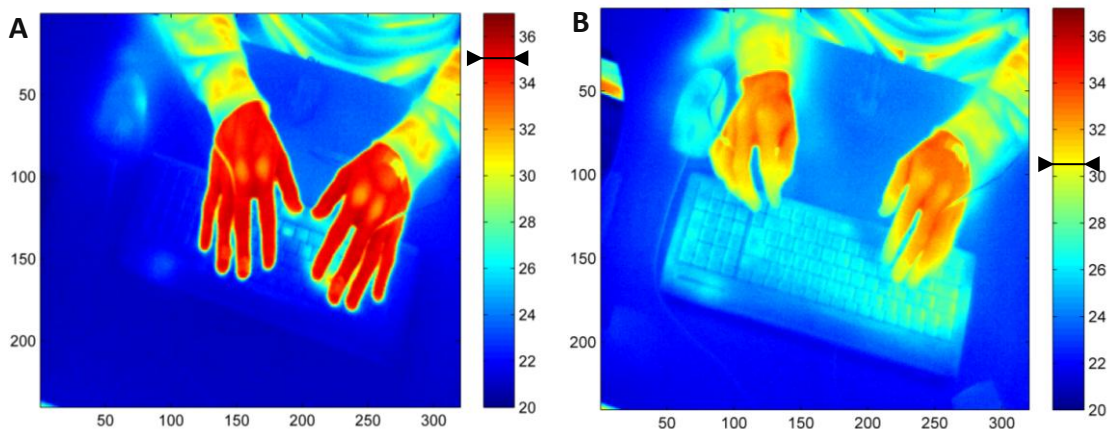


Figure 4.7 Thermographs of the upper-extremity skin temperature when finger temperature was controlled in a small bandwidth, session: 08-02-2012. Image A was taken at $t=10\text{min}$, and image B at $t=55\text{min}$. The color bars are in degree Celsius, and the finger temperature is indicated by the black arrow.

The measurement results are shown in Figure 4.8. In part A, the primary vertical axis shows the moving average fingertip skin temperature measured by IR thermography. The secondary vertical axis indicates if the hand-heating system was activated (1) or deactivated (0). The total power during activation was 98W. In part B, the overall thermal sensation (WB-TS) and local thermal sensation of the hands (TS-hands) are shown on the 7-point ASHRAE thermal sensation scale. In part C, the user preferences for a warmer, neither warmer nor cooler, or a cooler environment are presented. The mean environmental conditions and corresponding standard deviation (SD) are also included. To assess the thermal environment (without personal heating), the PMV was calculated according to the thermal sensation model of Fanger [Fanger, 1970]. Additionally, the mean skin temperature is included for comparison of the different cases.

From $t=0$ until $t=50\text{min}$, no hand-heating was required because the fingertip skin temperature did not reach the lower limit of the small bandwidth. After these 50min, a strong decrease in fingertip skin temperature was observed. After reaching the lower limit (29°C), the hand-heating was switched on until the finger temperature reached the upper limit (31.5°C). This pattern was repeated during the rest of the experiment. Throughout the entire session, there were only two moments that the user preferences were not maintained at the desired 'neither warmer nor cooler' level. This happened directly after the break ($t=140\text{min}$) and at the end of the session ($t=190\text{min}$).

In general, it was possible to maintain the thermal sensation at neutral or higher, and to keep user preferences unchanged.

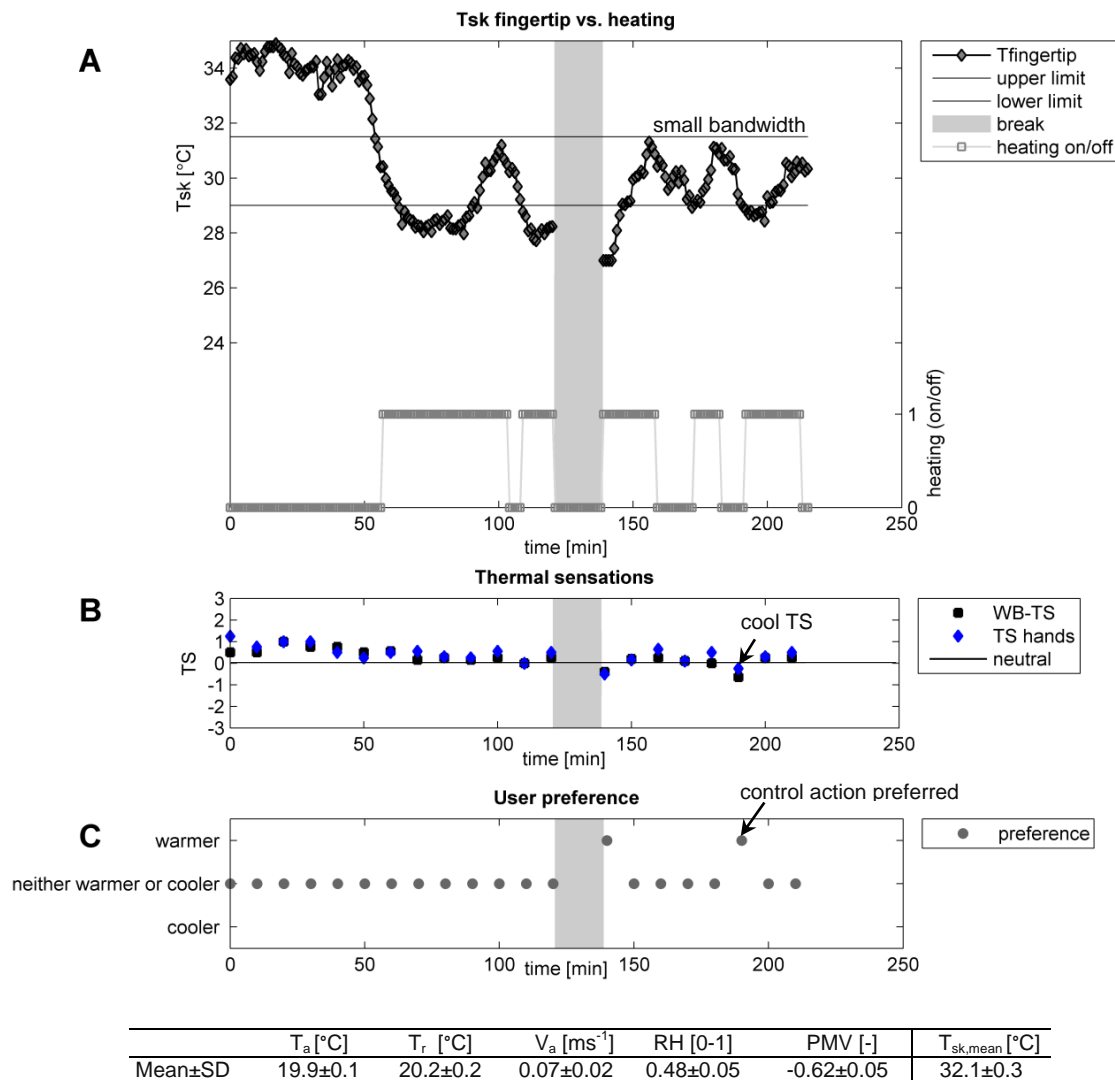


Figure 4.8 Upper-extremity skin temperature controlled in a small bandwidth. (A) Fingertip skin temperatures (moving average) versus heating level, (B) Whole-body and local thermal sensation, and (C) heating preferences. Session 08-02-2012: male subject.

4.4.2 Experiment 1: Small bandwidth, female subject

Figure 4.9 shows the results of the session in which finger skin temperature of the female subject was controlled in a small bandwidth. The influence of transitions out of the small bandwidth was examined on thermal sensation and preferences. Immediately after the 1st transition out of the small bandwidth ($t=55$ min), the local sensation dropped below neutral and extra heating was preferred. The preference for extra warmth disappeared ($t=70$ min), while skin temperatures were not yet in the small bandwidth. Also after the 2nd transition the local sensation votes dropped below neutral and a warmer environment was preferred. Environmental control actions were thus needed when the finger skin temperature dropped below the lower limit of the small bandwidth.

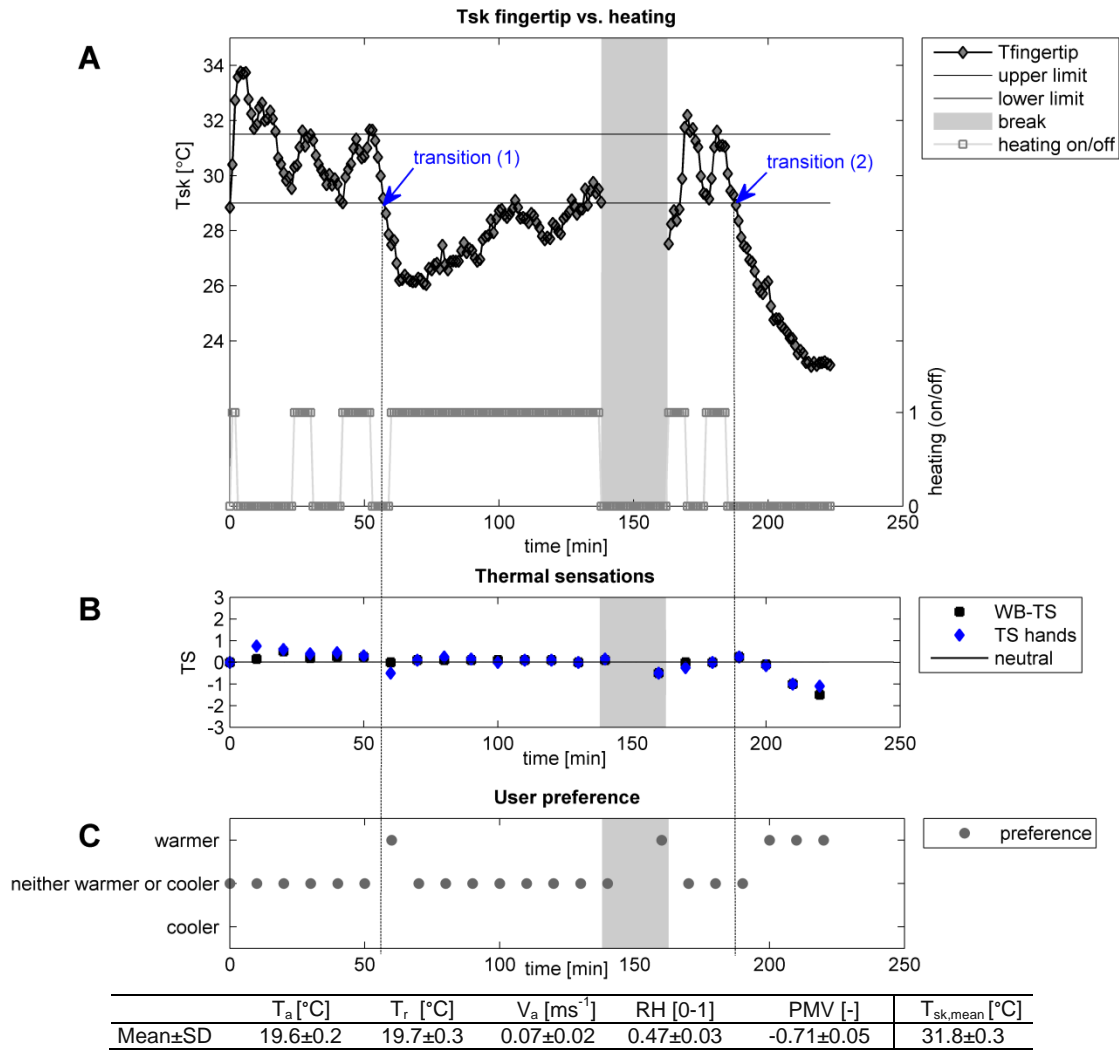


Figure 4.9 Upper-extremity skin temperature controlled in a small bandwidth with two transitions out of the bandwidth. (A) Fingertip skin temperatures (moving average) versus heating level, (B) Whole-body and local thermal sensation, and (C) heating preferences. Session 10-02-2012: female subject.

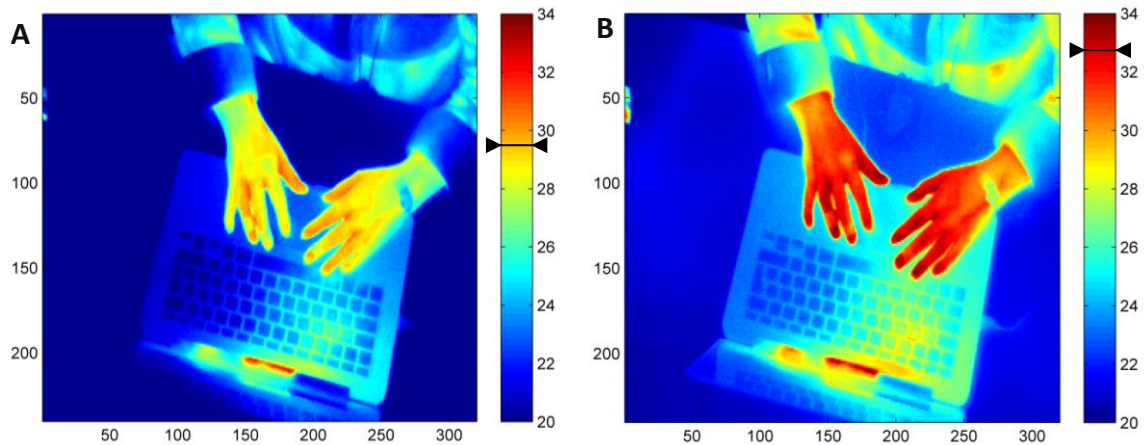


Figure 4.10 Thermographs of the upper-extremity skin temperature when finger temperature was controlled in a small bandwidth, session: 10-02-2012. Image A was taken at t=0min, and image B at t=15min. The color bars are in degree Celsius, and the finger temperature is indicated by the black arrow. The female subject used her own laptop.

Thermoreception

As mentioned before, humans do not sense temperature directly. Temperature information is coded into the firing rate of temperature sensitive neurons (§2.1.1). Kingma developed a model based on neurophysiology, which can capture the dynamic behaviour of thermal sensation during transients. This model uses thermoreceptor data as reported by [Zotterman, 1953]. For a detailed description of the model, see his PhD thesis [Kingma, 2011].

Using this model for the measured skin temperatures, the neuron discharge rate was simulated. The sum of the 1st 10 seconds of the neuron fire rate of the warm and cold-sensitive neurons are presented in Figure 4.11, part A. The sum is highly sensitive for quick changes in local skin temperature and may explain the dynamic character of thermal sensation. The thermal sensation votes are shown in part B.

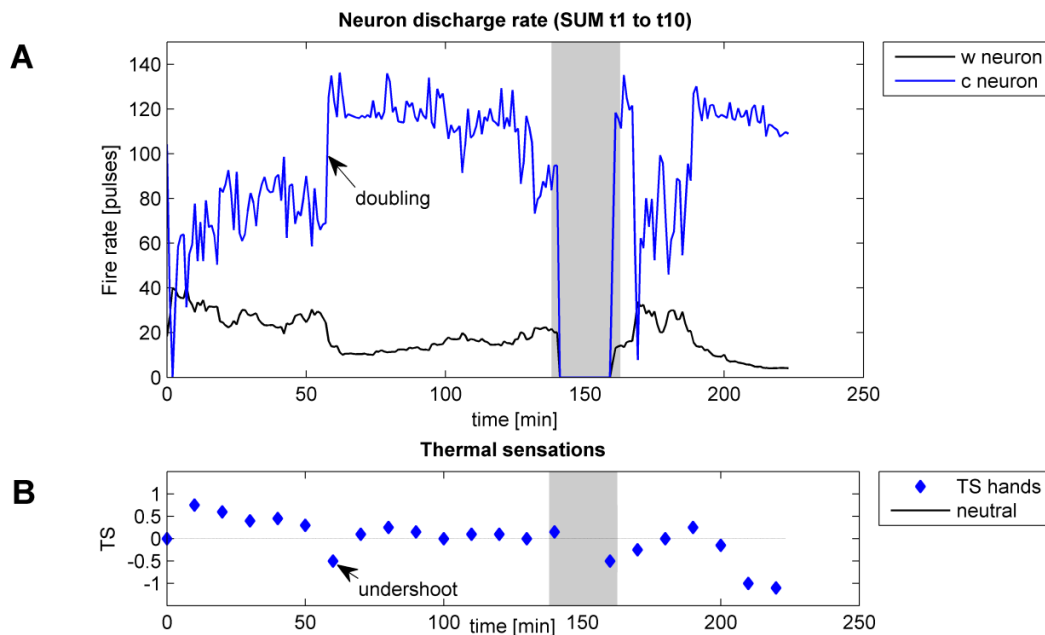
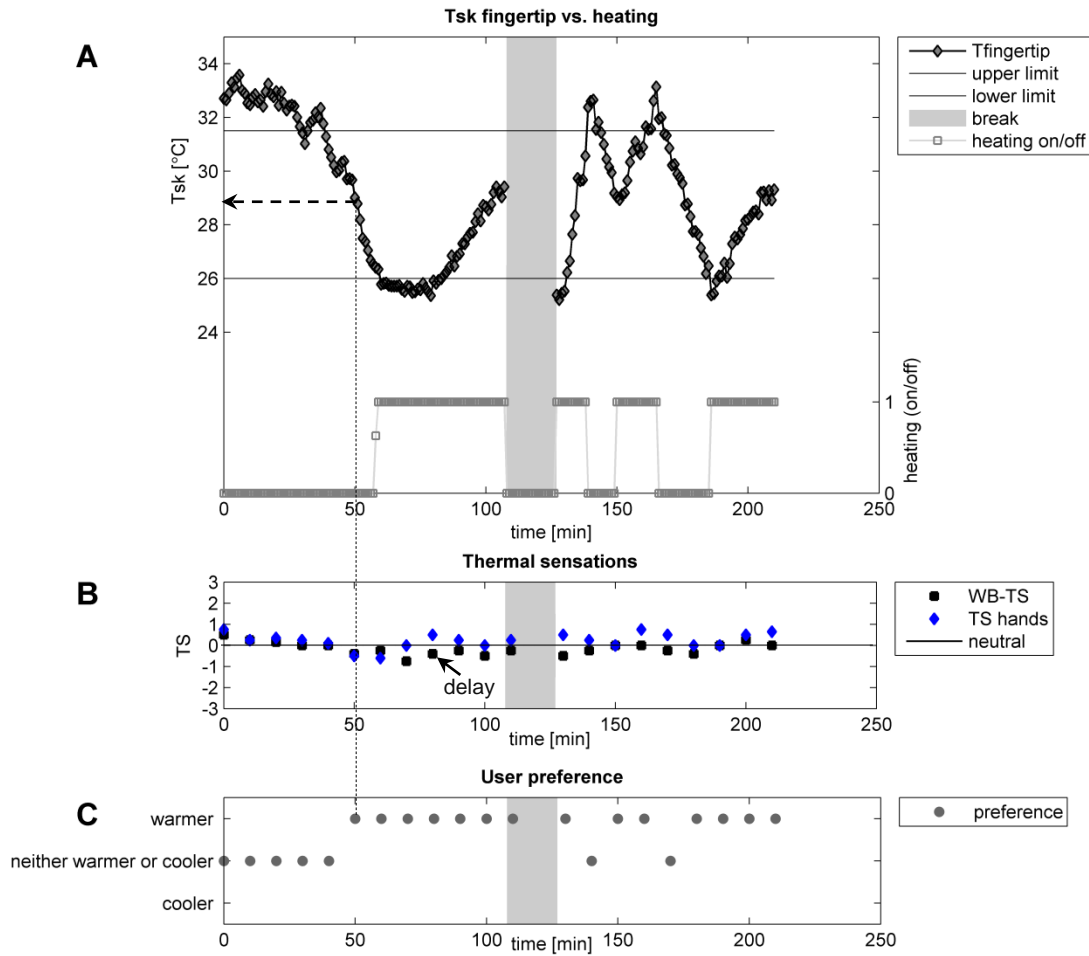


Figure 4.11 The dynamics of thermal sensation. (A) Neuron discharge rate of the cold and warm sensitive neurons for the measurement results of 10-02-2012, and (B) Local thermal sensations of the hands.

The significant decrease in skin temperature after 55min (i.e. transition 1, Figure 4.9) is clearly reflected by the strong increase in the neuron fire rate of the cold-sensitive neurons. As a result, the local thermal sensation of the hands strongly decreased, from 0.3 (t=40min) to -0.5 (t=50min), and then increased to 0.1 (t=60min): a typical 'undershoot' in thermal sensation.

4.4.3 Experiment 2: Medium bandwidth, male subject

The finger skin temperature was controlled in a medium bandwidth of 26-31.5°C (Figure 4.12). When the skin temperature dropped below 28°C (t=50min), the local and overall thermal sensations votes were assessed below neutral and a warmer environment was preferred. The application of local heating had a strong effect on the local sensation, but was not sufficient to bring overall sensation to a positive level (t=70 until t=100min). Moreover, the subject asked for a warmer environment throughout the entire session. For this reason the medium bandwidth appears to be unable to respond on user thermal preferences.



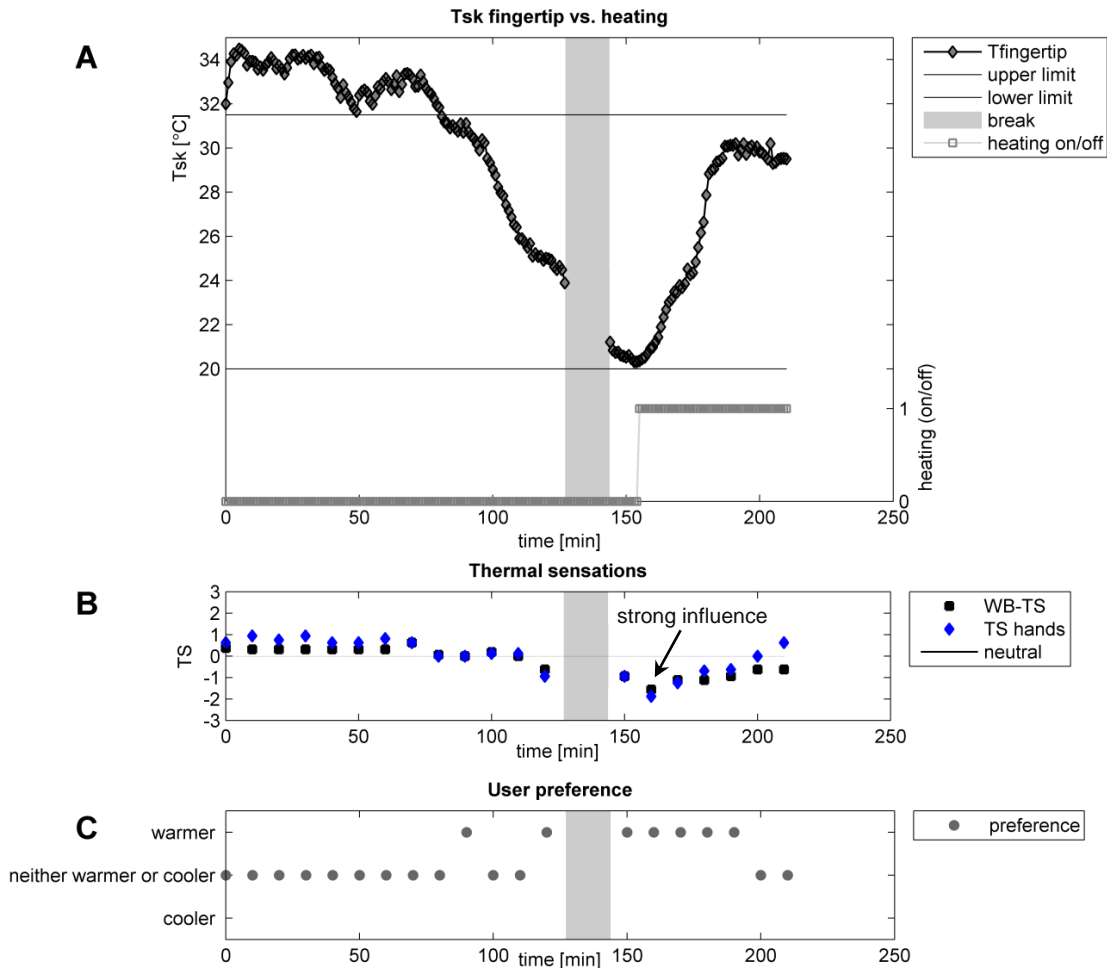
	T_a [°C]	T_r [°C]	V_a [ms ⁻¹]	RH [0-1]	PMV [-]	$T_{sk,mean}$ [°C]
Mean±SD	19.7±0.2	19.6±0.3	0.08±0.03	0.42±0.02	-0.70±0.05	32.1±0.21

Figure 4.12 Upper-extremity skin temperature controlled in a medium bandwidth. (A) Fingertip skin temperatures (moving average) versus heating level, (B) Whole-body and local thermal sensation, and (C) heating preferences. Session 07-02-2012: male subject.

4.4.4 Experiment 3: Large bandwidth, male subject

In Figure 4.13 the upper-extremity skin temperature was controlled in a large bandwidth (20–31.5°C). The purpose of this experiment was to detect at which skin temperature the user-preferences changed from ‘neither warmer nor cooler’ into ‘warmer’ and to show influence on thermal sensation.

From $t=0$ min to $t=80$ min, the upper-extremity skin temperature remained in between 32–35°C. Thereafter, skin temperature decreased until it reached a minimum temperature of 20°C, which was near-ambient air temperature of 19.6°C. From $t=120$ until $t=190$ min the user consistently preferred a warmer environment. This is also reflected by the local sensation of the hands, which was below neutral ($TS < 0$). Heating of the hands had again a strong effect on local sensation, it was however not sufficient enough to bring overall sensation to a positive level ($t=160$ min until $t=210$ min). Remarkable is that after 200min no extra heat was preferred, while whole-body thermal sensation remained below neutral.



	T_a [°C]	T_r [°C]	V_a [ms ⁻¹]	RH [0-1]	PMV [-]	$T_{sk,mean}$ [°C]
Mean±SD	19.6±0.1	19.7±0.2	0.08±0.02	0.49±0.03	-0.71±0.04	32.0±0.45

Figure 4.13 Upper-extremity skin temperature controlled in a large bandwidth. (A) Fingertip skin temperatures (moving average) versus heating level, (B) Whole-body and local thermal sensation, and (C) heating preferences. Session 09-02-2012: male subject.

4.4.5 Statistic results of all experiments

This paragraph describes the statistic results of all experiments with regard to automatic climate control purposes. In total 7 experiments were performed (see Appendix I).

Thermal- preference and acceptance of the environment

The turning point from 'neither warmer nor cooler' to a 'warmer' preferred thermal environment is the central point of interest. In fact this point describes if the finger temperature can be used as critical performance indicator (CPI) for individual local heating. In Figure 4.14 a boxplot for the user thermal preferences is shown. The lower limit of the small bandwidth (29°C) is also included. If no change in the thermal environment was preferred, 75% of the measurement results were above the threshold of 29°C. This pattern is reversed when looking at the preference for a warmer environment. The temperature of 29°C can be seen as a threshold, separating 'warm preferences' from 'neither warmer nor cooler' preferences, with an overlap of 25%. Notice that this threshold can only be applied to the subjects which participated in this research. It is expected that among

individual this threshold can significantly vary. Nevertheless it shows the major influence of upper-extremity temperature on the thermal preferences.

In Figure 4.15 the boxplot for the user acceptance of the thermal environment and the fingertip skin temperature is shown. As with the user thermal preference, the lower limit ($T_{sk}=29^{\circ}\text{C}$) of the small bandwidth is included. When the thermal environment was assessed as 'just unacceptable', the finger skin temperature was below 29°C . The difference between 'just acceptable' and 'clearly acceptable' cannot be explained by the finger temperature.

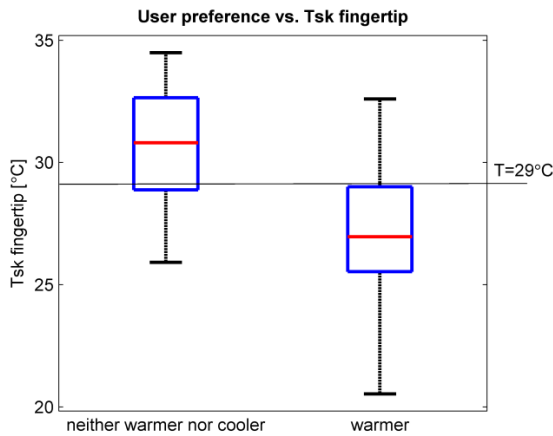


Figure 4.14 Boxplot of the user thermal preference vs. fingertip skin temperature.

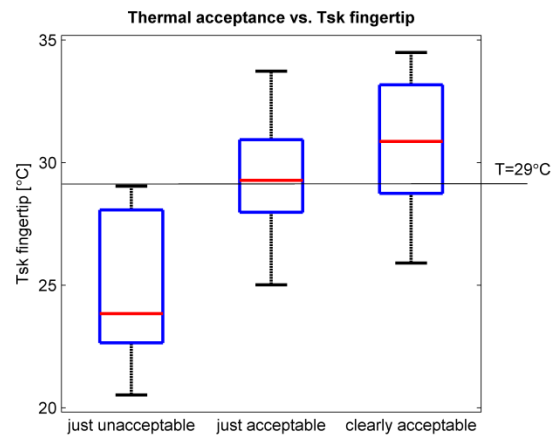


Figure 4.15 Boxplot of the user thermal acceptance vs. fingertip skin temperature.

Overall thermal sensation vs. finger temperature

The correlation between the overall thermal sensations and the fingertip skin temperature is shown in Figure 4.16. The overall thermal sensations votes for active hand-heating are separated from the data when hand-heating was inactive. Spearman's rank correlation coefficient has been used as a non-parametric measure of statistical dependence between fingertip skin temperature and overall sensations. The Pearson correlation coefficient, which is more sensitive for strong outliers, is also calculated. Most of the sensation votes fluctuate around neutral (-0.5 to 0.5), but a clear trend is recognizable too. The Spearman correlation coefficient of $r_s=0.67$ ($r^2=0.45$) indicates a medium positive correlation.

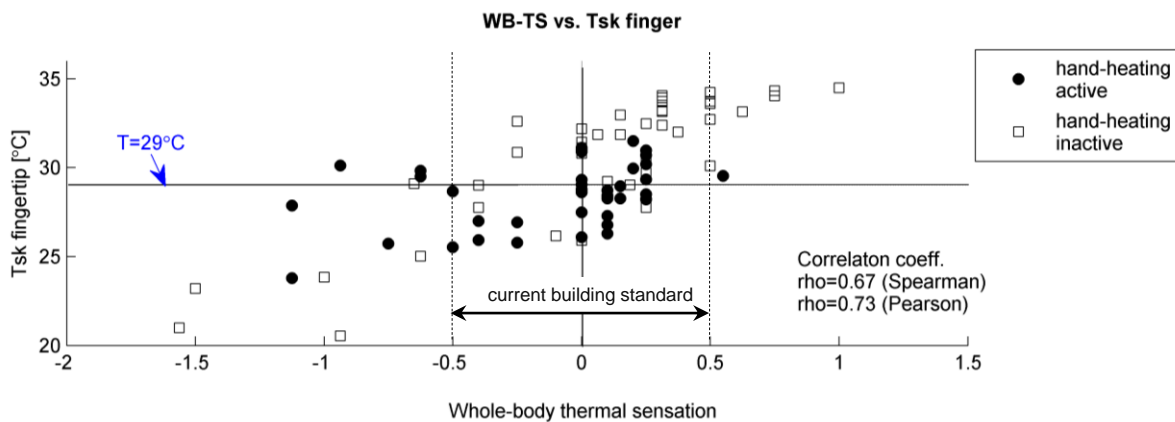


Figure 4.16 Correlation between the finger skin temperature and whole-body thermal sensation. The vertical line (at WB-TS=0) represents a neutral overall sensation. The horizontal line (at $T=29^{\circ}\text{C}$) represents the lower limit of the small bandwidth. The data-points when hand-heating was active / inactive are separated from each other.

4.5 Discussion on measurement results

General observations

- The upper-extremity skin temperature of subjects' right hand (computer mouse) was consistently cooler than the left hand (keyboard). In addition, the index fingers of both the hands were much cooler (about 1.5K) than the middle (3rd) and ring (4th) fingers.
- During almost all experiments, the upper-extremity skin temperature decreased after 30-60min, while the subjects were already thermally acclimatized for 20 minutes. This means that the first hour no environmental control actions were needed.
- A difference between the cooling behaviour of the hands of the female and male subject was observed. The hands of the female subject cooled down much faster and were more easily to influence by heating than the hands of the male subject. It should be noted that the surface area of the hands of the female subject was smaller (i.e. lower mass) than of the male subject. See Figure 4.17.

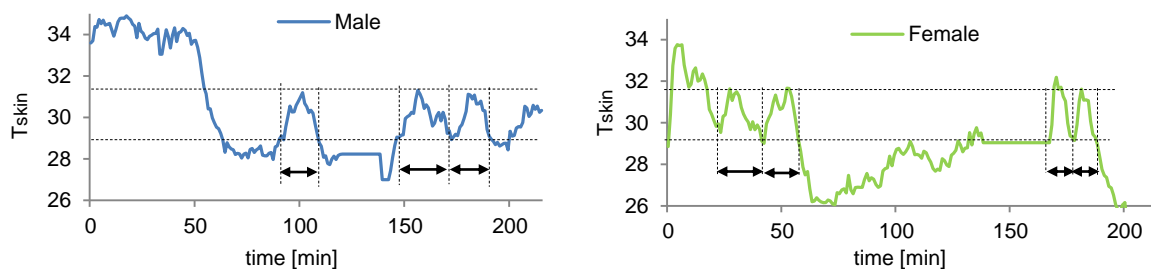


Figure 4.17 Differences in the cooling-time of the fingers between the male and female subject.

The finger as feedback control signal

- By controlling the finger temperature in a small bandwidth ($T=29-31.5^{\circ}\text{C}$), it was possible to automatically respond on user thermal preferences. Small changes in the skin temperature ($\leq 2.5\text{K}$) were not perceived as cool by the subject. The minimal observed cooling time of the finger temperature in the small bandwidth took about 5min. This time was available for detection and reaction by the heating control system.
- During the experiments the moving average (over 120s) finger temperature was used as control signal. The moving average is less sensitive for quick changes; however it increases the overall response time. Using a signal filter to eliminate the oscillating effect can overcome this problem. See Figure 4.18

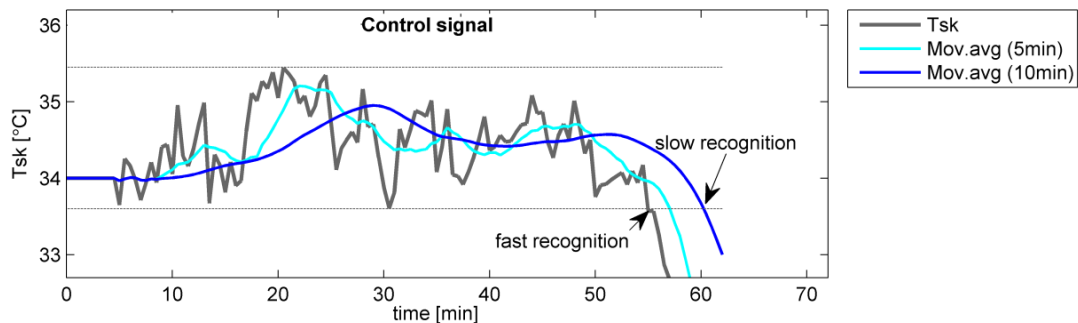


Figure 4.18 The measured finger temperature by IR thermography (T_{sk}), the moving average signals based on 5- and 10minute data, and the overall filtered area. Session 08-02-2012: male subject.

- The on/off control algorithm as applied during the experiments had some disadvantages. When the heating system was abruptly switched off, a short-duration 'undershoot' in local thermal sensation occurred. A more smooth control process, for example by a PI controller, may solve this problem.
- The small bandwidth in which finger temperature is controlled will differ per individual. From literature (§2.3) it was concluded that the finger skin temperature varies between individuals due to different thermoregulatory set-points. An example is the percentage of body fat which significantly affects the upper-extremity skin temperature [Savastano et al., 2009]. By learning from the individual preferences, the small bandwidth might be applicable to other individuals. This means for example that the bandwidth for an obese office worker lies higher than for a normal weight office worker (Figure 4.19).

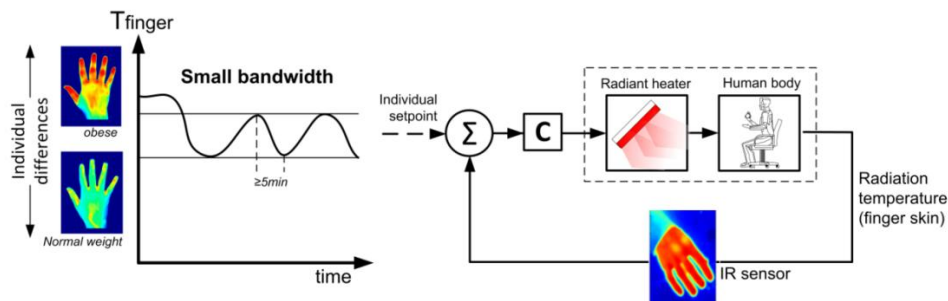


Figure 4.19 The individual 'small bandwidth' as set-point for the proposed control strategy. Based on literature it was concluded that the bandwidth for an obese office worker lies higher than for a normal weight office worker.

Comparison with literature

- In Figure 4.20 the finger temperatures and overall thermal sensation as measured in this study, are compared to the results obtained by Wang et al. (2007). The results of Wang show a much larger dispersion in thermal sensation votes. This can be explained by the wide range of temperatures (17.5~20.7°C) in which in the indoor temperature was controlled, in comparison to this study (19.6-19.9°C). In addition, Wang applied convective heating instead of radiant heating. The range of skin temperatures fluctuating near-neutral (26-32°C) is much larger for this study, however Wang (2007) only performed limited measurements in this range which makes the comparison complicated.

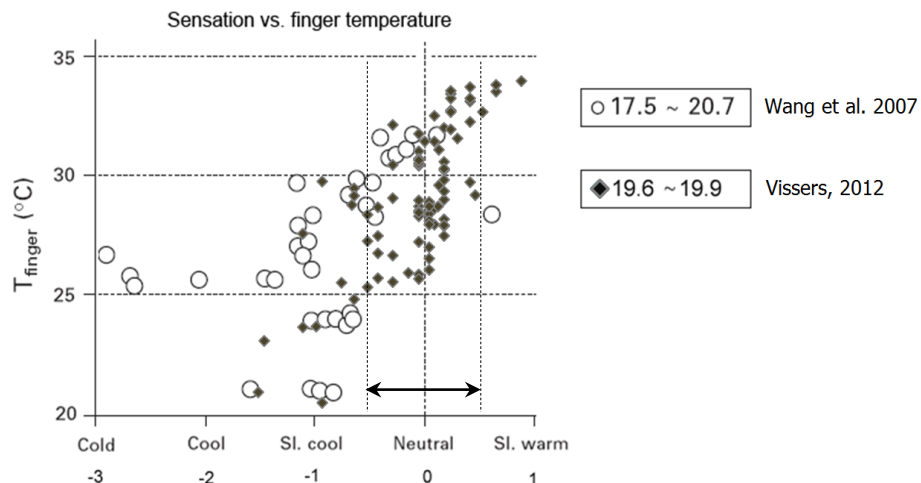


Figure 4.20 Comparison of the finger temperature and overall thermal sensation as measured in this study (called Vissers, 2012) and the results obtained by Wang et al. (2007) for different chamber temperatures. The current building standard ($-0.5 < TS < +0.5$) is indicated by the arrow between the dashed lines.

5. Energy saving potential

5.1 Introduction

This chapter elaborates on the energy saving potential of the proposed human in the loop control strategy during an average winter period in the Netherlands. The energy saving potential results from the fact that the room ambient conditions can be less strict when individual controlled heating is applied. From §4.4, it was concluded that the set-point for basic room air temperature can be lowered from 22 to 19.5°C. So less energy is needed to condition the entire room. The energy use for local heating, about 98W per occupant, should however also be taken into account. The principle is schematically shown in Figure 5.1.

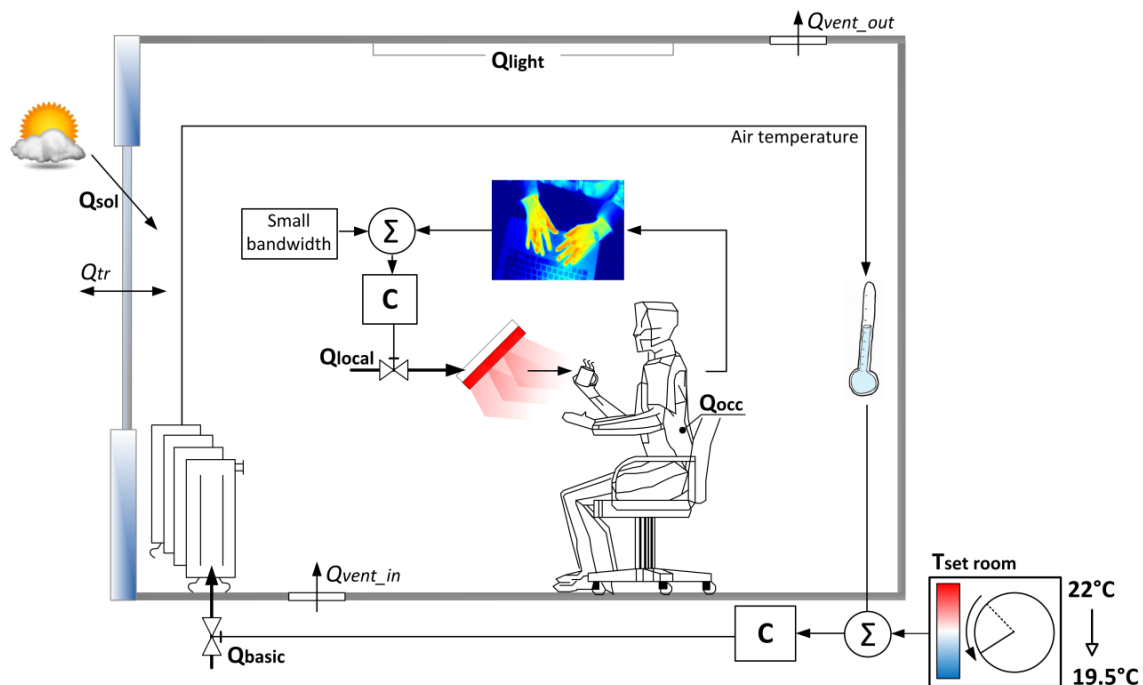


Figure 5.1 Block diagram of the global and local control loop and the energy flows into the room. The energy saving potential results from the decreasing set-point of the room temperature.

5.2 Case study

In this graduation project the energy saving potential is simulated for an office building in the Netherlands during an average winter period. The simulation is performed using a whole building model programmed in the MATLAB HAMBBase environment. A reference project was chosen to make the results more realistic. In contrary to earlier research by [Zhang et al., 2009], this study takes into account the real occupancy profiles, the appliances use, lighting profiles and the energy needed for personalized conditioning of the occupants.

5.2.1 Building description

An office building of Royal Haskoning (an international engineering company) located in Rotterdam, the Netherlands, was chosen for the case study as it is a typical state-of-the-art rented office which are most common in the Netherlands (see Figure 5.2). The building was completed in 2006 and the total floor surface is about 1000m². A part of the 4th floor was chosen for the energy

simulation. Real occupancy profiles and appliances use on this floor were measured for a 6-week winter period by [Maaijen, 2012]. The office workers mainly performed computer, design and calculation work.

The 4th floor consists of an open plan office (14 workplaces, 121m²), cell offices, a meeting room and a corridor. The floor plan and construction properties are presented in Figure 5.3. The specific heat capacitance of the construction materials is assessed at 840Jkg⁻¹K⁻¹, with the exception of the expanded polystyrene (1470Jkg⁻¹K⁻¹).



Figure 5.2 The Royal Haskoning office building in Rotterdam, the Netherlands.

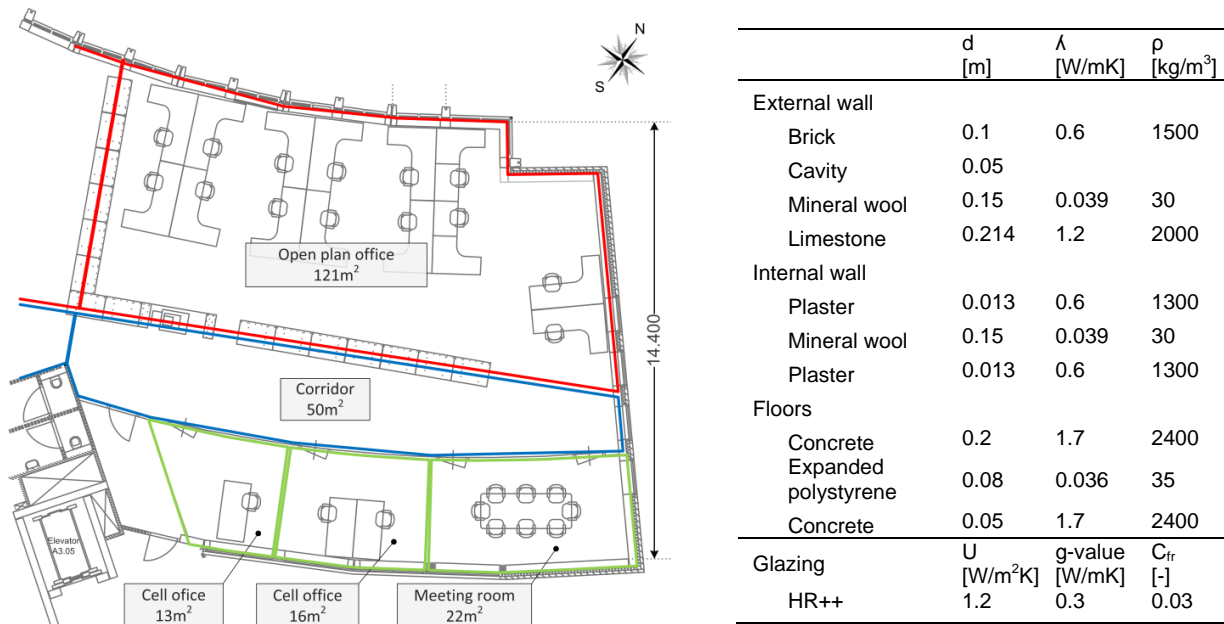


Figure 5.3 Floor plan, and construction properties of the 4th floor (used for simulation) of the Royal Haskoning office building in Rotterdam, the Netherlands.

5.2.2 Internal heat gains

The occupancy contributes to both sensible and latent heat load in the room. The activity level of the occupants was assessed at 1.1met (1met=58.2W/m², A_o=1.8m²), which is standard for office activities such as typing according to ASHRAE (2004). In the simulation model, the measured heat load due to electrical appliances (laptops, printer, screens etc.) was also applied. The artificial lighting was switched on in between 8.00 and 20.00h with a heat load of 8W/m².

In Figure 5.4, the measured profiles for occupancy and appliances are shown for a typical reference day in the open plan office. The occupancy is presented as a fraction of the full occupancy. During this day the maximum occupancy equals 80%. For the appliances the total heat load is presented. Remarkable point to mention is that even when the occupancy decreases (e.g. during the lunch break at 12.00h), the heat load by appliances does not significantly change.

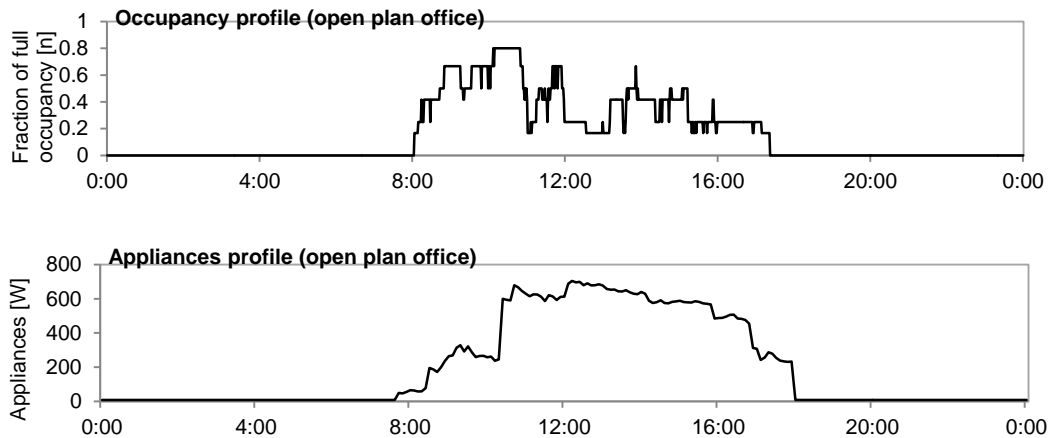


Figure 5.4 Measured profiles for occupancy and appliances for a typical winter day [Maaijen, 2012].

5.2.3 Room conditioning

The conditioning of the rooms is provided by an all-air HVAC system. From 7.30 until 18.00h the HVAC keeps the indoor air temperature at 22°C. During the night the indoor air temperature is controlled at 18°C. In the weekend, the day-time/night-time profile is 20/18°C. These temperature levels were based on measurements performed in the Royal Haskoning office building. Each zone in the simulation model has an own proportional controller for controlling the indoor conditions. The specific time constant of the HVAC system equals $\tau=10\text{min}$. A ventilation rate of 3h^{-1} is applied during office hours and during the night the ventilation rate is reduced to 1h^{-1} .

5.2.4 Local heating

For the simulation each of the workplaces was thought to be equipped with a local hand-heating system ($P=98\text{W}$). Again, the energy required for hand-heating is based on the measurement results as presented in §4.4.1. In reality the heating profiles will vary among individuals. However it is assumed to be an acceptable approximation for the average energy demand.

For all occupants the hand heating is only switched on when they are present on their workplace. By multiplying the local hand heating power with the occupancy profile the total power needed for local conditioning can be calculated. By integrating this power demand over time, the total energy usage is determined. See equation 5.1.

$$Q_{\text{local}}(t) = \int_0^t (P_{\text{local}} * \text{occ}) dt \quad (5.1)$$

5.3 Simulation model

The energy balance of the different zones (Figure 5.1) can be written using the general energy balance, see equation 5.2.

$$V_c \rho \frac{dT_a}{dt} = \dot{Q}_{\text{in}}(t) - \dot{Q}_{\text{out}}(t) \quad (5.2)$$

It can be assumed that the energy flows into the room constitutes:

- Energy supplied for space heating/conditioning by the central HVAC system (Q_{basic});
- Energy supplied for personalized conditioning of the occupants (Q_{local});
- Direct solar gains (Q_{sol});
- Internal heat gains from lighting, occupants and appliances.

$$\dot{Q}_{\text{in}}(t) = \underbrace{\dot{Q}_{\text{basic}}(t)}_{\text{Basic conditioning}} + \underbrace{\dot{Q}_{\text{local}}(t)}_{\text{Personalized heating}} + \underbrace{\dot{Q}_{\text{sol}}(t) + \dot{Q}_{\text{light}}(t) + \dot{Q}_{\text{occ}}(t) + \dot{Q}_{\text{app}}(t)}_{\text{Internal heat gains}} \quad (5.3)$$

The energy outflow of the zone constitutes heat losses from the building envelope towards the external conditions (Q_{tr}) and ventilation losses (Q_{vent}). Heat is stored and released by the building construction.

The HAMBBase model

A simplified sketch of the simulation model in Simulink is shown in Figure 5.5. The building construction properties are included in the HAMBBase model (see Appendix J). Climate data of the measured 6-week winter period is coupled to the whole-building model. The indoor air temperature of the zones is the output of the whole-building model. This information is used as feedback signal for the control algorithms of the individual zones. A demultiplexer (demux) is used for selecting the data-output from this feedback signal. A multiplexer (mux) is used for combining several data lines into one single signal line.

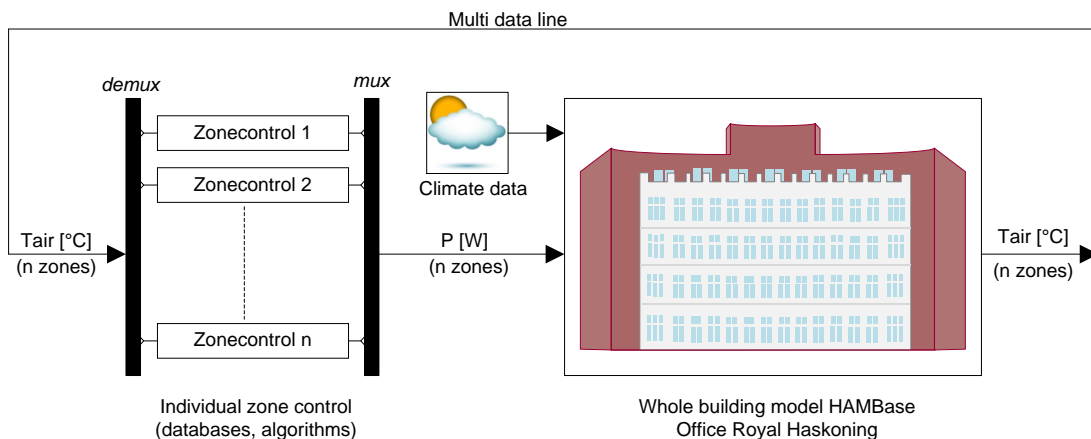


Figure 5.5 Simplified sketch of the simulation model in Matlab/Simulink. The air temperature is used as feedback control signal for the individual zone models.

Zone model

Each zone has its own control loop for regulating the indoor air temperature (see Figure 5.6). For the basic room heating (P_{basic}) a proportional control algorithm is applied. The feedback control signal is the indoor air temperature, and a time-dependent set point was applied. The internal heat gains (P_{intern}) are provided by the databases of the measured occupancy profiles, electrical appliance use and artificial lighting profiles. The power needed for local heating (P_{local}) depends on the occupancy. The total heating power flowing into the zone consists of the sum of basic heating, local heating and the internal heat gains. See equation 5.3.

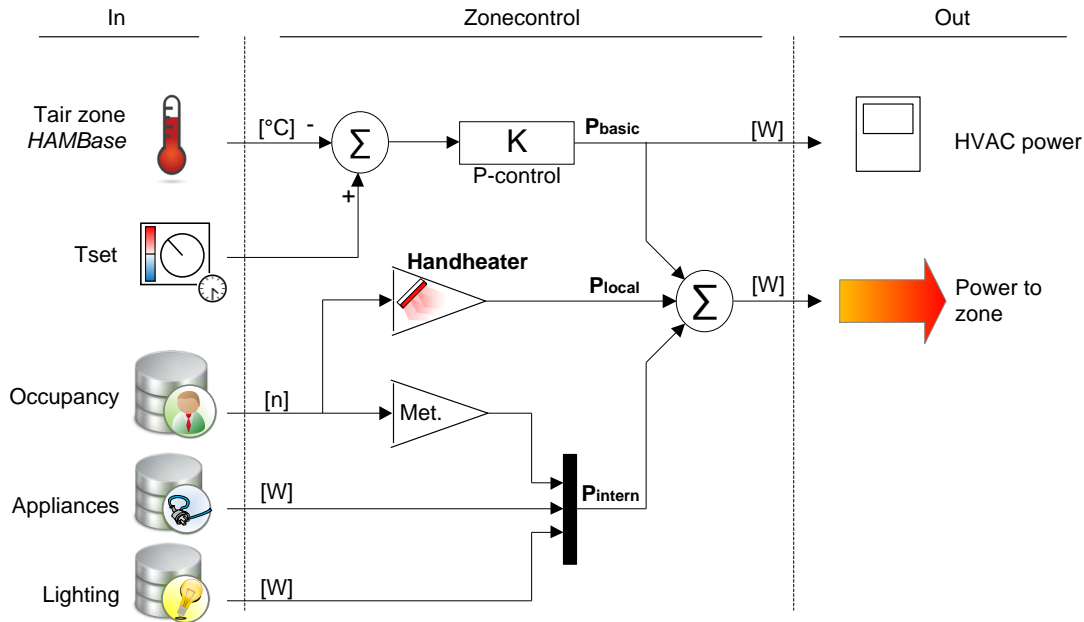


Figure 5.6 Simplified sketch of the individual zone control model in Matlab/Simulink. The power provided to the zone consists of the basic heating, local heating, and the internal heat gains by occupants, appliances and lighting.

Cases

The energy saving potential is simulated for different basic room air temperatures. A reference case was chosen in which the indoor air temperature was controlled at 22°C by a central HVAC system and where no personalized heating was applied.

In all other cases the basic room air temperature set-point was consistently reduced by 0.5K, to a minimum indoor air temperature of 18°C. The applied power for local heating at an indoor air temperature of 19.5°C was 100W. For room temperature set-points below this 19.5°C, an increase in heating power was assumed of 20W per 0.5K.

5.4 Results

The (primary) energy saving potential is calculated according to equation 5.4. The energy needed for the case is divided by the energy needed for the reference situation. The results are presented in Figure 5.7. The current situation, the proposed 'human-in-the-loop' control strategy and the future direction are also included.

$$\text{energy saving} = 1 - \frac{(Q_{\text{basic}} + \sum Q_{\text{local}})_{\text{case}}}{(Q_{\text{basic}})_{@22^{\circ}\text{C}}} \tag{5.4}$$

From §4.4.1 and 4.4.2 it was concluded that by controlling the finger temperature in a small bandwidth the overall thermal sensation was maintained at neutral or slightly higher, while an indoor air temperature of 19.5°C was applied. The energy saving potential for heating is 17% when lowering the set point of the indoor air temperature from 22°C to 19.5°C and taking into account personalized heating of 98W per occupant.

	Basic room air temperature									
	18°C	18.5°C	19°C	19.5°C	20°C	20.5°C	21°C	21.5°C	22 °C	
Saving potential	25%	23%	20%	17%	14%	11%	8%	4%	0%	

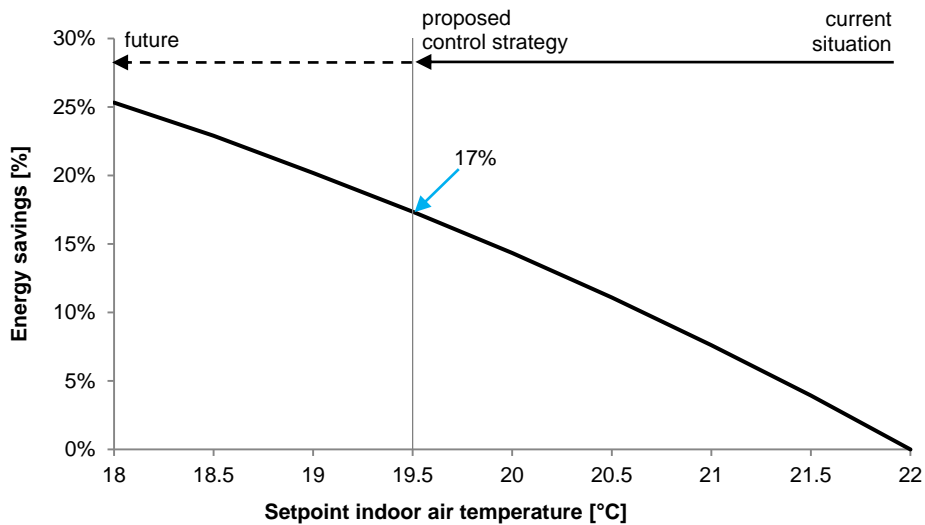


Figure 5.7 Energy saving potential for heating energy calculated for a 6-week winter period, by decreasing the indoor air temperature set-points and applying local heating per occupant. In the reference case the indoor temperature is controlled at 22°C without local heating.

Simulation results compared to literature

Zhang et al. (2010b) also reported the energy savings by expanding the dead-band⁵ in which the room temperature is controlled [Zhang et al., 2010b]. The annual energy savings, obtained by a numerical study, for different climate zones in the United States are shown in Figure 5.8 [Zhang et al., 2009]. The energy use of the local task-ambient conditioning (TAC) system itself is not taken into account. Therefore the energy savings, as found in this research, are less high compared to the graph of [Zhang et al., 2009].

In addition Van Oeffelen et al. (2010) simulated the energy potential for a typical winter situation in the Netherlands. They calculated an energy saving potential of about 25% for heating by decreasing the room temperature set point from 22°C to 20°C [Oeffelen et al., 2010], which is about 10% higher as found in this research. However, this research considered real occupancy profiles and energy use for individual local heating, which makes the results more realistic.

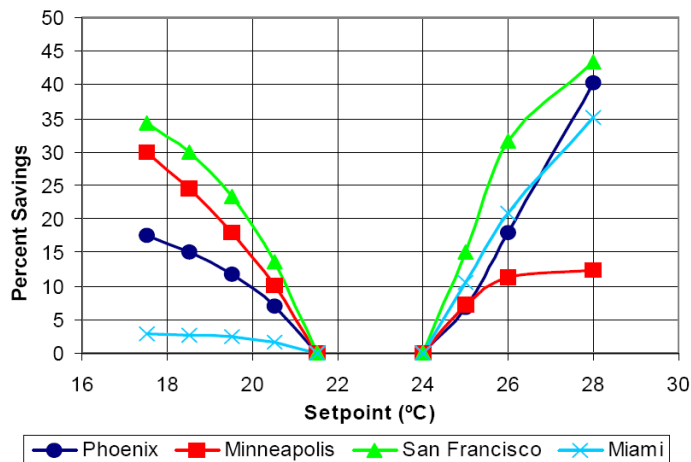


Figure 5.8 Percent energy savings for widened air temperature set points relative to conventional set point range for different climate zones in the United States. The energy for local heating/cooling is not included [Zhang et al., 2009].

⁵ Indoor temperature range between thermostat settings for heating and cooling.

6. Conclusion, discussion and future directions

6.1 Conclusions

The control paradigm for HVAC systems in the built environment has remained relatively unchanged: regulating one or more indoor environmental variables such as air temperature without including the thermal state of the individual occupant in the control loop. This graduation project presented a new control strategy, for personalized heating in mild cold office environments, which includes the human body as sensor in the thermal comfort control loop. The upper-extremity and facial skin temperature, both remotely sensed by IR thermography, were proposed as feedback control signals. This led to several research questions (§1.3) to which the following conclusions are drawn:

- I. A 'proof-of-principle' experiment demonstrated that the finger skin temperature is a critical performance indicator for the body thermal state in mild cold office conditions ($T_a=19\sim 20^\circ\text{C}$). The following observations were made:
 - a. By real-time infrared monitoring of the 4th finger temperature (and thus thermoregulatory response) it was possible to recognize the turning point from a neutral- to cool body thermal state, before any cool sensation was perceived. This turning point is induced by vasoconstriction, which reduces the skin blood flow in the fingers.
 - b. A decreasing finger temperature was clearly reflected by the local thermal sensation. In addition, a medium positive correlation between the 4th finger temperature and overall thermal sensation ($r_s=0.67$, $P<0.05$) was found.

- II. By using the 3rd finger skin temperature as control signal for local hand-heating, it was possible to feed-forward respond on user thermal preferences, while the basic room air temperature was lowered from 22 to 19.5°C. The local- and overall thermal sensation of the subjects were maintained at neutral or higher, and the subjects did not prefer any environmental control action. Specific requirements are:
 - a. The 3rd finger temperature should be controlled in a small bandwidth (29-31.5°C) near to the neutral zone of the occupant, so that skin temperature changes do not initialize any cool thermal sensation and local discomfort of the hands is avoided;
 - b. The mean average or filtered signal should be used to eliminate the oscillating effect of 1-2K in the 3rd finger temperature, which has been observed in the neutral zone.
 - c. A smooth control process (for example PI controlled) is required to avoid a local 'undershoot' in thermal sensation.
 - d. The small bandwidth should be adaptable to individual differences, as thermoregulatory set-points differ among individuals. Preference modeling that arises from the interactions with the user is therefore required.

- III. By applying the 'human-in-the-loop' control strategy energy savings are achieved in two ways, firstly because the basic-room air set-point can be lowered, and secondly the energy wasting behaviour by incorrect use of individual control is avoided. A case study for a state-of-the-art office building in Rotterdam, the Netherlands showed an energy saving potential of 17% for heating. This by decreasing the set point of the indoor air temperature from 22°C to 19.5°C, and taking into account local heating of 98W per occupant.

6.2 General discussion

The paragraph elaborates on the general discussion of the proposed human-in-the-loop control strategy. The measurement results were already discussed in detail in §3.5 and §4.5 for respectively the user-controlled and automatic controlled experiments.

- Experiments
This pilot study showed the possibilities for including the human body in the control loop of personalized heating systems by IR thermography. The obtained results can however only be applied to the two subjects (male and female) who participated in this research. It is already known that individual differences such as body fat percentage, and age, can have a significant influence on respectively the upper-extremity skin temperature and the degree of vasoconstriction [Savastano et al., 2009] [Schellen et al., 2010]. By modeling the preference that arises from the interactions with the user, this small bandwidth might be applicable to other individuals.
- Practical considerations
When applying the proposed control strategy in practice, the following factors should be taken into account: (1) the control signal can be highly influenced by occupant behaviour such as taking a hot drink or hand rubbing. In addition (2) the 3rd finger of the left hand was taken as control parameter, because the right hand (using the computer mouse) was less representative. For a left-handed person, this will be the opposite.
- Winter vs. summer situation
This research only considered a comfort control strategy for heating during a typical winter situation. For automatic control of local cooling in a summer situation the finger temperature alone may not be a good indicator of the whole-body thermal state, as the finger temperature than fluctuates in a very small range (35-37°C). From literature it was concluded that the finger-forehead temperature gradient may be a more sensitive indicator of hot sensations [Wang et al., 2007]. However the skin wettedness, for example measured at the forehead, seems to be a better predictor of warm discomfort [Toftum et al., 1998].
- Finger temperature vs. thermal sensation
This study showed that there is correlation between the 3rd finger temperature and overall thermal sensation ($r^2=0.48$, $P<0.05$). These results were compared to the findings of [Wang et al., 2007], see §4.5. From literature it was concluded that the most influential group having a dominant impact on overall sensation consist of the back, chest, and pelvis [Zhang et al., 2010a]. However the level of body cooling during the experiments was limited; so that these body parts were not perceived as cool. Only the extremities became cold and therefore local heating of the upper-extremities had a significant effect on overall sensation.
- 'Human in the loop' vs. 'human in control'
The human in the loop strategy is able to automatically respond to user thermal preferences by using the skin temperature. However this does not mean that the personal control devices are superfluous. An extensive field study by Huizenga et al. (2006) showed that the ability of personal control has a significant impact on occupant satisfaction. This asks for a system which combines (1) automatic control by using the skin temperature, and (2) an optional possibility for fine-tuning by a personal control device. This is expected to be the most effective way to achieve individual thermal comfort.

6.3 Future directions

6.3.1 Recommendations

General

This pilot study showed the possibilities for including the human body in the control loop of personalized heating systems by IR thermography. The obtained results can however only be applied to the two subjects (male and female) who participated in this research. The results are promising, so it is highly recommended to test the proposed strategy to more subjects, both in a climate chamber set-up and in a real office environment.

- Thereby, the individual differences should be assessed. The general hypothesis that women are more sensitive for cold extremities than man can be tested.
- In addition, it is advisable to investigate how the proposed control strategy is perceived when the room conditions are not controlled at a constant temperature, but when the indoor conditions are allowed to drift. Allowing the temperature to drift can result in 'higher energy savings' than the calculated 17%, and earlier research showed that this will not lead to dissatisfaction with the thermal environment [Schellen et al., 2010].

Local heating systems

- The development of fast-responding local heating systems, which can respond before the user is thermally dissatisfied, is of high importance. Therefore existing technologies should be improved or new technologies should be developed. The requirements are as follows:
 - a. A maximum response time of 5min is acceptable for automatic heating control purposes, before cool discomfort becomes a possibility. This is much faster than the response time (approximately 15min) of current HVAC systems as found in office buildings.
 - b. A limited contribution to warming of the indoor air (and room objects) is required, which require local heating technologies only targeting the specific body parts as with the radiant hand-heating system. The heating panels (Chapter 3) do not fulfill this requirement.
 - c. The system has to be easy implementable in office environments, so that the user does not experience a spatial disturbance as with the heating-lamps.
 - d. Additionally, the system has to be energy-efficient.

Infrared thermography

- Infrared thermography for control purposes shows high potential for further integration in office environments, because (1) the office worker is not disturbed and (2) it is an easy implementable technology (e.g. in laptops). However, image segmentation techniques should be developed for real-time extraction of the fingers from the thermal images, and smart data structures are needed which can deal with the large amount of image-data.
- Infrared thermography not only shows potential for monitoring body thermal state, but also for deriving the mean wall surface temperatures, the number of occupant, and the presence of other heat sources (e.g. printers, laptops) in an office room. It can, for example, be easily used to determine radiant asymmetry caused by glass surfaces. All this information can be used for real-time estimating of the energy balance and the comfort parameters in an office room.

Control parameter for local cooling

- Following the discussion in §6.2, it is recommended to investigate if the facial skin temperature or forehead skin wettedness may be good control indicators for local cooling. As with the heating systems, fast-responding cooling systems need to be developed, which can respond before warm discomfort becomes a possibility.

6.3.2 Future control of the thermal environment

In modern office buildings, the workplaces or open-plan offices, in which everyone has their own fixed workplace, are more often replaced by flexible workplaces. This means that the local heating system, located at a certain workplace, should be able to adapt to the individual preferences of the occupant. By using preference modeling that arises from the interactions with the user, it might be possible to learn from these preferences. In addition, smart sensor techniques are needed to localize the individual occupant in the office building. Recent work done by Maaijen (2012) showed that portable nodes (e.g. smart-phone) in combination with a wireless sensor network makes it possible to real-time localize the occupants [Maaijen, 2012]. Combining his work with this study resulted in a set-up for intelligent control of the thermal environment. See Figure 6.1.

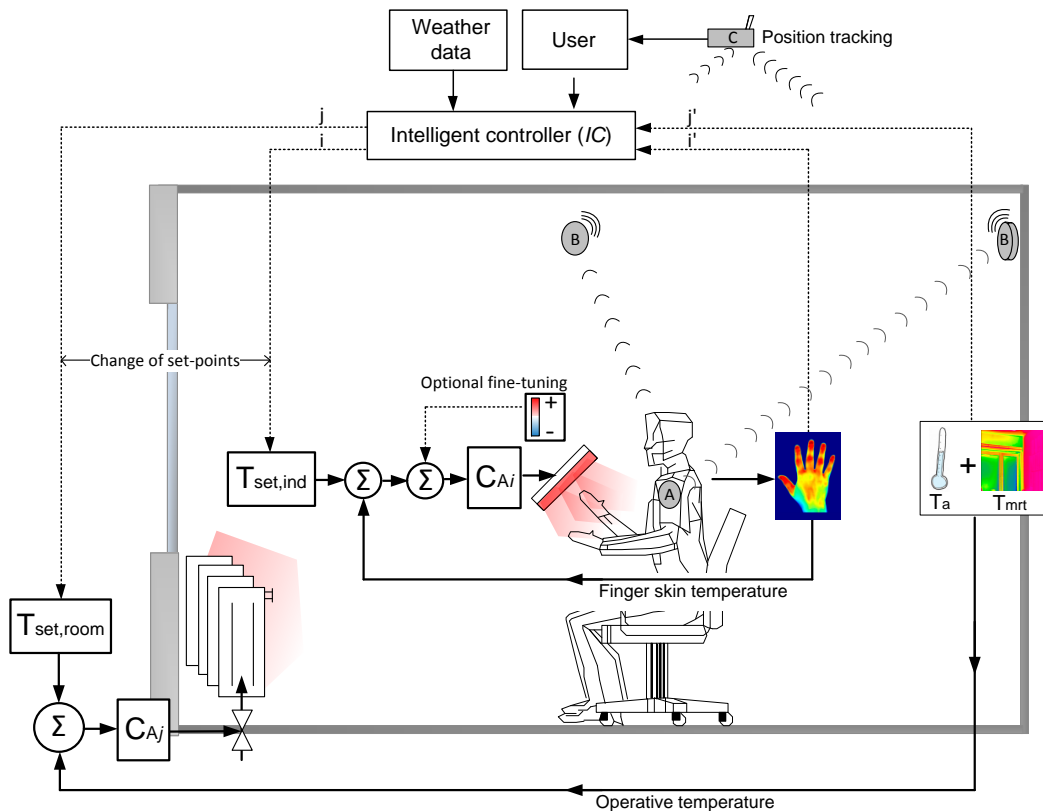


Figure 6.1. Set-up for intelligent control of the thermal environment. The local controller agents (CA) are guided by an intelligent coordinator (IC), which can be seen as a master agent [Dournis et al., 2009]. Based on human position tracking by A, B and C, the intelligent controller knows which occupant is present at the workplace. Individual set-points are provided to the different local control loops, and optional fine-tuning by a personal control device remains possible.

In this set-up the local controller agents (CA) are guided by an intelligent coordinator. Based on human position tracking by communication between the portable node (A) and the static room nodes (B), the localization network (C) knows which occupant is present at the specific workplace. The intelligent controller can load the individual preferences of this occupant, and providing the preferred set-points ($T_{set,ind}$) to the local control loop.

The basic room conditions will be controlled in an expanded dead-band using the operative temperature as feedback control signal. Thereby, the radiant temperature can be derived from IR monitoring. This control structure shows also high potential for inclusion of ventilation and lighting control loops. Future research should focus on the integration of the different local loops (heating, cooling, ventilation, and lighting) and intelligent communication between them.

List of symbols

Symbol	Description	Unit
A	Surface area	[m ²]
c _p	Specific heat	[J kg ⁻¹ K ⁻¹]
C	Convection heat loss	[W]
C _{fr}	Convection fraction	[-]
d	Thickness	[m]
E	Evaporative heat loss	[W]
h	Heat transfer coefficient	[W m ⁻² K ⁻¹]
H	Height	[m]
f _{cl}	Clothing surface area factor	[-]
F _{i-j}	View factor between surfaces i and j	[-]
g	Local acceleration due to gravity	[m s ⁻²]
Gr	Grashof number	[-]
J	Radiosity	[W m ⁻²]
K	Conductive heat loss	[W m ⁻²]
L	Characteristic length	[-]
LR	Lewis ratio	[K kPa ⁻¹]
M	Metabolic heat production	[W]
p	Partial vapor pressure	[Pa]
Pr	Prandtl number	[-]
q	Heat transfer	[W m ⁻²]
r _s	Spearman correlation coefficient	[-]
R	Radiation heat loss	[W m ⁻²]
Ra	Rayleigh number	[-]
RH	Relative humidity	[%]
S	Heat storage	[W m ⁻²]
sr	Steradian	[°]
t	Time	[s]
T	Temperature	[K]
\bar{T}_r	Mean radiant Temperature	[K]
V	Volume	[m ³]
v	Velocity	[m s ⁻¹]
x	Absolute humidity	[kg kg ⁻¹]
W	Work	[W]

Greek symbols	Description	Unit
α	Thermal diffusivity	[m ² s ⁻¹]
β	Volumetric expansion coefficient	[K ⁻¹]
ε	Emissivity	[-]
ρ	Mass density	[kg m ⁻³]
λ	Thermal conductivity	[W m ⁻¹ K ⁻¹]
ν	Kinematic viscosity	[m ² s ⁻¹]
σ	Stefan-Boltzmann constant	[W m ⁻² K ⁻⁴]

Subscripts

a	Ambient
air	Air
c	Convective
cl	Clothing
e	Evaporative
mean	Mean
occ	Occupancy
r	Radiative
res	Respiration
s	Surface
sat	Saturated
sk	Skin
sol	Solar

Abbreviations

ATC	Adaptive thermal comfort
AVA	Arteriovenous anastomoses
ASHRAE	American Society of Heating, Refrigerating and Air-Conditioning Engineers
C	Controller
CNS	Central nervous system
CPI	Critical performance indicator
FOV	Field of view
HVAC	Heating Ventilation Air Conditioning
LCT	Lower critical temperature
ICS	Individual controlled system
ICU	Individual control unit
IR	Infrared
NST	Non-shivering thermogenesis
PMV	Predicted Mean Vote
PPD	Predicted Percentage of Dissatisfied
RP	Radiant panel
TAC	Task-ambient conditioning
TNZ	Thermo-neutral zone
TS	Thermal sensation
UCT	Upper critical temperature
WB-TS	Whole-body thermal sensation

References

- Alvarez, G.E., Zhao, K., Kosiba, A.K., Johnson, J.M., 2006, Relative roles of local and reflex components in cutaneous vasoconstriction during skin cooling in humans. *Journal of Applied Physiology*, 100 (6): 2083-2088.
- Ardehali, M., Panah, N., and Smith, T., 2004, Proof of concept modeling of energy transfer mechanisms for radiant conditioning panels, *Energy Conversion and Management* 45: 2005-2017.
- Arens, E., Zhang, H., Huizenga, C., 2006a, Partial- and whole body thermal sensation and comfort – Part I: Uniform environmental conditions, *Journal of Thermal Biology*, 31: 53-59. - Part II: Non-uniform environmental conditions, *Journal of Thermal Biology*, 31: 60-66.
- Arens, E. and H. Zhang. 2006b, The Skin's Role in Human Thermoregulation and Comfort. *Thermal and Moisture Transport in Fibrous Materials*, eds N. Pan and P. Gibson, Woodhead Publishing Ltd, 560-602.
- ASHRAE Standard 55, 2004, Thermal Environmental Conditions for Human Occupancy.
- ASHRAE Fundamentals, 2009, Publisher: Amer Society of Heating | ISBN-10:1933742542.
- Bergersen, , 1993, A search of arteriovenous anastomoses in human skin using ultrasound Doppler. *Acta Physiologica Scandinavica* 147:195-201.
- De Carli, M., Olesen, B.J., Zarrella, A., Zecchin, R., 2007, People's clothing behaviour according to external weather and indoor environment; *Building and Environment* 42: 3965–3973.
- De Oliveira F., Moreau S., Gehin C, Dittmar A, 2007,: "Infrared Imaging Analysis for Thermal Comfort Assessment", 29th Annual International Conference of the IEEE Engineering in Medicine and Biology Society, France, Lyon, 23-26 august.
- De Oliveira F., Moreau S., 2009, Assessment of thermal environment sensations for various climatic conditions and fluctuating air flow, *EACWE 5*, Florence, Italy 19-23 July.
- Dournis A.I., Caraiscos C., 2009, Advanced control systems engineering for energy and comfort management in a building environment – a review, *Renewable and Sustainable Energy Reviews* 13: 1246-1261.
- Fanger, P.O., 1970, *Thermal Comfort: Analysis and Applications in Environmental Engineering*, McGraw-Hill, New-York.
- Filippini G.J.A., 2009, De mens centraal bij het ontwerp van het binnenklimaat: ontwerp en ontwikkeling van een duurzaam lokaal klimatiseringsstelsel, MSc thesis Technische Universiteit Eindhoven.
- Guyton A., Hall J., 2000, *Textbook of Medical Physiology*, London, New York, W.B. Saunders Company. Chapter 48: 607-609; Chapter 73: 889-901.
- Hardy, J.D., 1968, Heat Transfer, "Physiology of Heat Regulation and The Science of Clothing", edited by L.H. Newburg, Chapter 3: 78-109.
- He, Y., Zhang H.D., Wang, X., Shao, H.W., Mu L.Z., Zhang, J., 2010, Dynamic infrared imaging for analysis of fingertip temperature after cold water stimulation and neurothermal modeling study, *Computers in Biology and Medicine* 40: 650-656.

- Hensel, H., Kenshalo, D., 1969, Warm receptors in the nasal region of cats. *Journal of Physiology* 204 (1):99-112.
- Hensel, H., 1981, *Thermal Sensation and Thermal Receptors in Man*, courtesy of Charles C Thomas Publishers, Springfield, Illinois.
- Hoof van J., 2008, Forty years Fanger's model of thermal comfort: comfort for all?; *Indoor Air* 18:182-201.
- Houdas, Y., Ring, E.F.J., 1982, *Human Body Temperature, its Measurement and regulation*, New York, London, Plenum Press
- House J., Tipton, M., 2002, Using skin temperature gradients or skin heat flux measurements to determine thresholds of vasoconstriction and vasodilation. *European Journal of Applied Physiology* 88: 141-145.
- Huizenga, C., Zhang, H., Arens, E., Wang, D., 2004, Skin and core temperature response to partial- and whole body heating and cooling. *Journal of Thermal Biology* 29: 449-558.
- Huizinga, C., Abbaszadeh, S., Zagreus, L., and Arens, E., 2006, Air quality and thermal comfort in office buildings: results of a large indoor environmental quality survey. *Proceedings Healthy Buildings 3*: 393-397.
- ICNIRP, 2006, International commission on non-ionizing radiation protection, statement on far infrared radiation exposure, *Health Physics* 91 (6):630-645.
- ISO 9886, 2004, *Ergonomics – Evaluation of thermal strain by physiological measurements*: International Standards Organization
- Janna, W.S. & Janna W., 2000, *Engineering Heat Transfer*, Second Edition. Taylor & Francis Ltd.
- Karjalainen, S., Koistinen, O., 2007, User problems with individual temperature control in offices, *Building and Environment* 42:2880-2887.
- Kataoka, T. and Kumada, T., 2008, A Matrix Infrared Sensor System for Improving Thermal Comfort in Passenger Compartments, SAE Technical Paper 2008-01-0835 (2008), Presented at world congress Detroit, Michigan, April 14-17.
- Kellogg, D.L., Jr., 2006, In vivo mechanisms of cutaneous vasodilation and vasoconstriction in humans during thermoregulatory challenges. *Journal of Applied Physiology* 100(5): 1709-1718.
- Kenshalo, D.R., 1970, Psychophysical studies of temperature sensitivity. In J.W. Neff (Ed.), *Contributions to sensory physiology*. New York Academic Press,.
- Kingma, B. 2011, *Human Thermoregulation: A synergy between physiology and mathematical modeling* PhD thesis. <http://arno.unimaas.nl/show.cgi?fid=24017>
- Korukçu, M.O., Kilic, M., 2012, Tracking hand and facial skin temperatures in an automobile by using IR-thermography during heating period, *Gazi University Journal of Science* , 25 (1):207-217.
- Maaijen, H.N., 2012, *Occupant-oriented energy control by taking the human in the control loop of building systems*, MSc thesis Technische Universiteit Eindhoven.
- NEN-EN-ISO 7726, 1998, *Ergonomie van de thermische omgeving - Instrumenten voor het meten van fysische grootheden*

- NEN-EN-ISO 7730, 2005, Ergonomics of the thermal environment – Analytical determination and interpretation of thermal comfort using calculation of the PMV and PPD indices and local thermal comfort criteria.
- Oeffelen van E., Zundert van K., Jacobs P., 2010, Persoonlijke Verwarming in Kantoorgebouwen, TVVL magazine.
- Opstelten J., Bakker J.E., Kester J., Borsboom W., Elkhuizen B. van, 2007, Bringing an energy neutral built environment in the Netherlands under control, ECN-M-07-062, Petten.
- Parsons, K.C., 2003, Human thermal environments. The effects of hot, moderate, and cold environments on human health, comfort and performance; Taylor & Francis, London.
- Pedersen, C., Fisher, D., Lindstrom, P., 1997, Impact of Surface Characteristics on Radiant Panel Output, University of Illinois at Urbana-Champaign, Department of Mechanical and Industrial Engineering, ASHRAE 876 TRP.
- Rubinstein E., Sessler D., 1990, Skin-surface temperature gradients correlate with fingertip blood flow in humans, *Anesthesiology* 73:541–545.
- Sabatini E., Revel G.M., Arnesano, M., 2010, A new thermography based system for real-time energy balance in the built environment, *Proceedings Clima 2010*, May 10-12, Antalya.
- Savastano, D.M., Gorbach, A.M., 2009, Adiposity and human regional body temperature, *The American Journal of clinical nutrition* 90:1124 - 1131.
- Schellen L., Marken Lichtenbelt van, W., Loomans, M., Toftum, J., Wit de M., 2010, Differences between young adults and elderly in thermal comfort, productivity, and thermal physiology in response to a moderate temperature drift and a steady-state condition. *Indoor Air* 20: 273-283.
- Stolwijk, J., 1971, A mathematical model of physiological temperature regulation in man. NASA Report CR-1855, Washington D.C.
- Taniguchi, U., Aoki, H., Fujikake, K., Tanaka, H., Kitada, M., 1992, (*Toyota Central R&D Lab*), Study on car air conditioning system controlled by car occupants' skin temperatures. Part 1. Research on a method of quantitative evaluation of car occupants' thermal sensations by skin temperatures. Design and performance of climate control systems. SAE special publications, Vol. 916, paper 920169, 1992. Part 2. Development of a new air-conditioning system. Design and performance of climate control systems. SAE special publications, Vol. 916, paper 920170.
- Toftum, J., Jorgensen, A., Fanger P.O., 1998, Upper limits for indoor air humidity to avoid uncomfortably humid skin, *Energy and Buildings* 28: 1-13.
- Van Marken Lichtenbelt W., Daanen H., Wouters L., Fronczek R., Raymann R., Severens N. and Van Someren E., 2006, Evaluation of wireless determination of skin temperature using ibuttons *Physiology and Behaviour* 88:489-497.
- Vastamäki, R., Sinkkonen, I., Leinonen, C., 2005, A behavioural model of temperature controller usage and energy saving, *Personal and Ubiquitous Computing* 9:250–259.
- Wang, D., Zhang, H., Arens, E., Huizenga, C., 2007, Observations of upper-extremity skin temperature and corresponding overall-body thermal sensations and comfort, *Building and Environment* 42: 3933-3943.

- Watanabe, S., Melikov, A., Knudsen, G., 2010, Design of an individually controlled system for an optimal thermal microenvironment, *Building and Environment* 45: 549-558.
- Wissler, E.H., 2008, A quantitative assessment of skin blood flow in human. *Eur J Appl Physiol.*, 104 (2):145-157.
- Zeiler, W., Houten, M.A van, Besselink, H., Filippini, G.J.A. & Veerman, J. ,2010, Microklimatisering. *TVVL Magazine*, 39 (7/8): 4-7.
- Zhang, H., Huizenga, C., Arens, E., Yu, T., 2001, Considering individual physiological differences in a human thermal model, *Journal of thermal biology* 21:401-408.
- Zhang, H., 2003, Human Thermal Sensation and Comfort in Transient and Non Uniform Thermal Environments, PhD Thesis;
<http://repositories.cdlib.org/cedr/cbe/ieq/Zhang2003Thesis/>
- Zhang, H., Hoyt, T., Lee, K.H., Arens, E., Webster, T., 2009, Energy savings from extended air temperature set points and reductions in room air mixing, *International conference on Environmental Ergonomics*, August 2-7.
- Zhang, H., Arens, E., Huizenga, C., Han, T., 2010a, Thermal sensation and comfort models for non-uniform and transient environments: Part I: Local sensation of individual body parts, *Building and Environment* 45:80-388. - Part II: Local comfort of individual body parts, *Building and Environment* 45:389-398. - Part III: Whole body sensation and comfort, *Building and Environment* 45:399-410.
- Zhang, H., Arens, E., Kim, D., Buchberger, E., Bauman, F., Huizenga, C., 2010b, Comfort, perceived air quality, and work performance in low-power task-ambient conditioning system, *Building and Environment* 45:29-39.
- Zhou, M., 1998, Human-centered control of the indoor thermal environment, PhD Thesis;
<http://dspace.mit.edu/bitstream/handle/1721.1/10072/39241895.pdf>
- Zotterman, Y., 1953, Special senses: thermal receptors. *Annual Review Physiology* 15:357-72.

Software

- LabVIEW SP1, National Instruments (2010).
- MATLAB/Simulink R2010b, version 7.11.0.584, 32-bit (win 32). MathWorks, Inc.
- Mircosoft Office 2010 Professional
- RADIANCE, open source: <http://radsite.lbl.gov/radiance/>
- ThermaCAM Researcher Pro 2.8 SR-1, FLIR systems AB (2004).

Appendices

Appendix A: Background on thermal radiation

Thermal radiation is the emission of electromagnetic waves from all matter that has a temperature higher than absolute zero (0K). It represents a conversion of thermal energy into electromagnetic energy.

If a radiation-emitting object meets the physical characteristics of a black body in thermodynamic equilibrium, the radiation is called blackbody radiation. Planck's law describes the spectrum of blackbody radiation, which depends only on the object's temperature. Wien's displacement law determines the most likely frequency of the emitted radiation, and the Stefan–Boltzmann law gives the radiant intensity.

A.1 Planck's law

Planck (1858–1947) was able to describe the spectral distribution of the radiation from a blackbody by means of the following formula:

$$W_{\lambda b} = \frac{(2\pi hc^3)}{\lambda^5 \left(e^{\frac{hc}{\lambda kT}} - 1 \right)} (10^{-6}) \left[\frac{W}{m^2 \mu m} \right] \quad (\text{A.1})$$

When plotting Planck's formula for various temperature levels, a family of curves can be shown. The spectral emittance is zero at $\lambda = 0$, then increases rapidly to a maximum at a wavelength λ_{max} and after passing it approaches zero again at very long wavelengths. The higher the temperature, the shorter the wavelength at which maximum occurs. See Figure A.2.

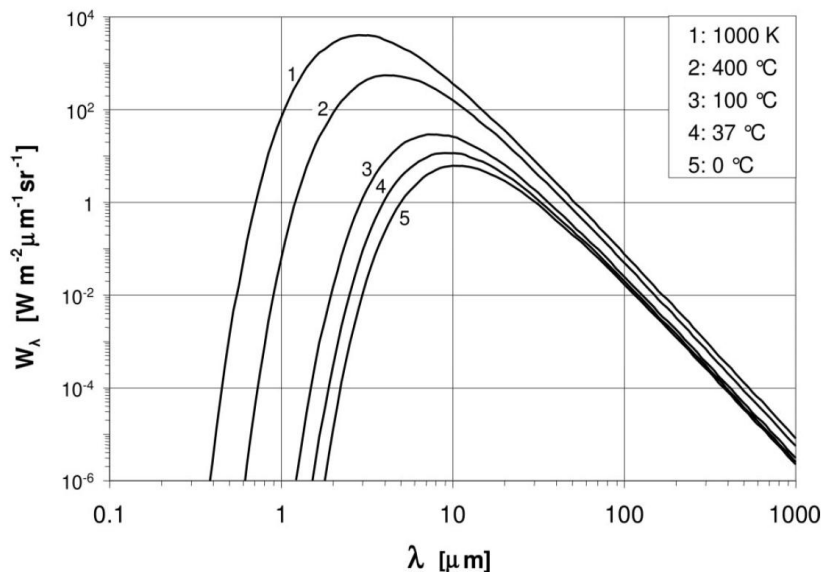


Figure A.2 Dependence of spectral radiant exitance W_{λ} (Planck's Law) for theoretically perfect blackbodies with temperatures between 273 K (0°C) and 1000 K as a function of wavelength λ (μm) [ICNIRP, 2006].

A.2 Wien's displacement law

Wien's formula can be obtained by differentiating Planck's formula with respect to λ . It expresses mathematically the common observation that colors vary from red to orange or yellow as the temperature of the thermal radiator increases.

$$\lambda_{max} = \frac{(2898)}{T} [\mu m] \quad (\text{A.2})$$

The sun (approximately 6000K) emits yellow light, peaking at about $0.5 \mu\text{m}$ in the middle of the visible light spectrum. At room temperature (300K) the peak of radiant emittance lies at $9.7 \mu\text{m}$ in the far infrared spectrum.

A.3 Stefan Boltzmann's law

By integrating Planck's formula from $\lambda=0$ to $\lambda=\infty$, the total radiant emittance of a blackbody can be obtained ($\sigma = 5.67 * 10^{-5} [\frac{\text{W}}{\text{m}^2\text{K}^4}]$).

$$W_b = \sigma T^4 \left[\frac{\text{W}}{\text{m}^2} \right] \quad (\text{A.3})$$

The total emissive power of a blackbody is proportional to the fourth power of its absolute temperature. For non-ideal or non-black bodies, the emitted energy or radiation is a function of the fourth power of the temperature of a material multiplied by the Stefan-Boltzmann constant and the material emittance (ϵ).

$$W = \epsilon \sigma T^4 \left[\frac{\text{W}}{\text{m}^2} \right] \quad (\text{A.4})$$

Figure A.3 provides the specific emissive power for a perfect blackbody in comparison with data for bodies of different total emissivity's at temperatures from 300K to about 3000K.

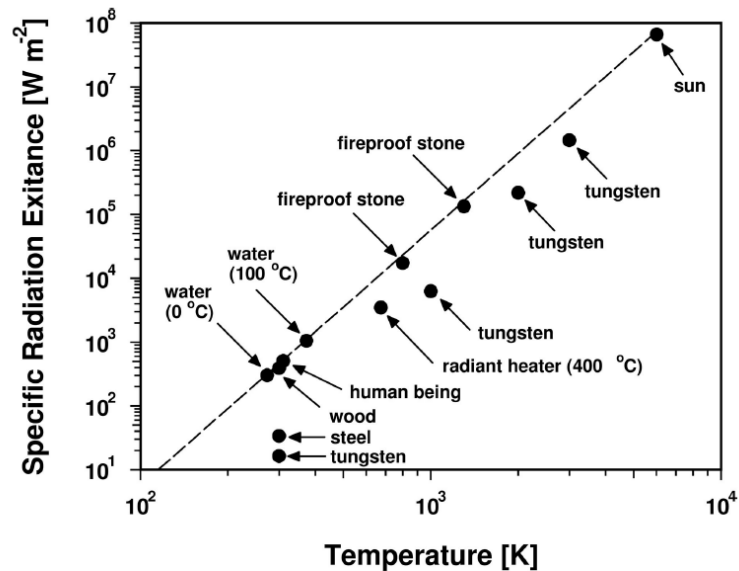


Figure A.3 Specific radiation exitance (W m^{-2}) as a function of absolute temperature (K) for a perfect black body (dashed line) and for bodies of different temperature and total emissivity's [ICNIRP, 2006].

A.4 Viewfactors

Emission of radiant energy from a surface element travels in all directions. The rate at which energy is transferred must include the quantity of energy transferred, the geometry, the solid angle, and the wavelength. These factors are combined into what is called the intensity (I) of radiation [Janna et al., 2000].

The radiation heat transfer rate depends on the orientation of the surfaces relative to each other as well their radiation properties and temperatures. To account for the effects of the orientation for radiation heat transfer the view factor can be introduced. The view factor is purely geometric quantity and is independent on surface characteristics or temperatures.

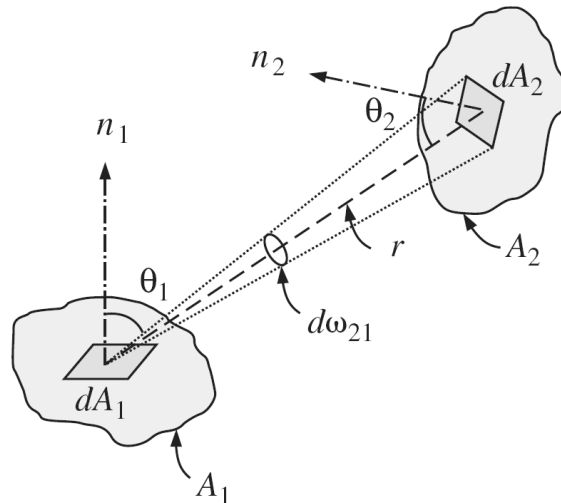


Figure A.4 Determination of the view factors between surface A_1 and A_2 .

The total rate at which radiation leaves the entire surface A_1 can be calculated by:

$$\dot{Q}_{A_1} = J_1 A_1 = \pi I_1 A_1 \text{ [W]}, \text{ where the radiosivity } J_1 = \varepsilon(\sigma T_1^4) + (1 - \varepsilon)G_i \left[\frac{\text{W}}{\text{m}^2} \right]$$

The portion of the radiation leaving A_1 , which strikes A_2 can be calculated by:

$$\dot{Q}_{A_1 \rightarrow A_2} = \int_{A_1} \int_{A_2} \frac{I_1 \cos \theta_1 \cos \theta_2}{r^2} dA_1 dA_2 \quad (\text{A.5})$$

Dividing this by the radiation leaving A_1 gives the fraction of radiation leaving A_1 that strikes A_2 , which is the view factor:

$$F_{A_1 \rightarrow A_2} = F_{1 \rightarrow 2} = \frac{\dot{Q}_{A_1 \rightarrow A_2}}{\dot{Q}_{A_1}} = \frac{1}{A_1} \int_{A_1} \int_{A_2} \frac{\cos \theta_1 \cos \theta_2}{\pi r^2} dA_1 dA_2 \quad (\text{A.6})$$

In this thesis formula A.7 will be applied to calculate the net radiant energy exchange between surface 1 and 2.

$$\dot{Q}_{1 \rightarrow 2} = \sigma \varepsilon (T_1^4 - T_2^4) A_1 F_{1 \rightarrow 2} \quad (\text{A.7})$$

Appendix B: Measurement set-up and equipment

The main environmental parameters that influence thermal comfort are air temperature, air velocity, and mean radiant temperature (surface temperatures). Also relative humidity plays a role in comfort prediction models. The measurement of these local comfort measurement positions are indicated in Figure B.1, B.2 and B.3, where I indicates the measurement position of the local comfort measurements near the occupant (see B.2), and J indicates the room comfort measurement.

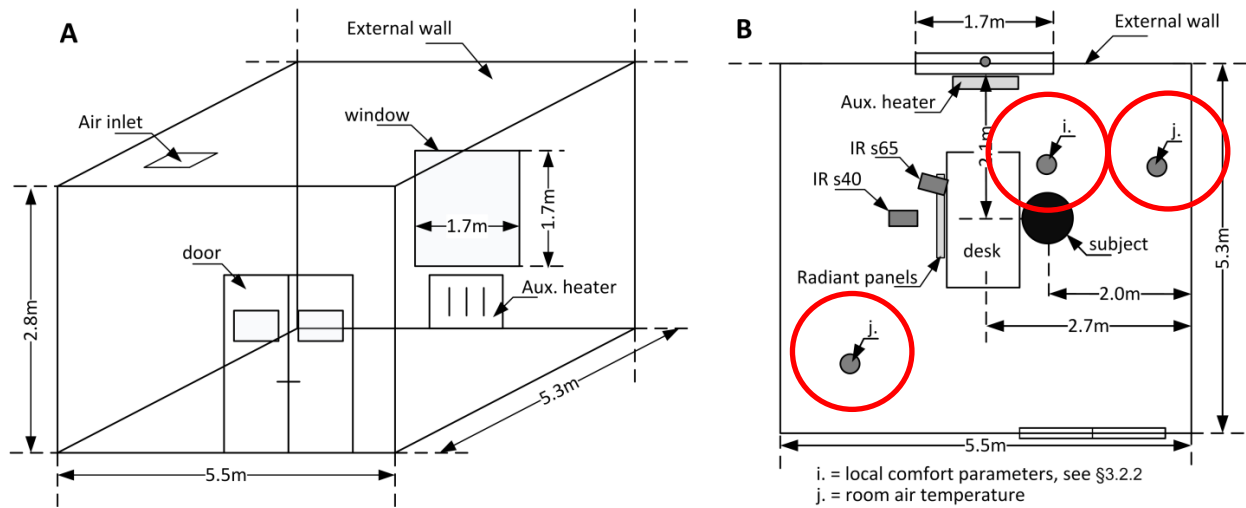


Figure B.1 Test room in the Building Physics and Services (BPS) laboratory of the TU/e. (A) 3D sketch of the test-room, and (B) position of the desk and occupant relative to the internal- and external walls. The positions of the IR cameras and the comfort measurements at local (i) and room (j) level are also indicated. No scale was applied.

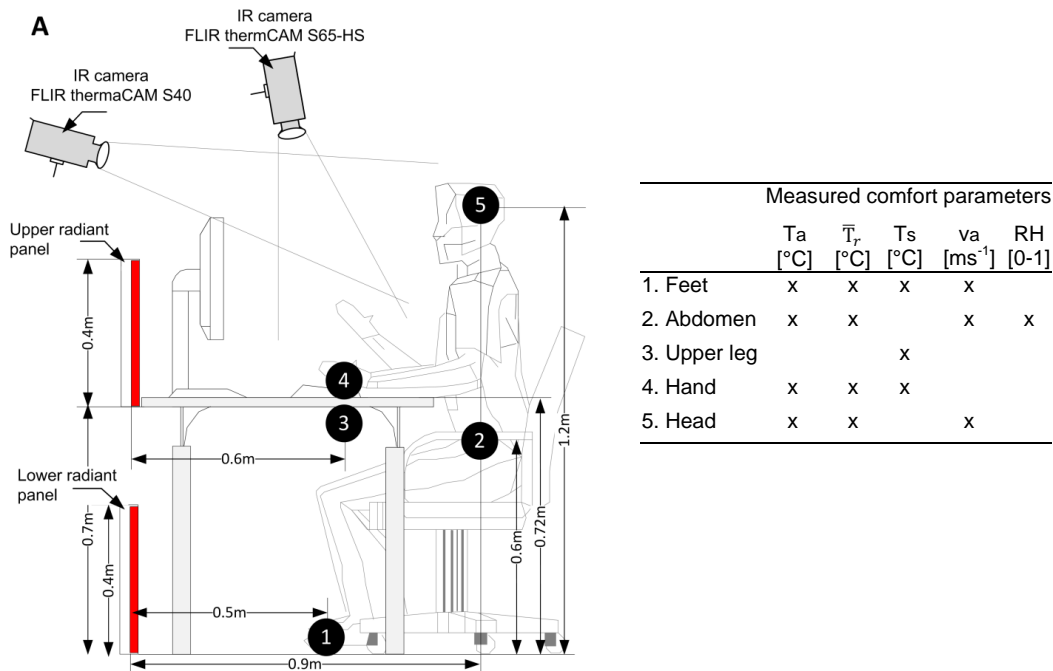


Figure B.2 Experimental workplace set-up. (A) Two infrared cameras for physiological measurements of the upper-extremities and face. The black circles indicate the measurement positions of the local comfort parameters, where 1=feet, 2=abdomen, 3=upper leg, 4=hands and 5=head level. (B) Digital control panel, as programmed in LABview, for regulating the surface temperature of the radiant panels.

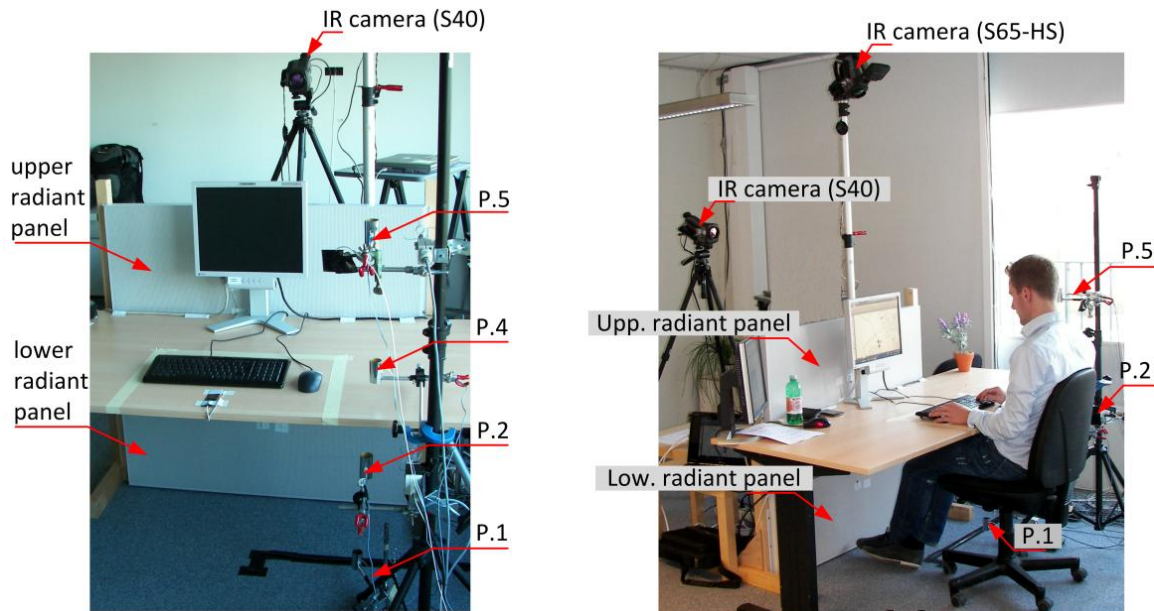


Figure B.3 Two impressions of the experimental workplace set-up. The positions of the radiant panels, IR cameras and the measurement positions (P.1-P.5) of the local comfort parameters are indicated.

B.1 Physical measurements

The physical measurements concern the measurements of the local comfort parameters such as air temperature, radiant temperature, air velocity and relative humidity. These variables were measured according to ISO 7726.

Air temperature

The air temperature was measured using a NTC thermistor (Type DC95, Sensor data BV), suitable over the range of -80 to 150°C, with a time constant of 10s. Based on the resistance of a Negative Temperature Coefficient (NTC) Thermistor the air temperature in the room can be determined. The electrical resistance of a NTC Thermistor decreases when the environmental air temperature increases. The resistance was calculated by:

- $R = (10000 \cdot V) / (5 - V)$;
- $T = -22.39 \cdot \ln(R) + 195.41$.

Mean radiant temperature

The mean radiant temperature (\bar{T}_r) is one of the most important environmental parameters governing human energy balance. The mean radiant temperature was measured by a black-globe thermometer. The globe temperature depends on both convection and radiation transfer, however by effectively increasing the size of the thermometer bulb the convection transfer coefficient is reduced and the effect of radiation is proportionally increased. Because of local convective air currents the globe temperature T_g typically lies between the air temperature T_a and the true mean radiant temperature \bar{T}_r . According to [ASHRAE, 2004] the mean radiant temperature can be calculated from the globe temperature by:

$$\bar{T}_r = (T_g + 273.15)^4 + \frac{(1.1 \cdot 10^8 v_a^{0.6})}{(\epsilon D^{0.4})} (T_g - T_a) - 273.15$$

Where: T_g = globe temperature ($^{\circ}\text{C}$), v_a = air velocity (ms^{-1}), T_a = air temperature ($^{\circ}\text{C}$), D = globe diameter (mm) and ε = emissivity (0.95 for a black globe).

During the experiments the surface temperatures of the walls, windows, floor and ceiling were measured for determination of the mean radiant temperature. The specific view factors (i.e. angle factor F) are calculated according to [ASHRAE, 2004].

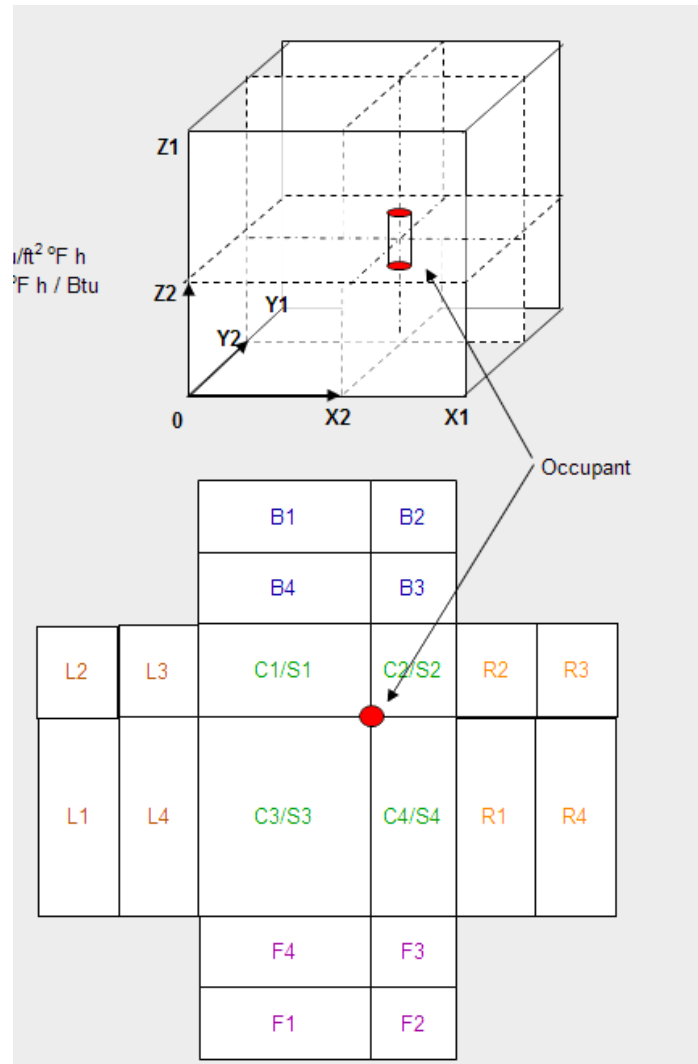


Figure B.3 Calculation of the mean radiant temperature according to ASHRAE (2004).

The mean radiant temperature can be calculated from the surface temperatures of the walls, which were measured at 2 locations of each wall by U-thermistors using the following viewfactors:

$f1=2.86/100$; $f2=5.00/100$; $f3=1.30/100$; $f4=2.14/100$;
 $b1=5.99/100$; $b2=4.29/100$; $b3=4.29/100$; $b4=5.99/100$;
 $l1=2.86/100$; $l2=1.72/100$; $l3=1.30/100$; $l4=2.14/100$;
 $r1=5.99/100$; $r2=4.29/100$; $r3=4.29/100$; $r4=5.99/100$;
 $s1=5.61/100$; $s2=4.62/100$; $s3=5.59/100$; $s4=6.99/100$;
 $c1=4.31/100$; $c2=3.04/100$; $c3=4.58/100$; $c4=4.83/100$;

Air velocity

The air velocities were measured by spherical air velocity sensors (type HT 400, sensor-electronic BV). The HT-400 system can be used for air temperature and low velocity measurements in rooms, as well as for measurements of flow inside air supply devices. The specific properties are as follows:

- type of velocity sensor:	omnidirectional, spherical, diameter 2mm
- measurement velocity range:	0.05 to 5 m/s
- repeatability:	range of 0,05 to 1m/s $\pm 0.02\text{m/s} \pm 1\%$ of readings range of 1 to 5m/s $\pm 3\%$ of readings
- accuracy of automatic temperature compensation:	better than $\pm 0.2\%/K$
- upper frequency f_{up}^{*1} :	min. 1Hz typ. 1.5Hz
- temperature range:	-10 to +50 °C
- accuracy of temperature measurement:	0.3 °C
- outputs of transducer unit:	analogue current 0-20mA or voltage 0-1V, 2V, 5V

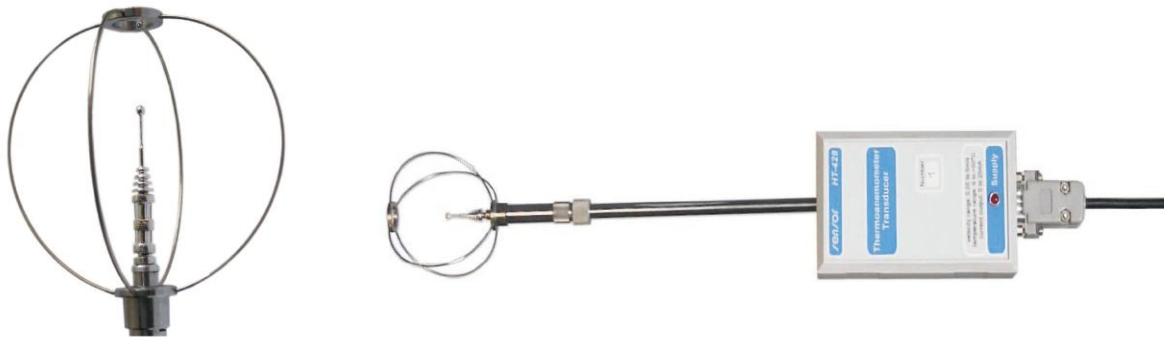


Figure B.4 Specific properties of the air velocity sensors.

The specific air velocity was calculated from the measured sensor voltage and the equation coefficients which were obtained by calibration in the $0.05\text{-}5\text{ms}^{-1}$ range.

$$\text{if } U_0 < U_v[V] < U_c (= 1.511), \text{ then } V_{\text{nom}} = (A_0 + A_1 U_v^2 + A_2 U_v^4 + A_3 U_v^6 + A_4 U_v^8)^2 \frac{\text{m}}{\text{s}}$$

The equation coefficients for the applied air velocity sensors (ID837 to ID840) are shown in below

ID0837		ID0838		ID0839		ID0840	
A0=	-1.06E-01	A0=	-1.05E-01	A0=	-0.087857	A0=	-1.02E-01
A1=	-4.16E-01	A1=	-3.71E-01	A1=	-0.45601	A1=	-3.84E-01
A2=	2.55E-01	A2=	1.88E-01	A2=	0.28568	A2=	1.98E-01
A3=	-1.03E-01	A3=	-6.85E-02	A3=	-0.11919	A3=	-7.39E-02
A4=	1.56E-02	A4=	9.56E-03	A4=	0.018786	A4=	1.07E-02

Relative humidity

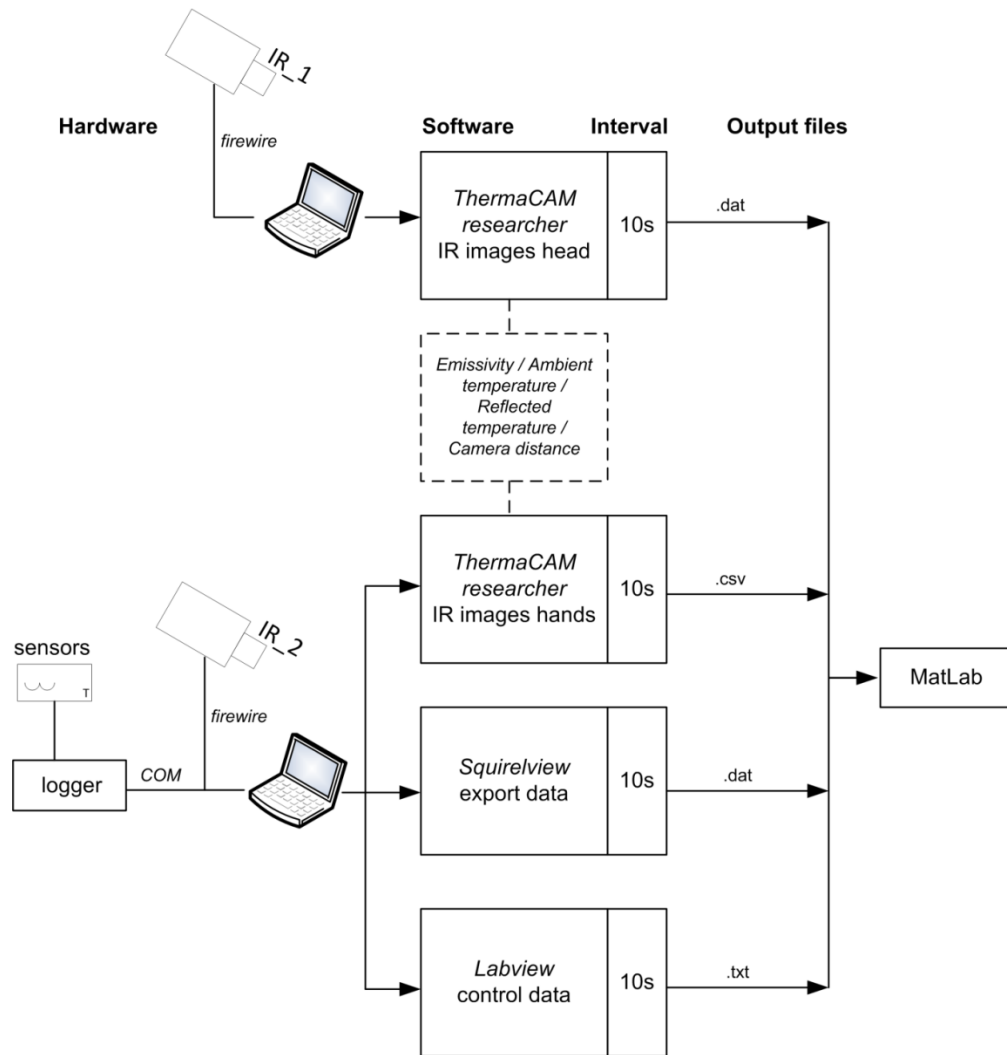
The relative humidity was measured by a humidity transmitter (type Rense sersie 732) with a standard accuracy of 2%RH. The working range lies in between 5 and 95% relative humidity. The output range lies in between 0-1V.

B.2 Infrared measurements and data-transfer

The skin temperature measurements were performed using two infrared cameras, the FLIR ThermaCAM S65-HS and the FLIR thermaCAM S40. The specific properties of both cameras are shown below:

THERMAL	
Field of view/min focus distance	24° x 18° / 0.3 m
Spatial resolution (IFOV)	1.3 mrad
Image Frequency	60 Hz
Thermal sensitivity @ 50/60Hz	0.08 °C at 30 °C
Electronic zoom function	2.4, interpolating
Focus	Automatic or manual
Digital image enhancement	Normal and enhanced
Detector type	Focal plane array (FPA) uncooled microbolometer
Spectral range	320 x 240 pixels 7.5 to 13 µm

Both the cameras were connected a laptop and the software tool ThermaCAM researcher was used as data processing tool. From this tool, the data was send to MATlab for image analysis.



B.3 Sensor positions

The measurement positions are indicated in Figure B.4.

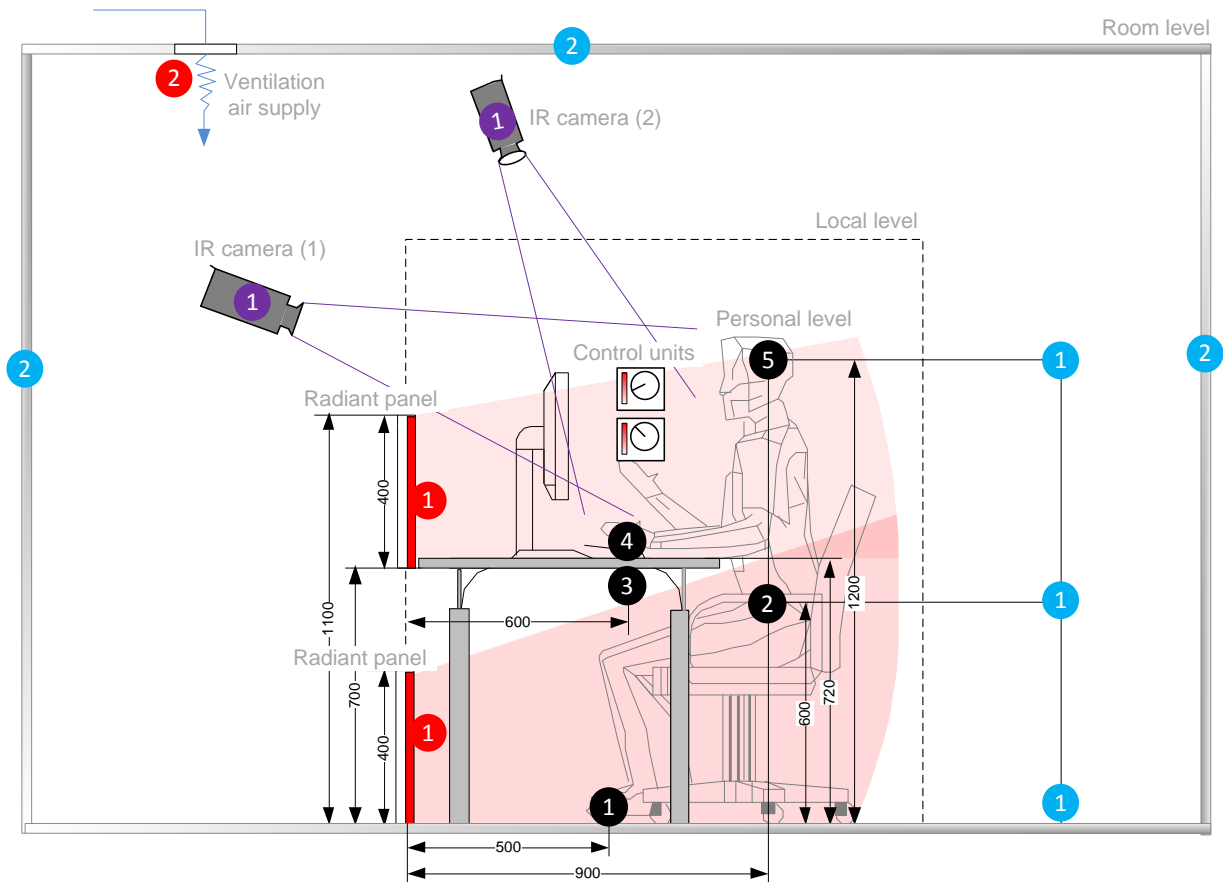




Figure B.4 Sensors positions at the experimental workplace

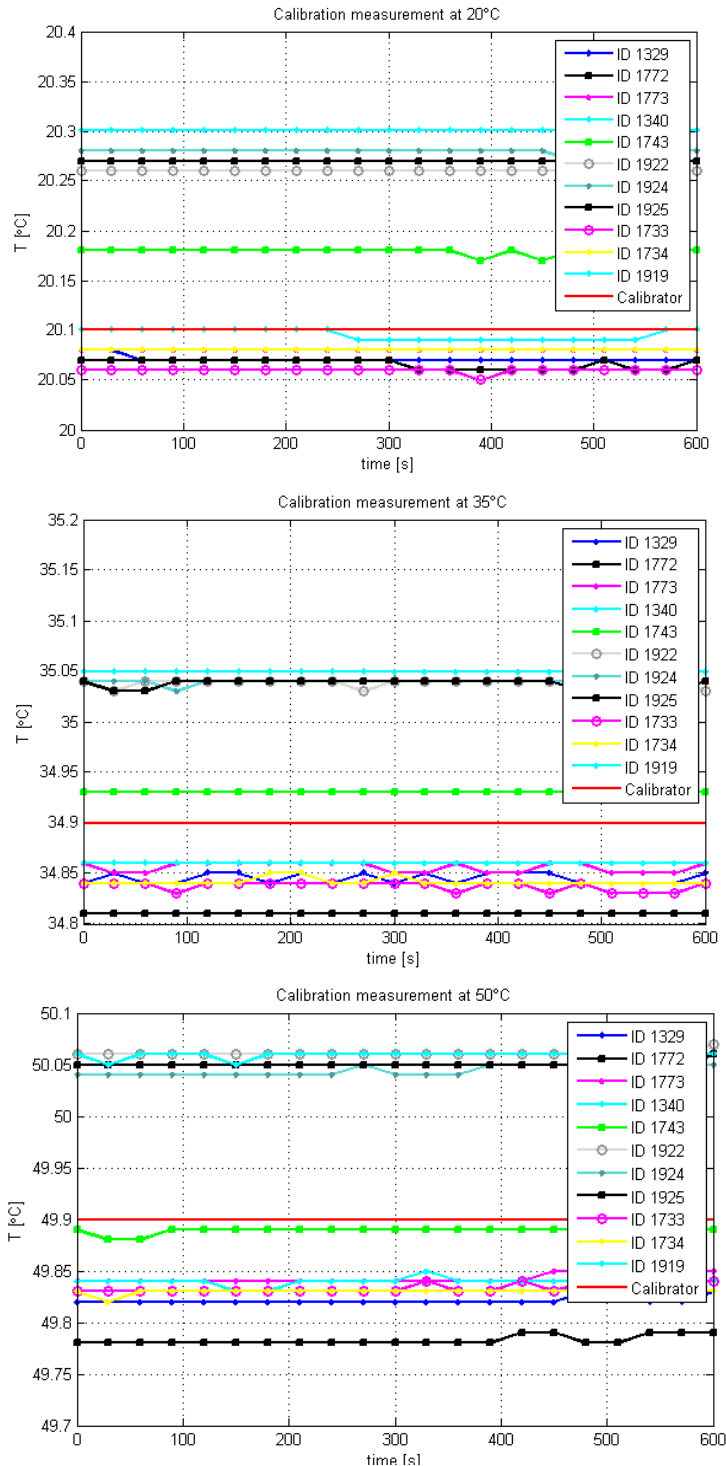
local level					
Position	Quantity	Unit	Description	Sensor ID / logger channel	Def
(1) Feet level	T_a	[°C]	Air temperature	ID 1925 / ch. B4	✓
	\bar{T}_r	[°C]	Mean radiant temperature	ID 1243 / ch. D2	
	v_a	[m/s]	Air velocity	ID 0840 / ch. H4	✓
	T_{s_floor}	[°C]	Surface temperature floor	ID 2235 / ch. C4	✓
(2) Abdomen level	T_a	[°C]	Air temperature	ID 1924 / ch. B3	✓
	\bar{T}_r	[°C]	Mean radiant temperature	ID 1754 / ch. D3	
	v_a	[m/s]	Air velocity	ID0839 / ch. H3	✓
	RH	[%]	Local relative humidity	ID0334 / ch. K2	✓
(3) Upper leg level	T_{s_desk}	[°C]	Surface temperature desk	ID 1340 / ch. A4	✓

			(under)		
(4) Hand level	T_a	[°C]	Air temperature	ID 1922 / ch. B2	√
	\bar{T}_r	[°C]	Mean radiant temperature	ID 2143 / ch. D4	
	T_{s_desk}	[°C]	Surface temperature desk (above)	ID 1773 / ch. A3	√
	T_{s_ref}	[°C]	Reference point IR measurement, surface temperature copper plate.	ID 2065 / ch. J2	√
(5) Head level	T_a	[°C]	Air temperature	ID 1743 / ch. B1	√
	\bar{T}_r	[°C]	Mean radiant temperature	ID 1214 / ch. D1	
	v_a	[m/s]	Air velocity	ID 0838 / ch. H2	√
	T_{s_ref}	[°C]	Reference point IR measurement, surface temperature copper plate.	ID2056 / ch. J1	√

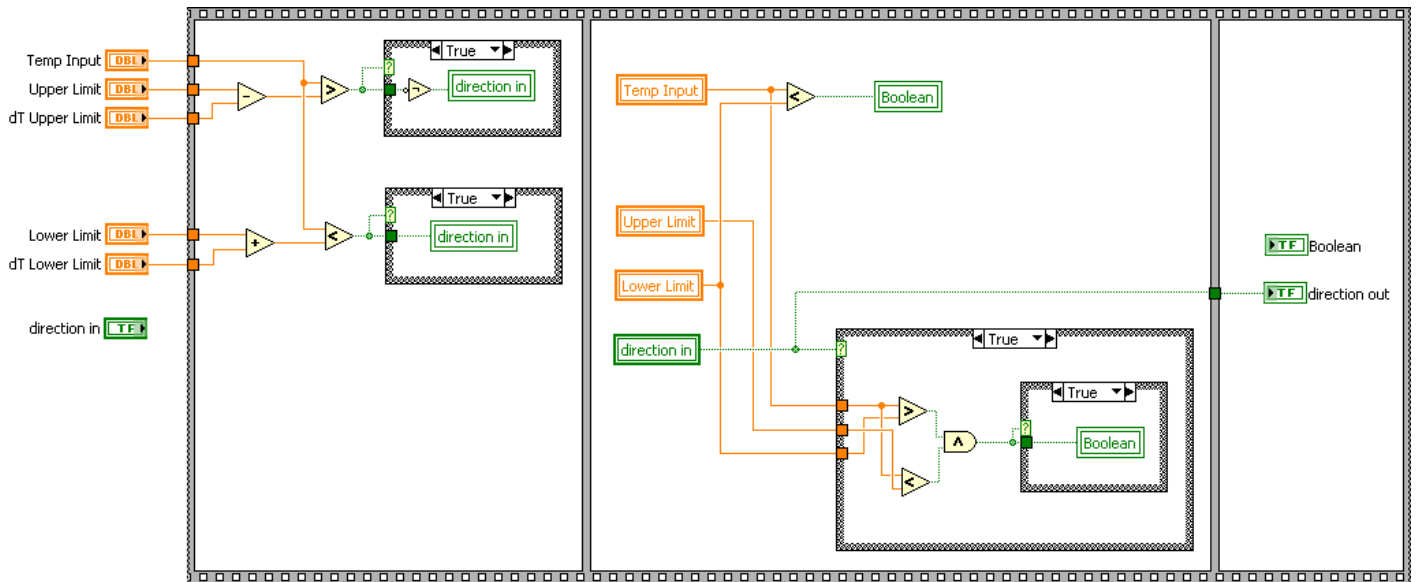
 room level					
<i>Position</i>	<i>Quantity</i>	<i>Unit</i>	<i>Description</i>	<i>Additional</i>	<i>Def</i>
(1) Room conditions	$T_{a_0.1}$	[°C]	Air temperature (0.1m)	ID 1733 / ch. C1	√
	$T_{a_0.6}$	[°C]	Air temperature (0.6m)	ID 1734 / ch. C2	√
	$T_{a_1.2}$	[°C]	Air temperature (1.2m)	ID 1919 / ch. C3	√
	RH	[%]	Overall relative humidity	ID 0335 / ch. K3	√
(2) Radiant temperatures	T_{s_walls}	[°C]	Surface temperature(s) wall(s)	ID 2055, 2057, 2058, 2059 / ch. G1 to G4.	√
	T_{s_window}	[°C]	Surface temperature window		√
 system level					
<i>Position</i>	<i>Quantity</i>	<i>Unit</i>	<i>Description</i>	<i>Additional</i>	<i>Def</i>
(1) Radiant panels	$T_{s_RP (up)}$	[°C]	Surface temperature upper panel	ID 1772 / ch. A2	√
	$T_{s_RP (low)}$	[°C]	Surface temperature lower panel	ID 1329 / ch. A1	√
	$E_{RP (up)}$	[kWh]	Energy usage upper panel		√
	$E_{RP (low)}$	[kWh]	Energy usage lower panel		√

B.4 Calibration measurements

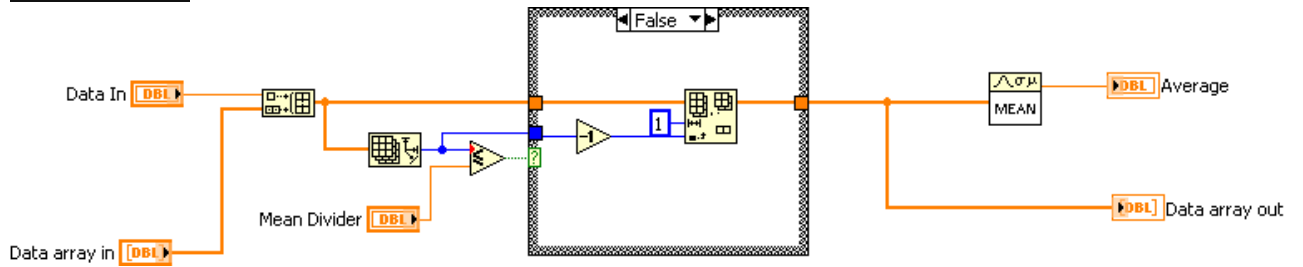
When using temperature sensors, actually a voltage is measured which can be related to what the operating temperature of the sensor must be. To determine the deviation of the individual sensor measurements to the so-called standard, a calibration measurement is required. The calibration measurements done during my research consist of temperature measurements in the range of 20 to 50°C. Below the results are presented for a steady state situation after a 2 hour test.



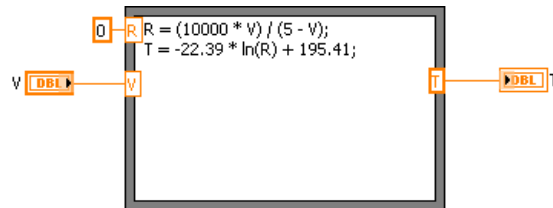
tempcontrol2.vi



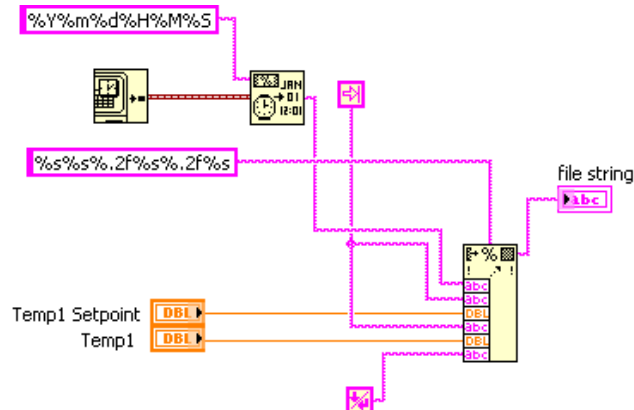
meanfilodata.vi



convert.vi



createfilestring.vi



Appendix D: Modeling radiant panel heat transfer

In this research two vertical mounted radiant panels ($A=0.44\text{m}^2$) were applied. The heat transfer through and from the panel surface is modeled using a simple thermal resistance network (Matlab Files). The simple resistance network includes the resistance between the heating element and panel surface, the convective and radiant resistance from the panel surface towards the environment, and the heat loss from the back of the panel.

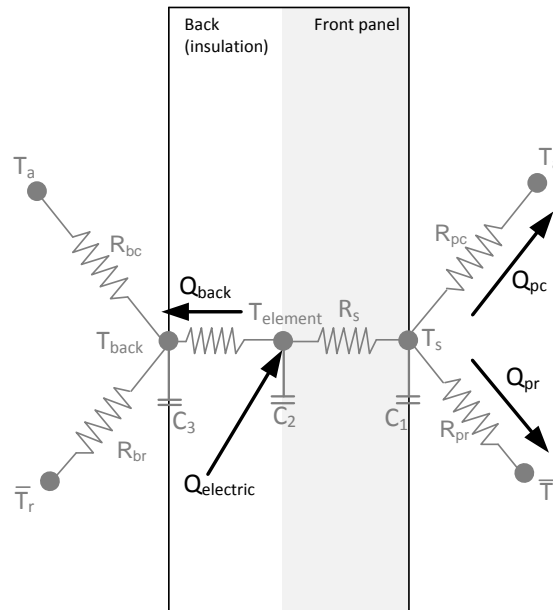


Figure D.1 Thermal resistance network for the electric radiant panel.

For a control volume around the radiant panel the energy balance is shown in equation D.1:

$C_1 \frac{dT_s}{dt} = \frac{T_e - T_s}{R_s} - Q_{pc} - Q_{pr} \text{ [W]}$	(D.1)
$C_2 \frac{dT_s}{dt} = Q_e - \frac{T_e - T_s}{R_s} - \frac{T_e - T_{back}}{R_{back}} \text{ [W]}$	
$C_3 \frac{dT_s}{dt} = \frac{T_e - T_{back}}{R_{back}} - Q_{bc} - Q_{br} \text{ [W]}$	

D.1 Convection

The heat transfer by convection is calculated according to equation D.2:

$\dot{Q}_{pc} = h_{pc} A_p (T_s - T_a) \text{ [W]}$	(C.2)
---	-------

The convective heat transfer coefficient was derived from equations D.3 to D.6.

$h_{pc} = \frac{(Nu \lambda)}{L} \left[\frac{W}{m^2 K} \right]$	(D.3)
--	-------

$\text{Nu} = \left(\frac{h_{pc} L}{\lambda} \right) = \text{CRa}_L^n = 1.53\text{Ra}_L^{0.14}$	(D.4)
---	-------

$\text{Ra}_L = \text{Gr}_L \text{Pr} = \frac{g\beta(T_s - T_a)L^3}{\nu\alpha}$	(D.5)
--	-------

$\text{Pr} = \frac{\nu}{\alpha}, \quad \alpha = \frac{\lambda}{\rho c_p} \left[\frac{\text{m}^2}{\text{s}} \right]$	(D.6)
--	-------

An empirical relation for convective heat transfer from vertical mounted radiant panels is given by Pedersen [Pedersen, 1997], see B.7.

$\dot{Q}_{pc} = A_p \left(\frac{1.87 (T_s - T_a)^{1.32}}{H^{0.05}} \right) [\text{W}]$	(D.7)
---	-------

D.2 Radiation

Using Stefan-Boltzmann's law, the radiant heat transfer between the radiant panel and the surroundings can be determined by:

$\dot{Q}_{pr} = A_p \varepsilon \sigma (T_s^4 - \bar{T}_r^4) [\text{W}]$	(D.8)
--	-------

The mean radiant temperature depends on the temperatures of the surrounding surfaces and the orientation relative to each other. The net heat transfer for different radiant panel temperatures towards the thermal environment ($\bar{T}_r = 20^\circ\text{C}$) are plotted in Figure D.2.

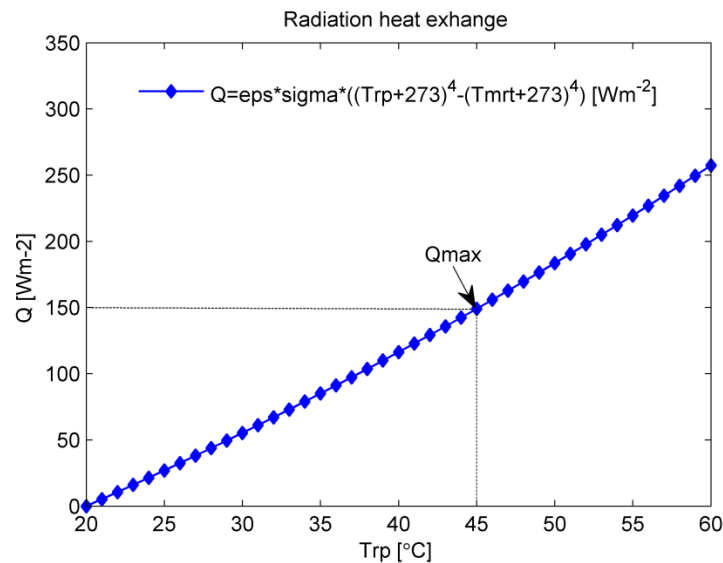


Figure D.2 Radiation heat transfer from the radiant panel (in Wm^{-2}) towards the thermal environment ($\bar{T}_r = 20^\circ\text{C}$) for different panel temperatures.

Using the equations as presented in section D.1 and D.2 the radiant panel response time was simulated for a step-change of 25K and a total electrical input power of 350W. The results and specific material properties are shown in Figure D.3.

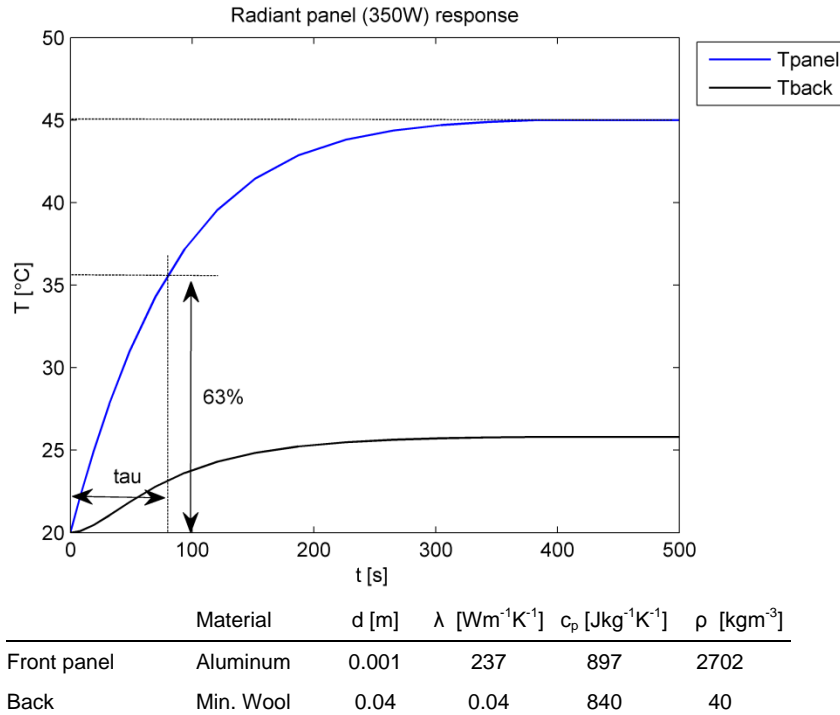
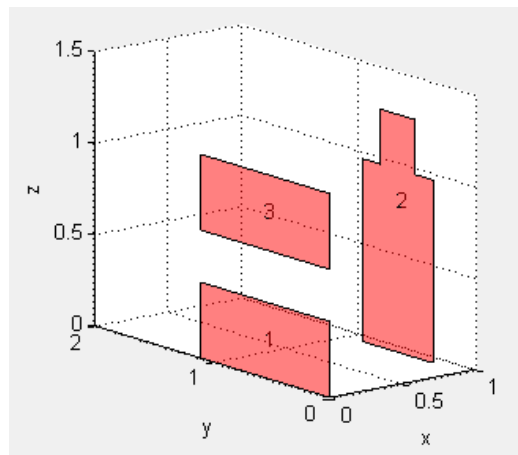


Figure D.3 Simulation of radiant panel surface temperature response after a step-change of 25K.

D.3 Viewfactor calculation

A simplified view factor calculation has been made to gain insight in the heat exchange between the radiant panels and the human body. See Figure B.4. The calculated view factors are:

$$F_{1-2} = 0.147, F_{2-1} = 0.097, F_{3-2} = 0.151, F_{2-3} = 0.099.$$



Nr.	Description	A [m ²]	ϵ [-]
1	Radiant panel	0.44	0.92
2	Human body (front)	0.69	-
3	Radiant panel	0.44	0.92

Figure D.4 Representation of the radiant panels (1 and 3) and the human body (2) as polygons. View factor calculation model is developed by N. Lauzier and D. Rousse, University of Laval (2003).
<http://www.mathworks.com/matlabcentral/fileexchange/5683-view-factors-with-gui>

D.4 Simplified approach

Using equation A.7 and the view factor obtained in section B.3, the net radiant heat transfer between the radiant panels and the human body can be calculated. Temperature T_1 is defined as the radiant panel temperature and T_2 as the surface temperature of the body exposed to the environment:

$$\dot{Q}_{1 \rightarrow 2} = \sigma \varepsilon (T_1^4 - T_2^4) A_1 F_{1 \rightarrow 2} = (5.67e^{-8})(0.92)((45 + 273)^4 - (26 + 273)^4)(0.44)(0.15) = 8W$$

Clothing temperature

The clothing temperature can be calculated from the skin temperature, the operative temperature and total sensible heat loss. For the calculation a radiation heat transfer coefficient of $4.7 \text{ Wm}^{-2}\text{K}^{-1}$ and a convective heat transfer coefficient of $4.0 \text{ Wm}^{-2}\text{K}^{-1}$ were applied. These values are typical for indoor thermal environments.

$$T_{cl} = T_{sk} - \frac{(R_{cl} * \dot{Q}_{R+C})}{A_{cl}} \approx 26^\circ\text{C}$$

Where,

$$T_{sk} = 32^\circ\text{C}, R_{cl} = 0.127 \frac{\text{m}^2\text{K}}{\text{W}} (0.82 \text{ clo}), A_{cl} = 1.8\text{m}^2, \text{ and } \dot{Q}_{R+C} = \frac{A_{cl} (T_{sk} - T_o)}{R_{cl} + \frac{1}{(h_R + h_C)}} = 89W$$

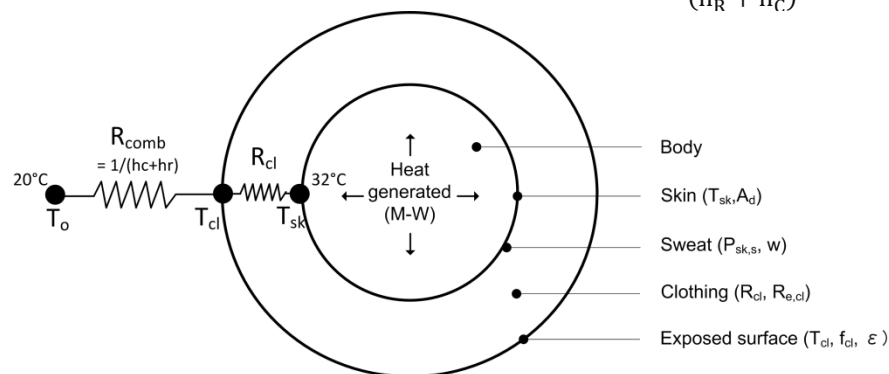


Figure D.5 Thermal interaction between the human body and its environment described by a cylindrical model [ASHRAE, 2004].

D.5 Advanced approach

To show the direct infrared radiation distribution from the heat sources towards the environment a simple view factor calculation is made and a sophisticated lighting simulation was made by Radiance (Figure D.6). Radiance is a radiometric measure that describes the amount of radiation such as light or radiant heat that passed through or is emitted by a particular area, and falls within a given solid angle in a specified direction.

The radiant panels are modeled as light sources in the far infrared spectrum by using identical RGB intensities. It should be noticed that this way only direct radiation from the light source towards the environment can be modeled. Radiation and reflection from surrounding surfaces are treated as zero. For diffuse emitters, the emitted radiation intensity is the same in all directions with the result that this can be written as:

$E = \pi I_1 \left[\frac{W}{\text{sr m}^2} \right]$	(C.9)
--	-------

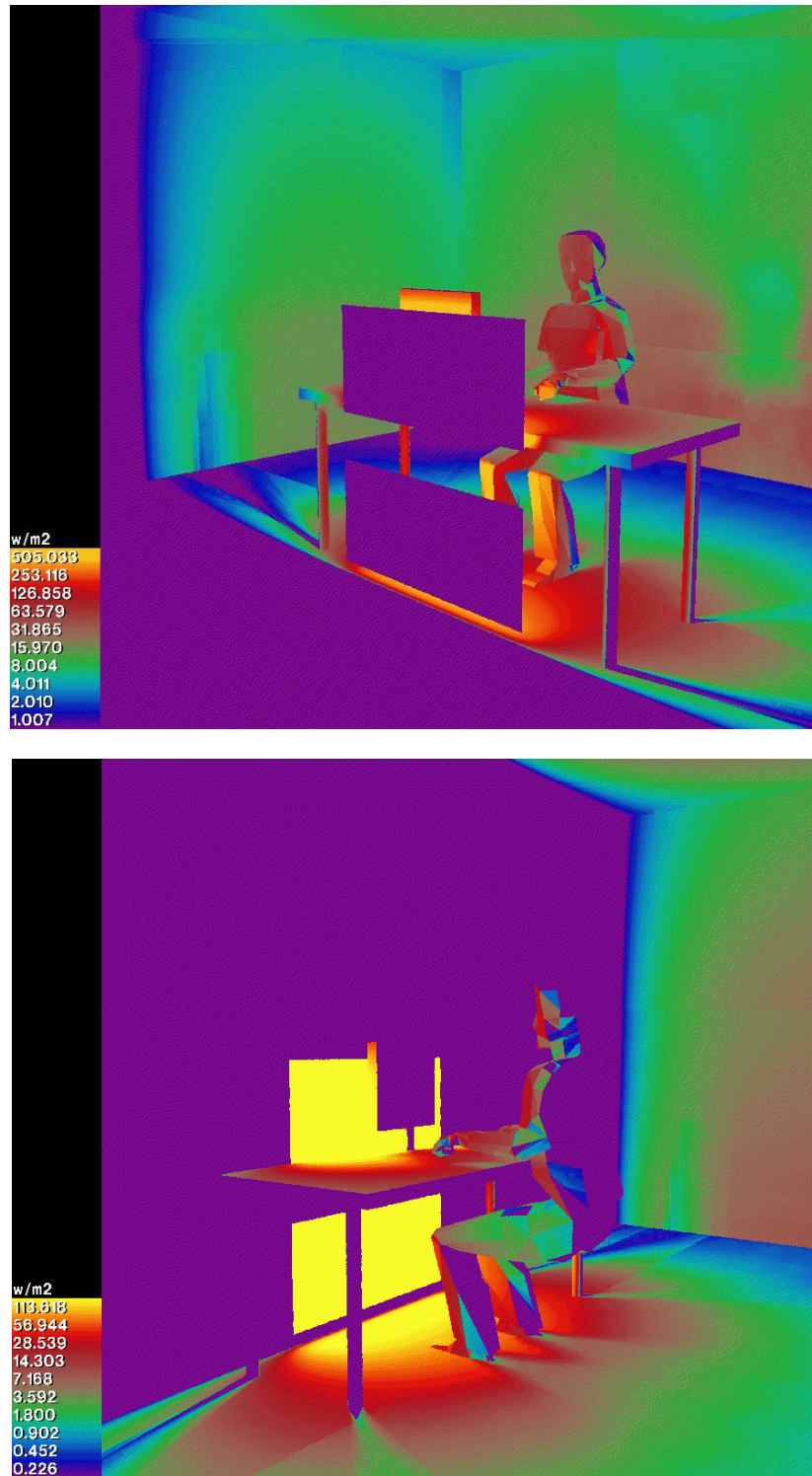


Figure D.6 Results of the radiance simulation to determine the heat transfer between the panels and the human body.

Appendix E: Radiant panels

E.1 Radiant panels

- 7 electrical heating elements;
- Aluminum coated front panel ($\epsilon=0.92$)



E.2 Influence on the thermal environment

- A correction should be made on the temperature levels of the radiant panels.

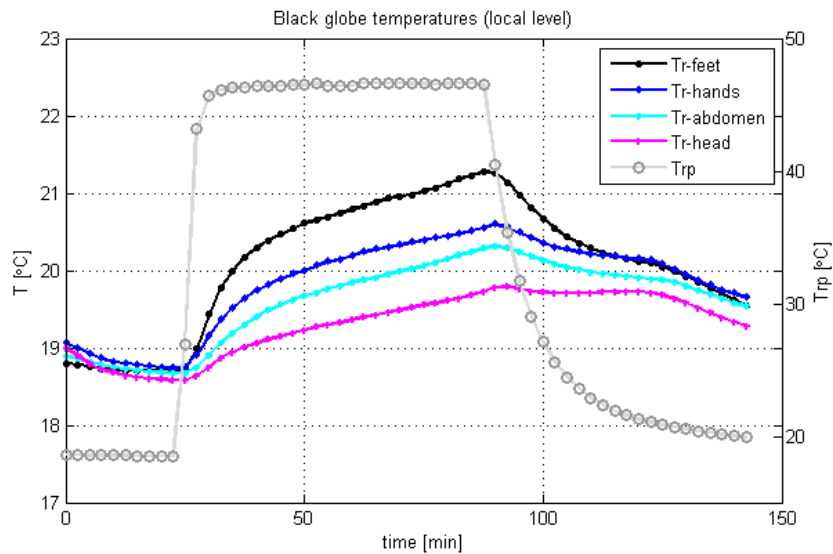


Figure E.1 Local black globe temperatures vs. radiant panel surface temperature (dd. 13-10-2011).

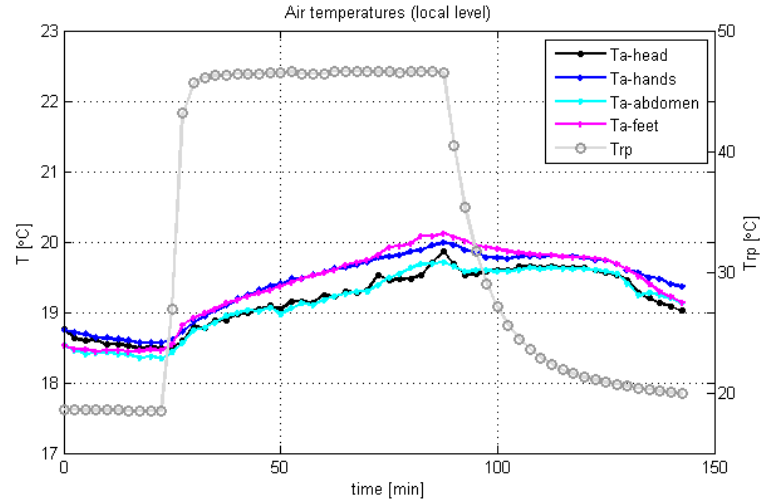


Figure E.2 Local air temperatures vs. radiant panel surface temperature (dd. 13-10-2011).

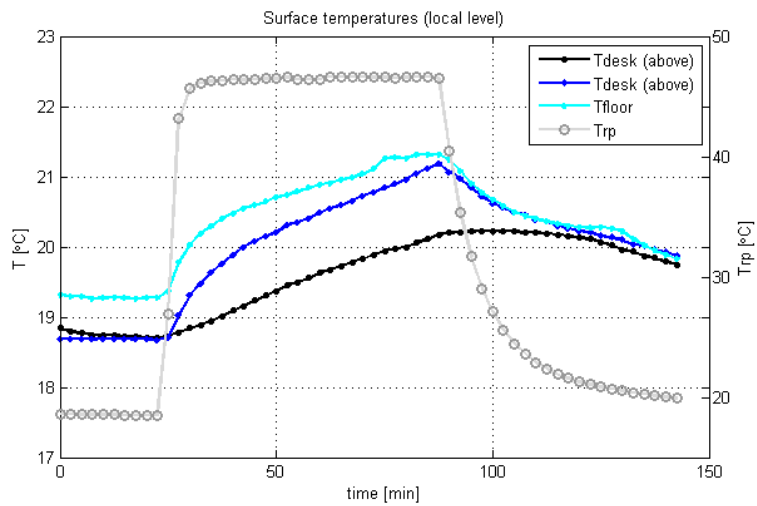


Figure E.3 Local surface temperatures vs. radiant panel surface temperature (dd. 13-10-2011).

Temperature distribution over panel surface

The emissivity of the radiation panel is 0.92; the ambient temperature was about 19°C; the reflective temperature is about 20°C; a relative humidity of 50%; and the distance of the camera to the radiant panel was 4.0m.

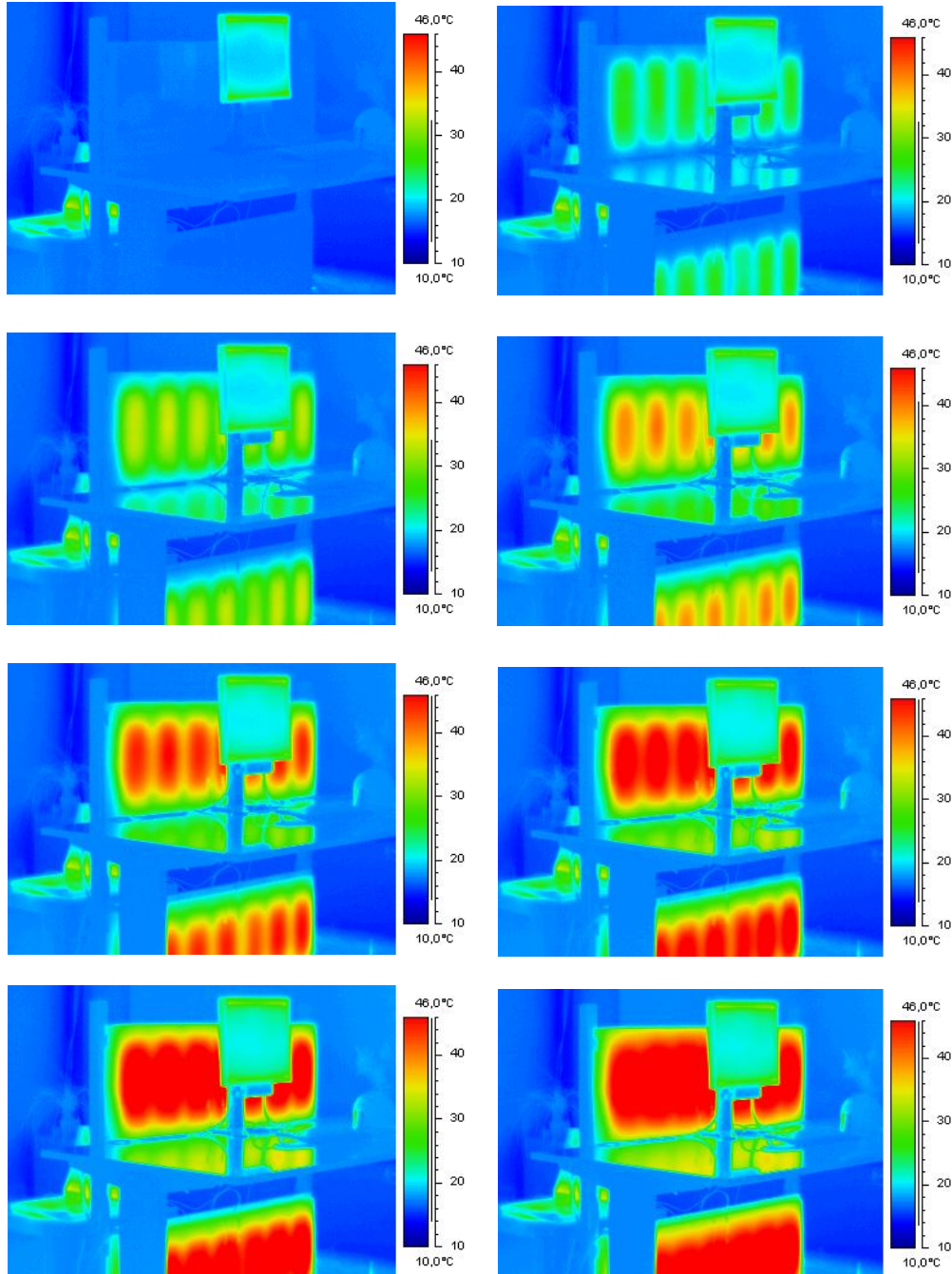
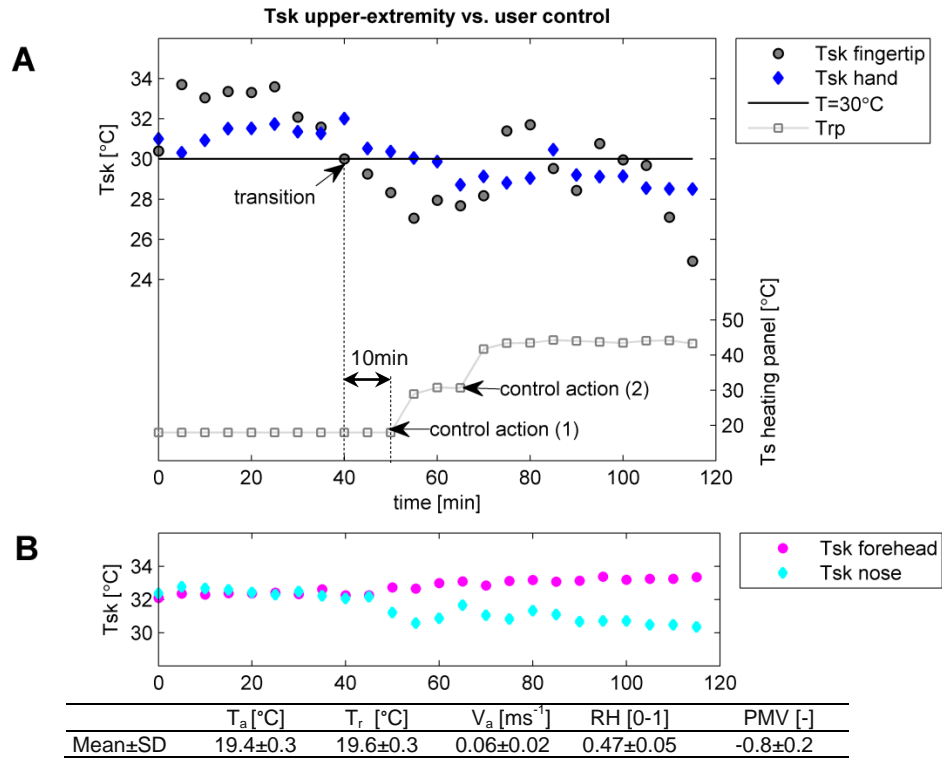


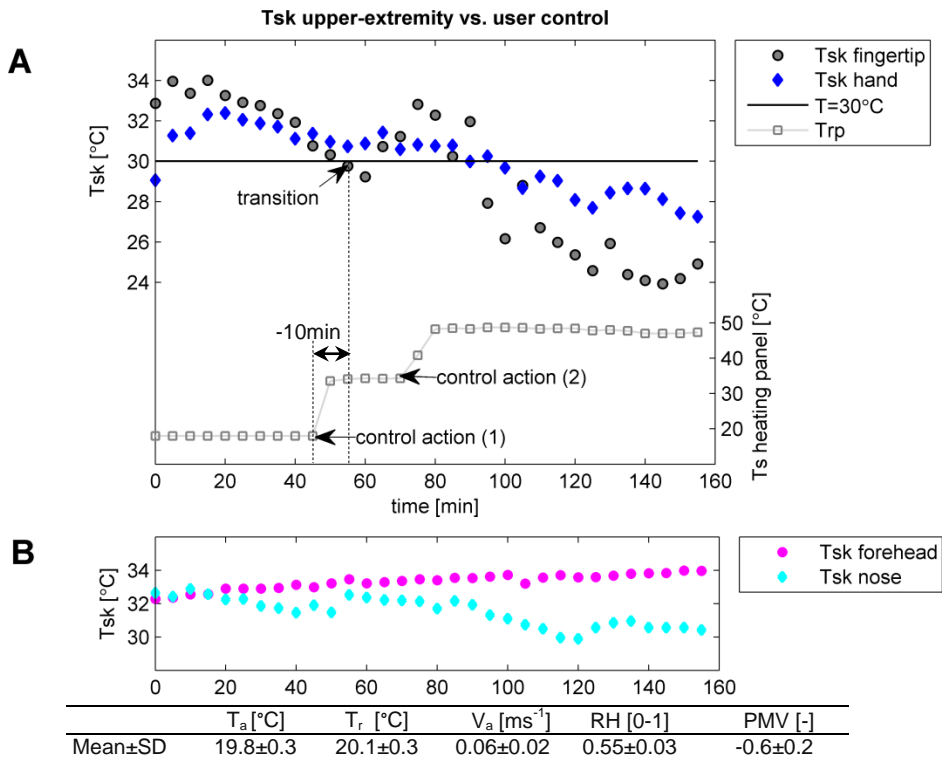
Figure E.4 Infrared measurements of temperature distribution over panel surface during heating curve (dd. 13-10-2011).

Appendix F: User-controlled experiments

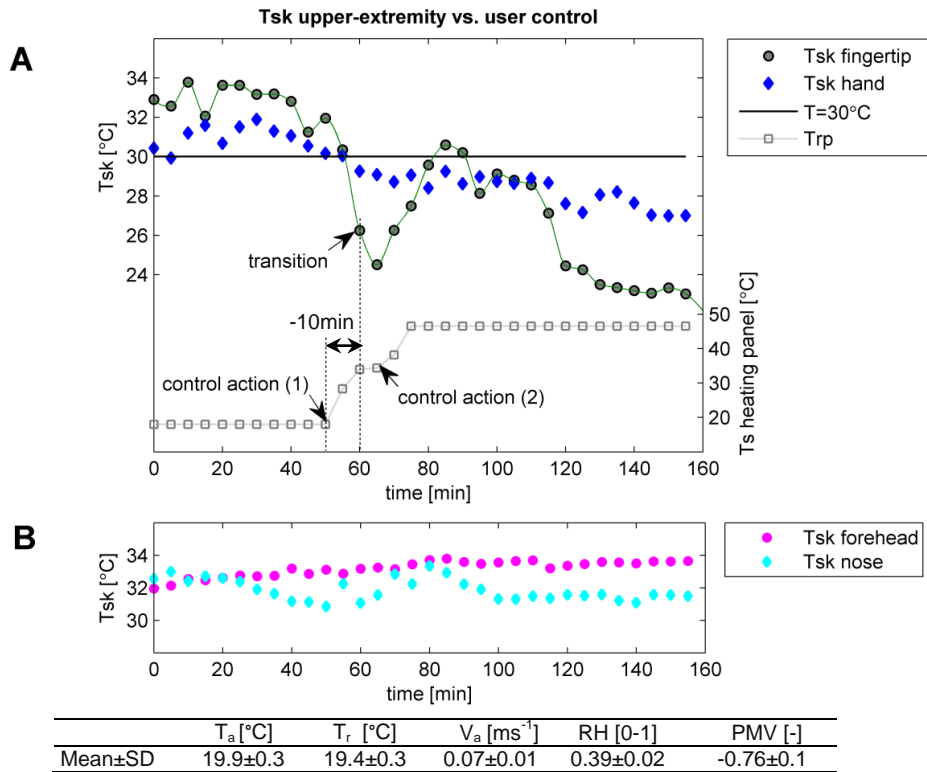
Session #1: 07-11-2011



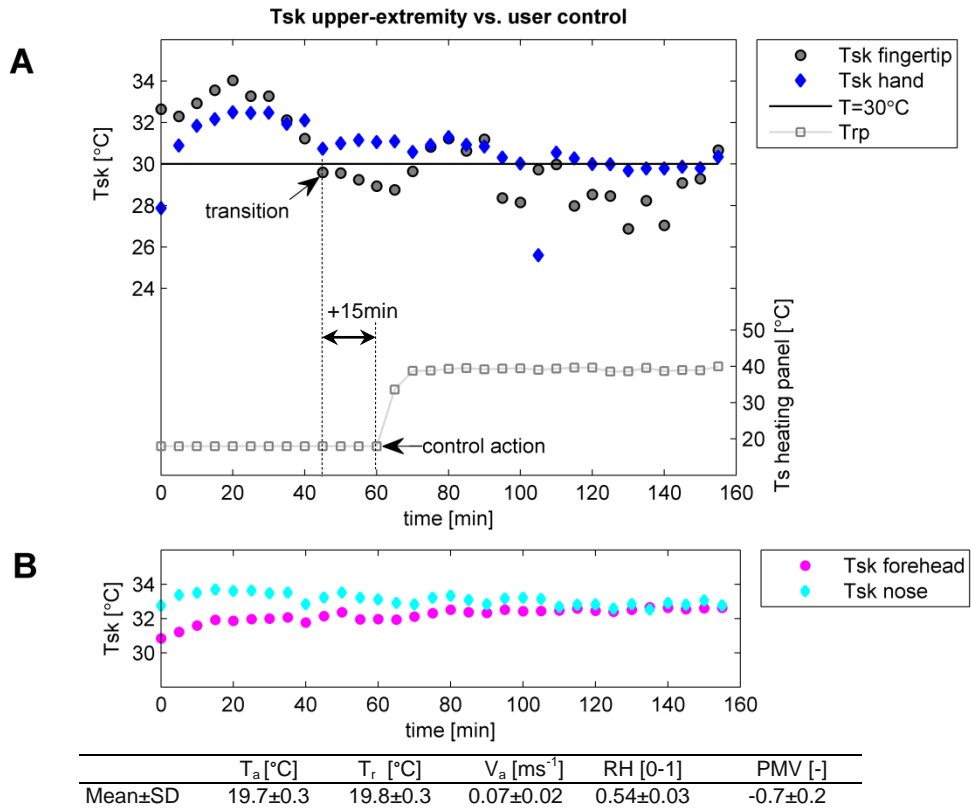
Session #2: 08-11-2011



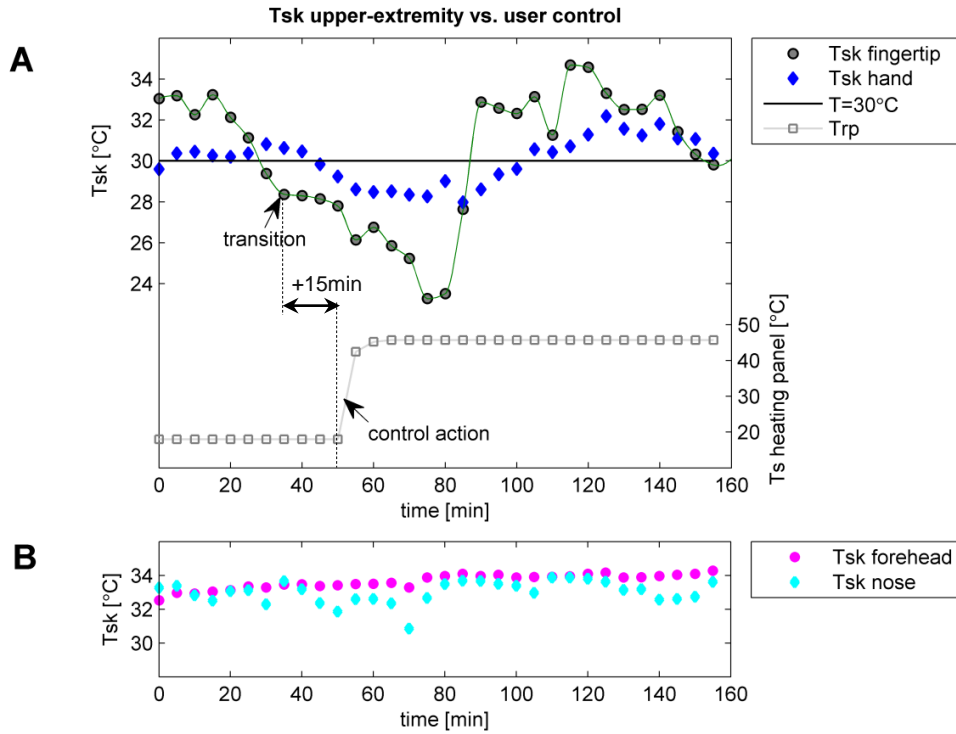
Session #3: 10-11-2011



Session #4: 11-11-2011

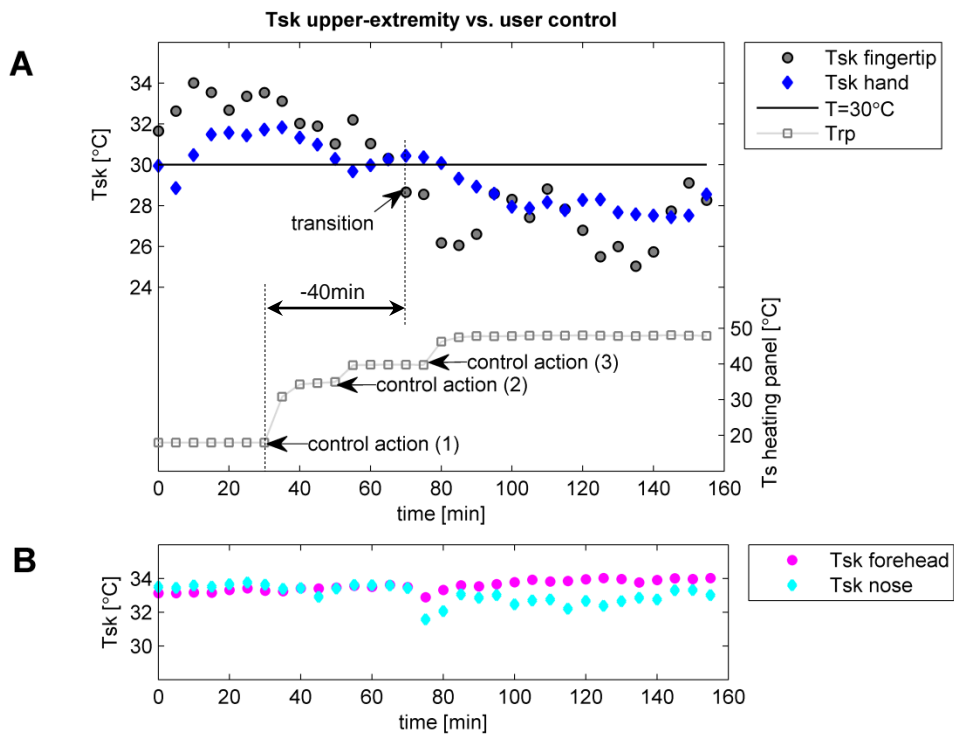


Session #5: 16-11-2011



	T_a [°C]	T_r [°C]	V_a [ms ⁻¹]	RH [0-1]	PMV [-]
Mean±SD	20.0±0.2	20.3±0.3	0.07±0.02	0.40±0.05	-0.65±0.1

Session #6: 17-11-2011

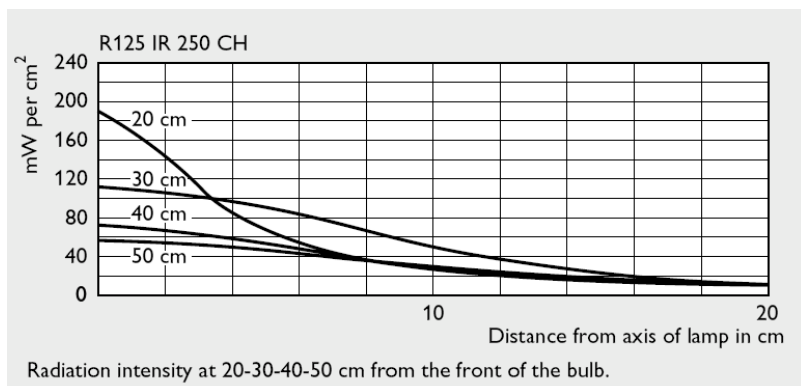
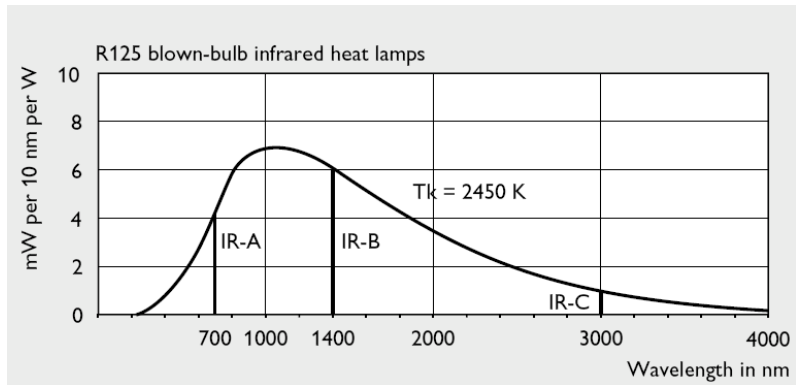


	T_a [°C]	T_r [°C]	V_a [ms ⁻¹]	RH [0-1]	PMV [-]
Mean±SD	20.1±0.1	20.2±0.2	0.07±0.02	0.48±0.05	-0.6±0.1

Appendix G: Heating lamp characteristics



- Philips incandescent reflector / industrial;
- 90% of energy is transmitted as infrared radiation.

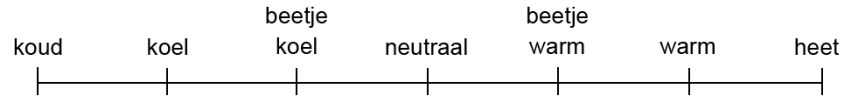


Source: Philips lighting: http://www.cpu.com.tw/kh/elec/pl/blb/ir250_series.pdf

Appendix H: Questionnaire

Begin

1. Hoe voel je je op dit moment?



2. Wat zou je op dit moment liever willen?

- kouder geen verandering warmer

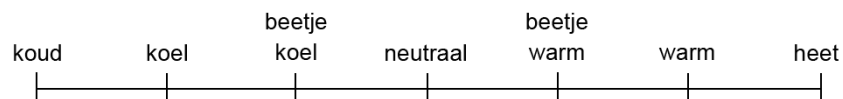
3. In welke mate zou je de temperatuur op dit moment willen beïnvloeden?

- veel koeler koeler beetje koeler geen verandering beetje warmer warmer veel warmer

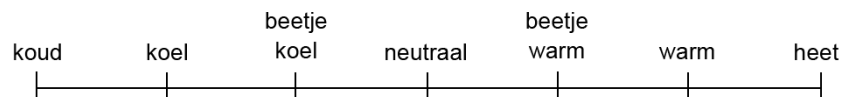
4. Hoe vind je de thermische omgeving?

- zeer acceptabel
net acceptabel
net onacceptabel
zeer onacceptabel

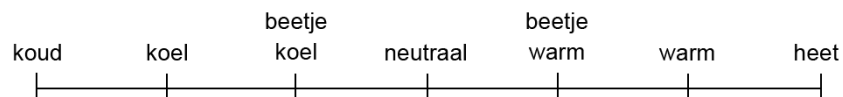
5. Hoe voelt op dit moment het **hoofd**?



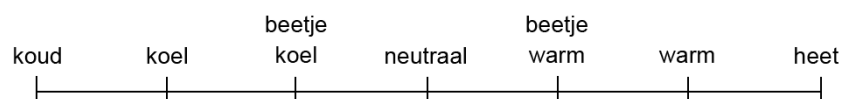
6. Hoe voelt op dit moment de **romp**?



7. Hoe voelen op dit moment de **handen**?



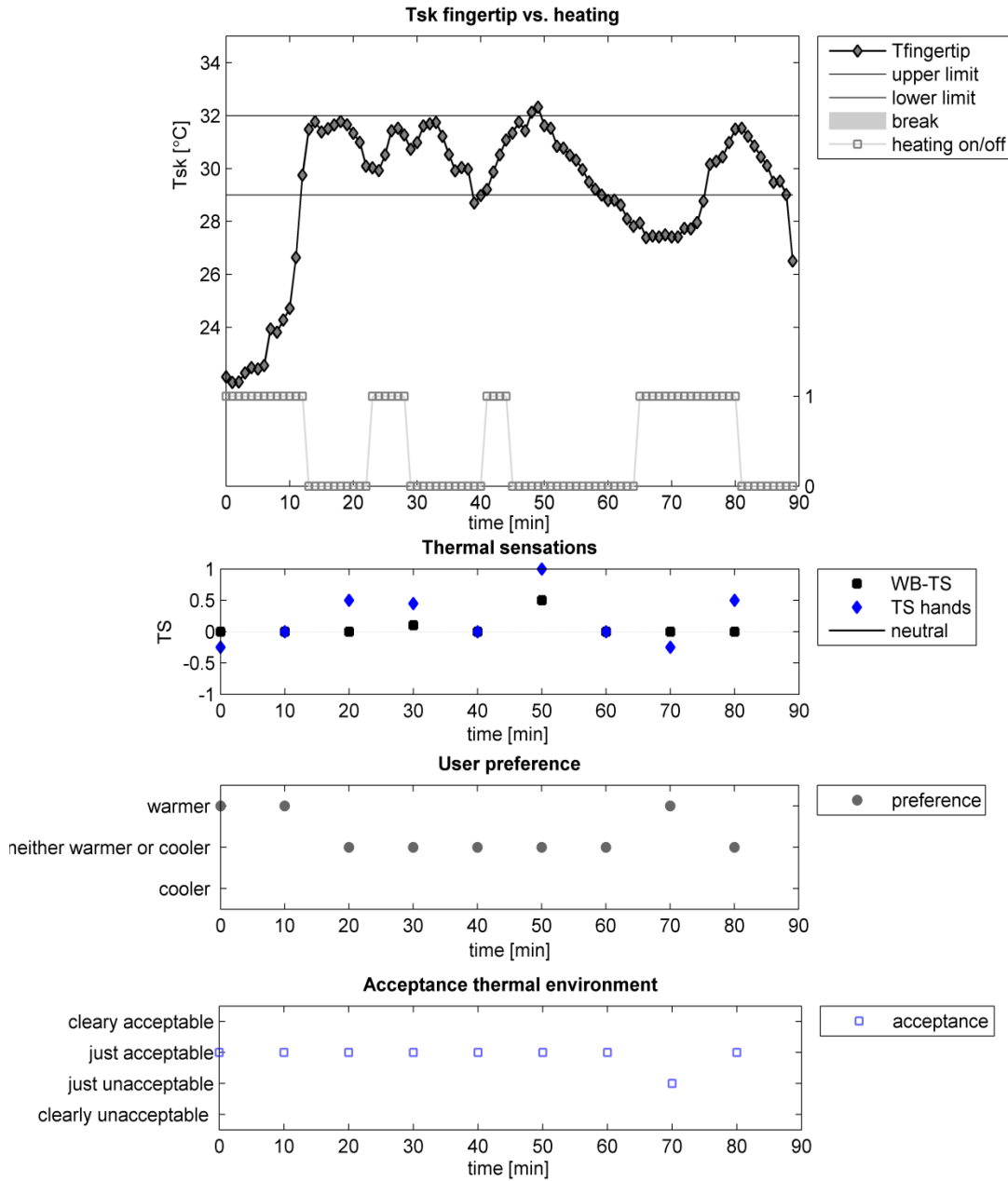
8. Hoe voelen op dit moment de **voeten**?



Einde

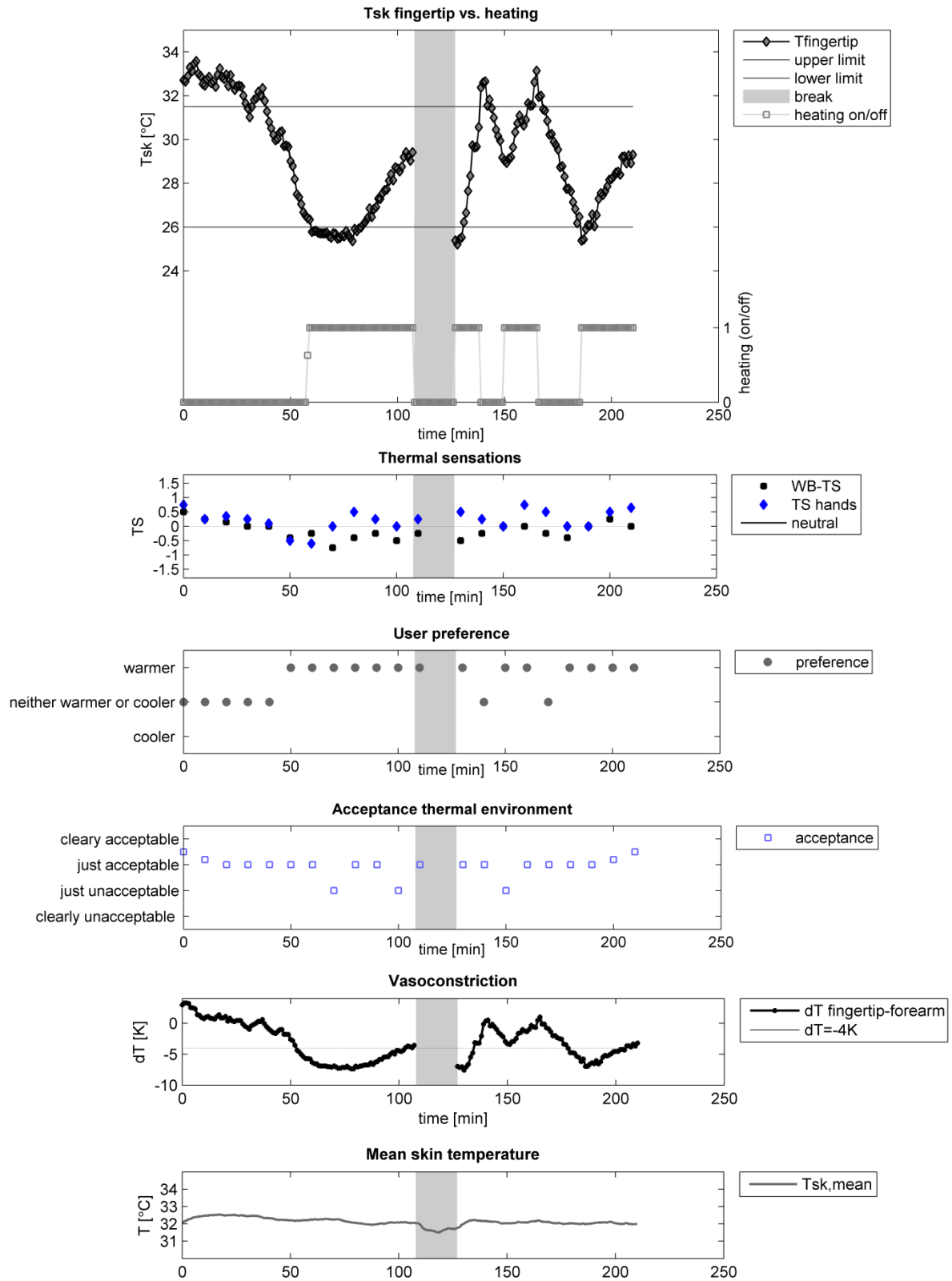
Appendix I: Automatic controlled experiments

Session #1: 01-02-2012: test experiment

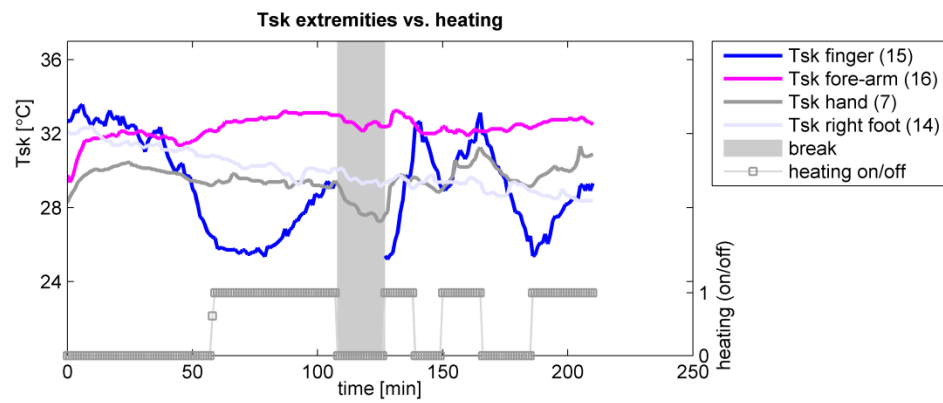
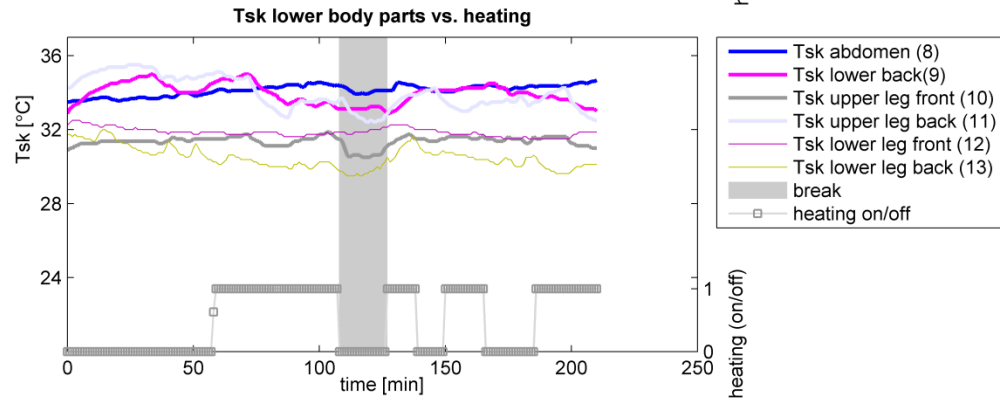
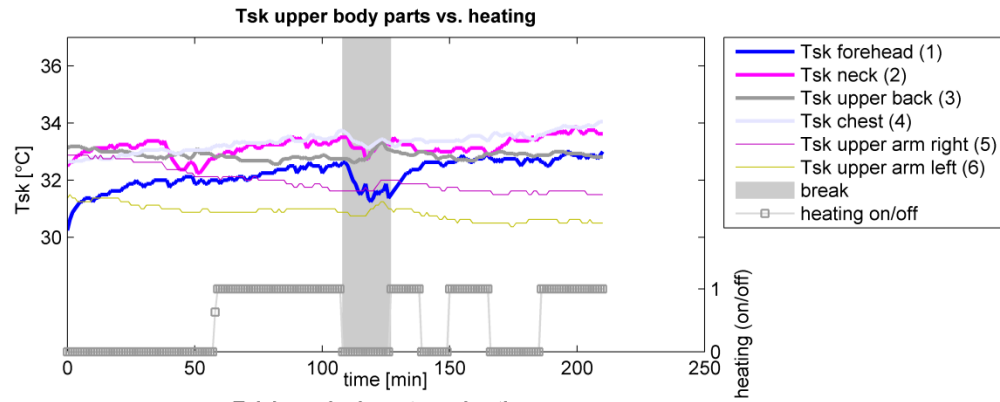


	T_a [°C]	T_r [°C]	V_a [ms ⁻¹]	RH [0-1]	PMV [-]
Mean±SD	19.9±0.2	20.2±0.3	0.06±0.03	0.42±0.02	-0.60±0.07

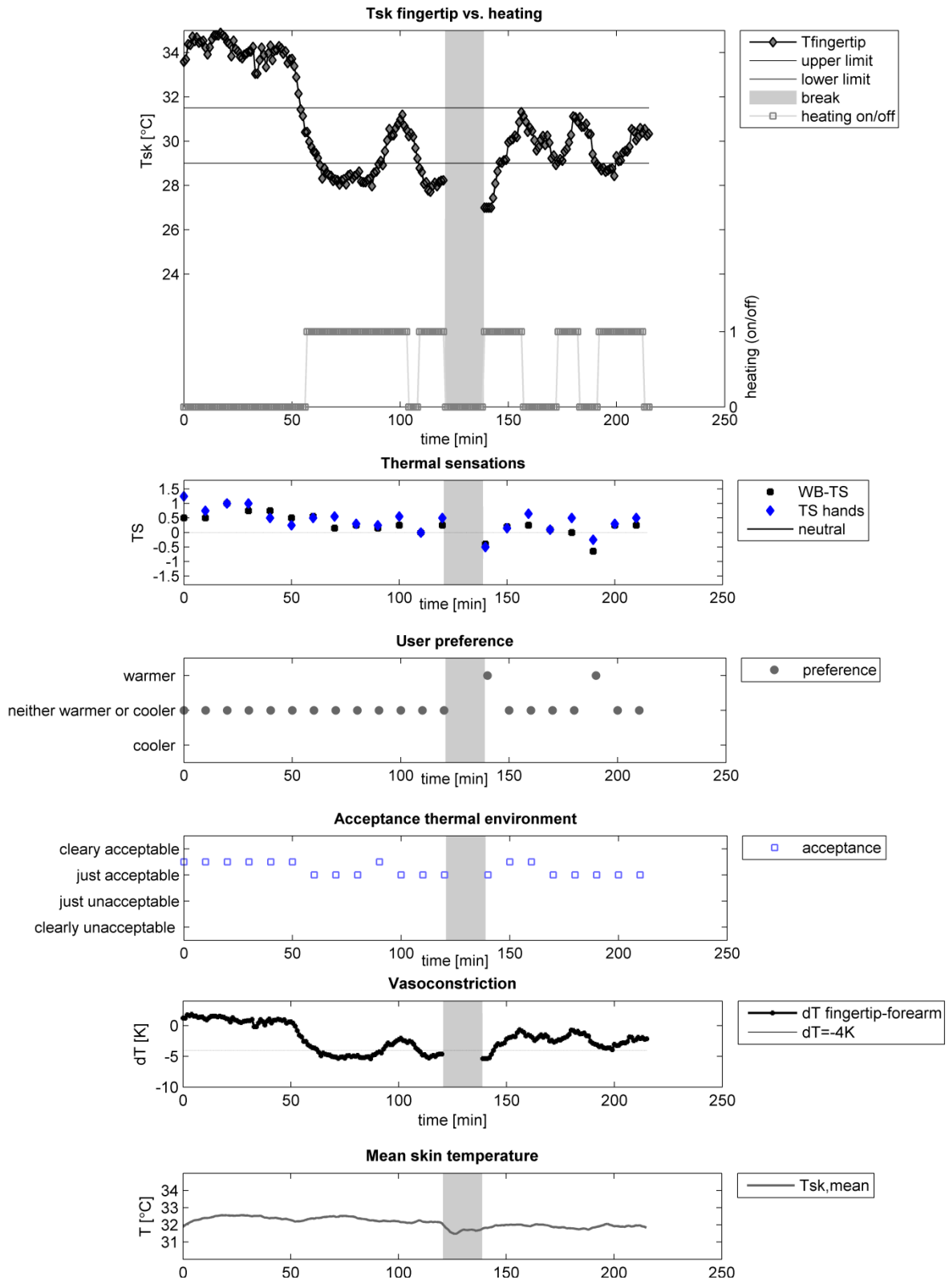
Session #2: 07-02-2012



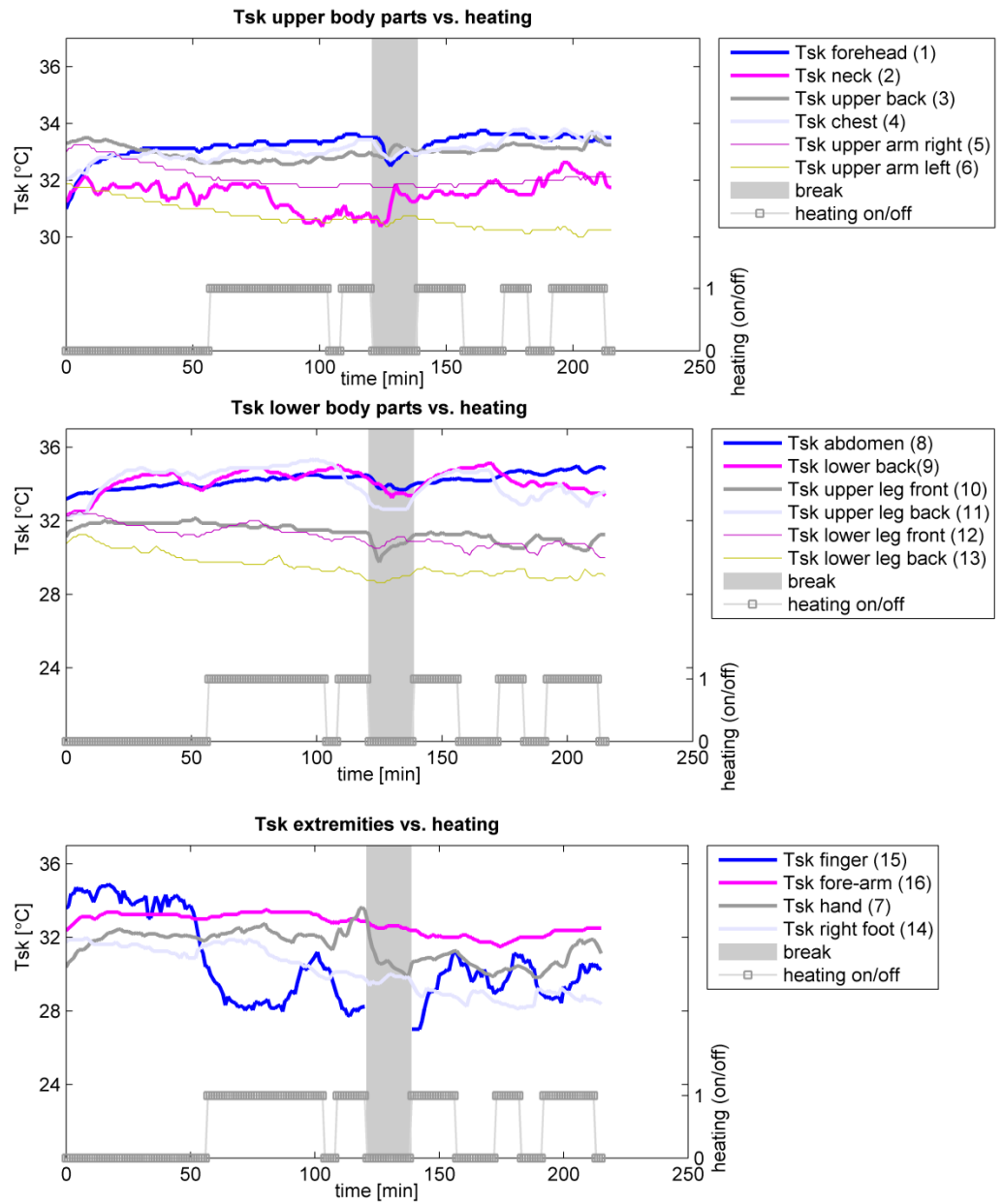
	T_a [°C]	T_r [°C]	V_a [ms ⁻¹]	RH [0-1]	PMV [-]	$T_{sk,mean}$ [°C]
Mean±SD	19.7±0.2	19.6±0.3	0.08±0.03	0.42±0.02	-0.70±0.05	32.1±0.21



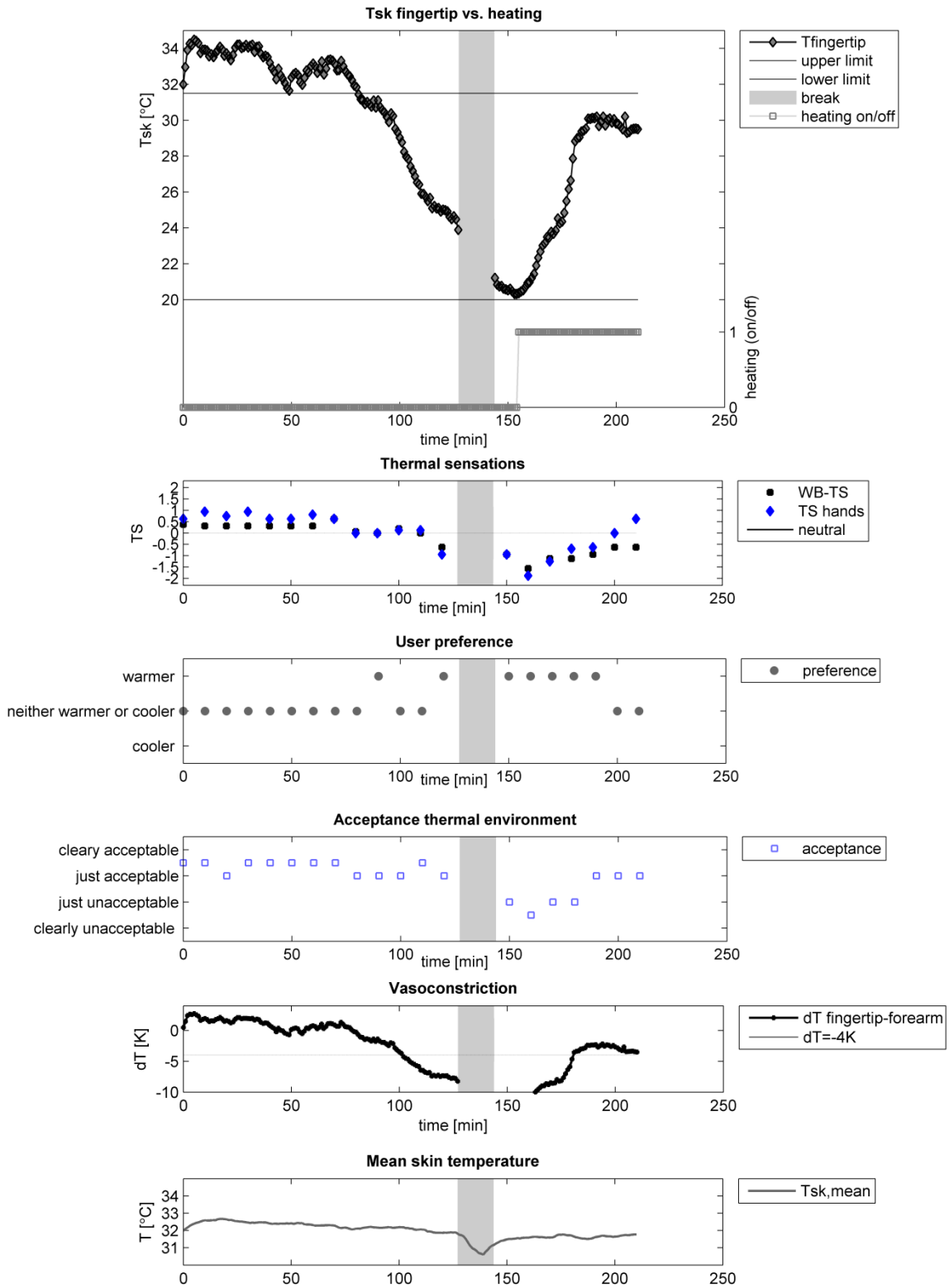
Session #3: 08-02-2012



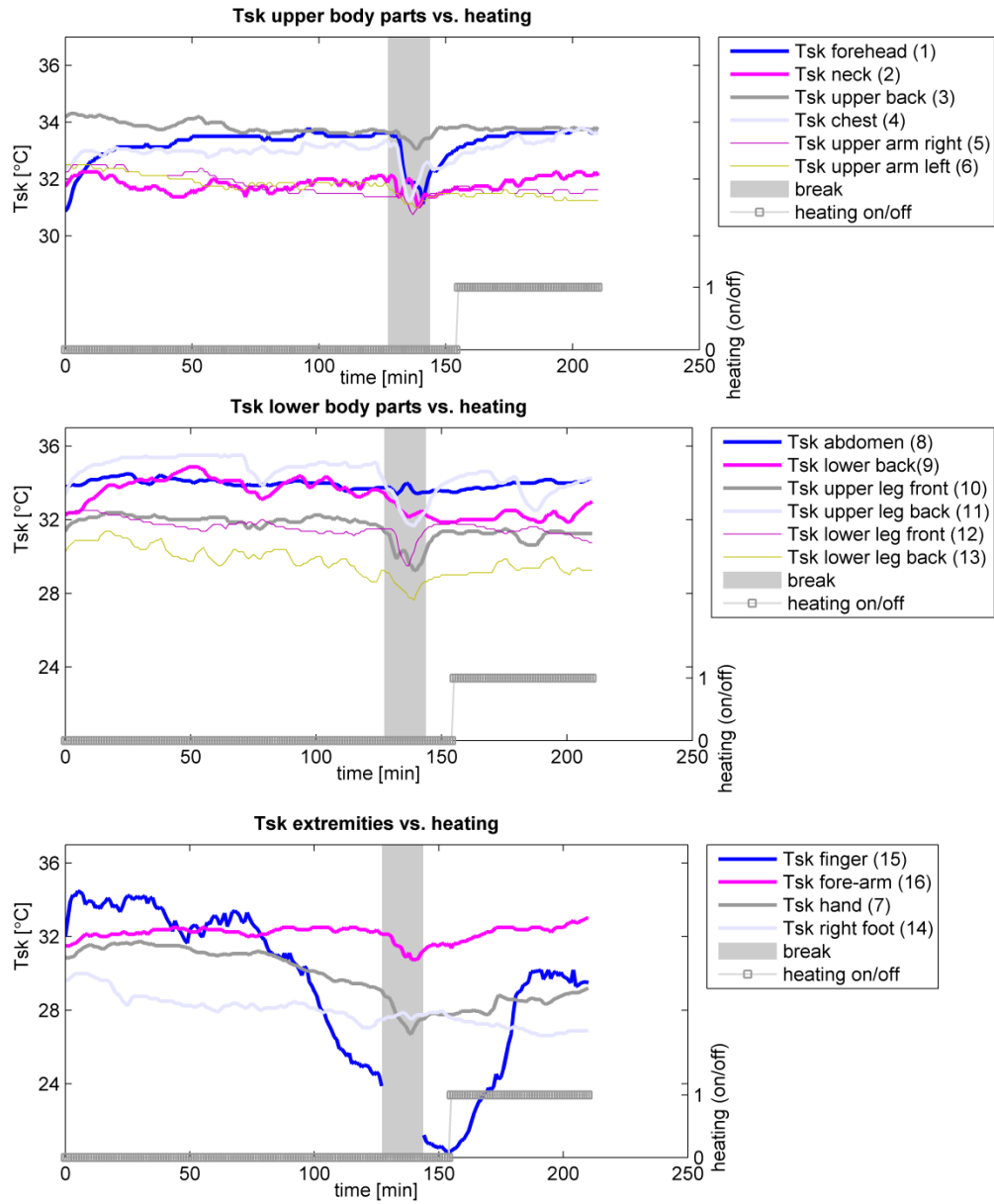
	T_a [°C]	T_r [°C]	V_a [ms ⁻¹]	RH [0-1]	PMV [-]	$T_{sk,mean}$ [°C]
Mean±SD	19.9±0.1	20.2±0.2	0.07±0.02	0.48±0.05	-0.62±0.05	32.1±0.3



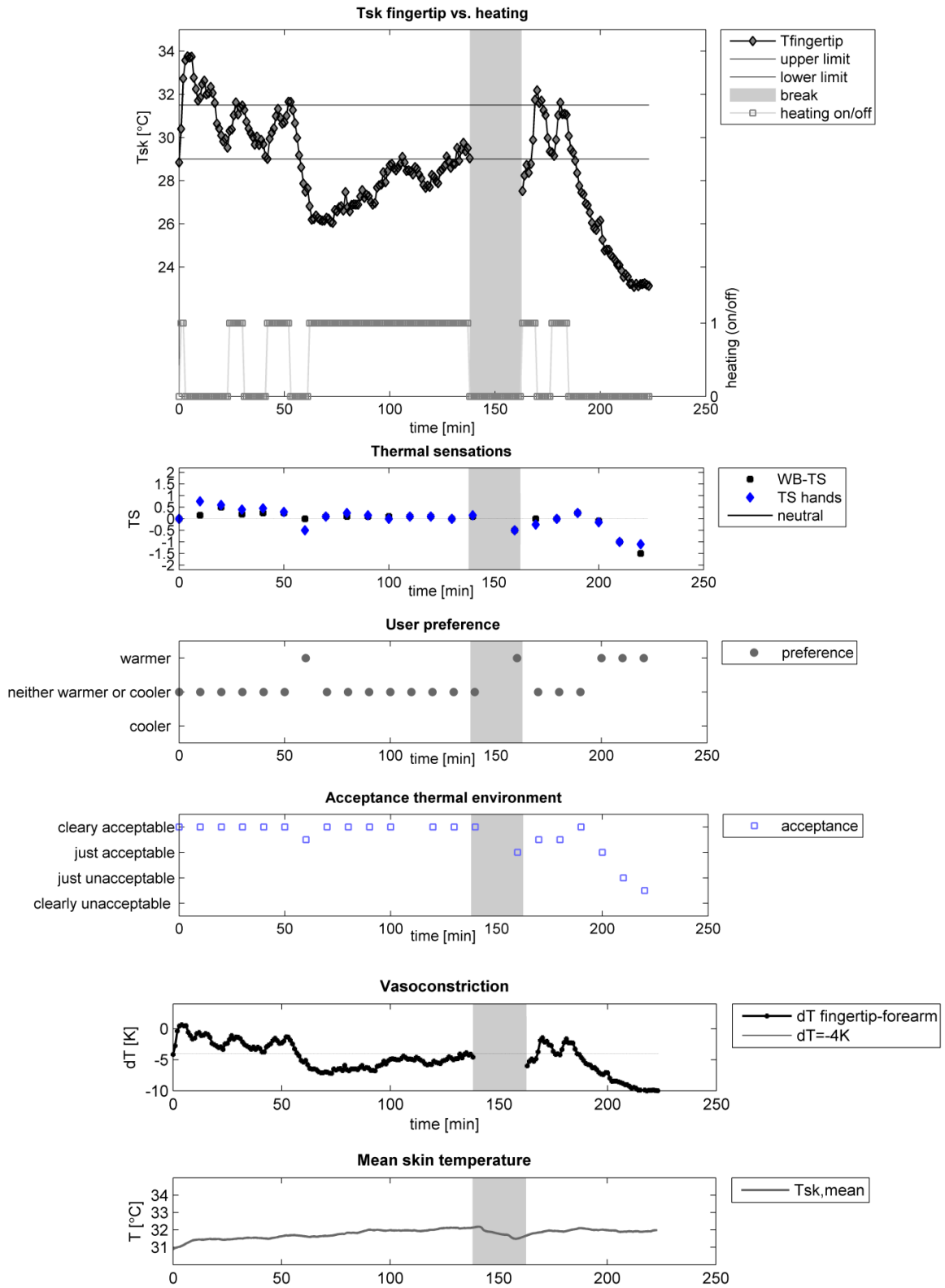
Session #4: 09-02-2012



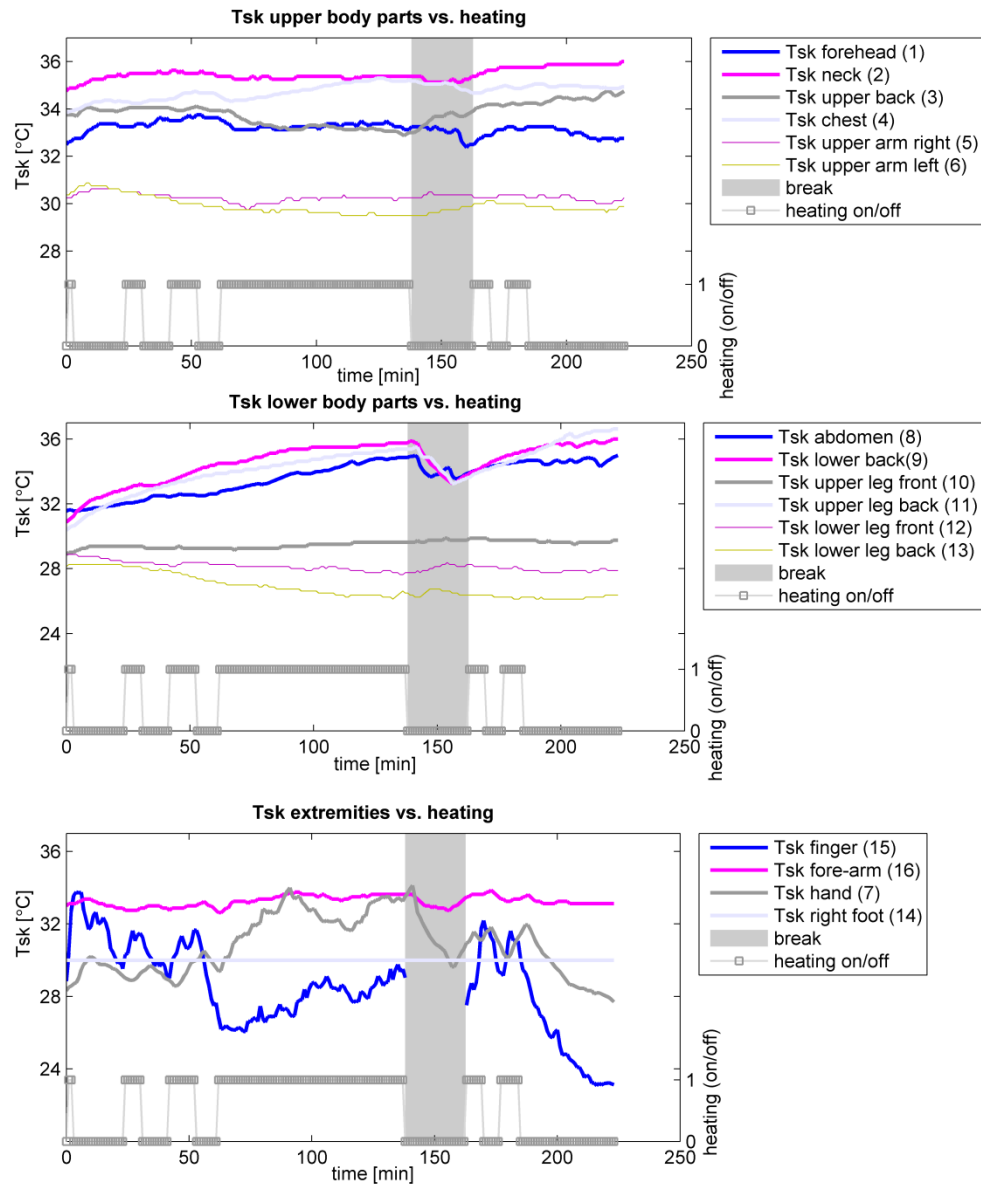
	T_a [°C]	T_r [°C]	V_a [ms ⁻¹]	RH [0-1]	PMV [-]	$T_{sk,mean}$ [°C]
Mean±SD	19.6±0.1	19.7±0.2	0.08±0.02	0.49±0.03	-0.71±0.04	32.0±0.45



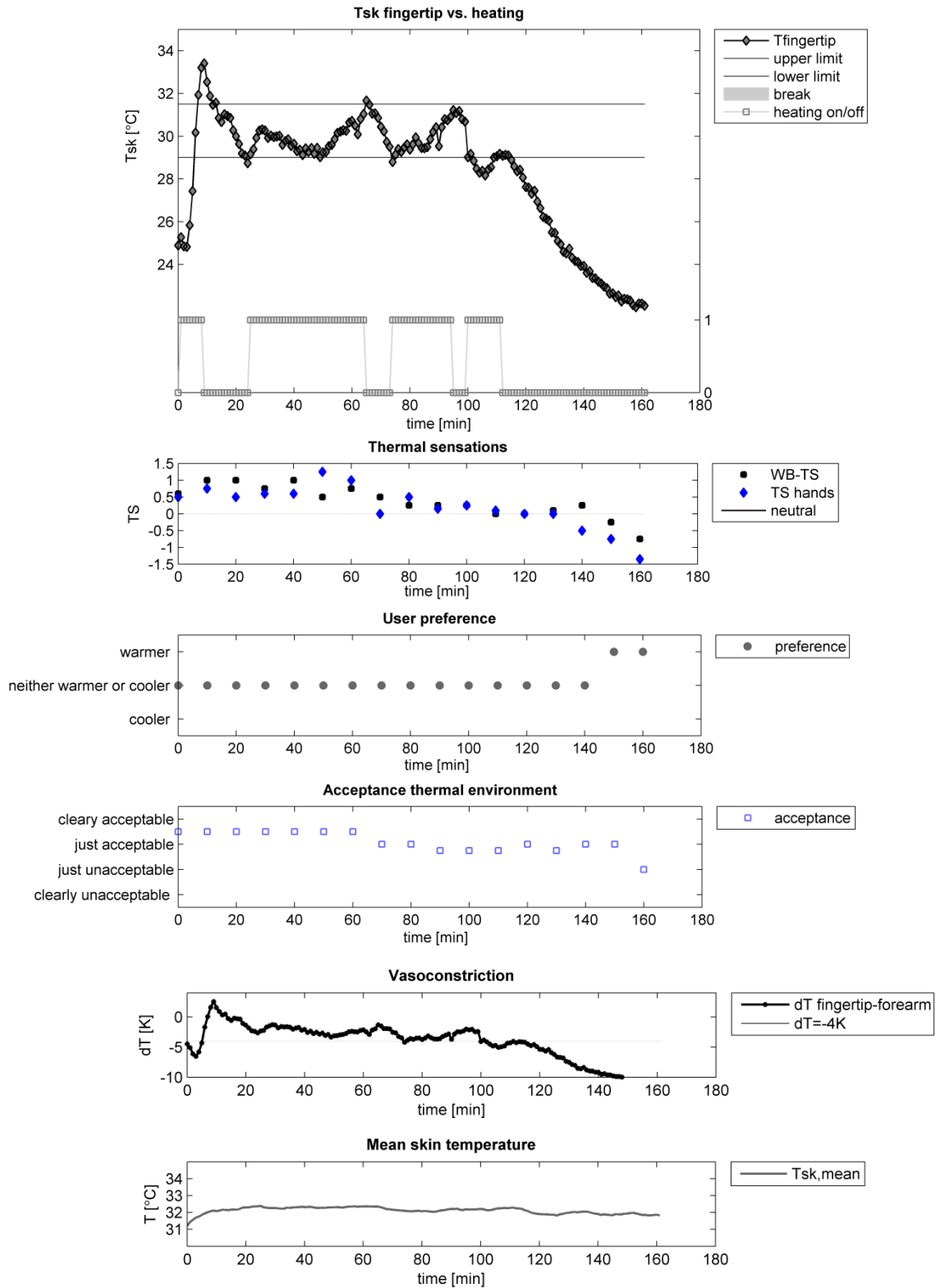
Session #5: 10-02-2012



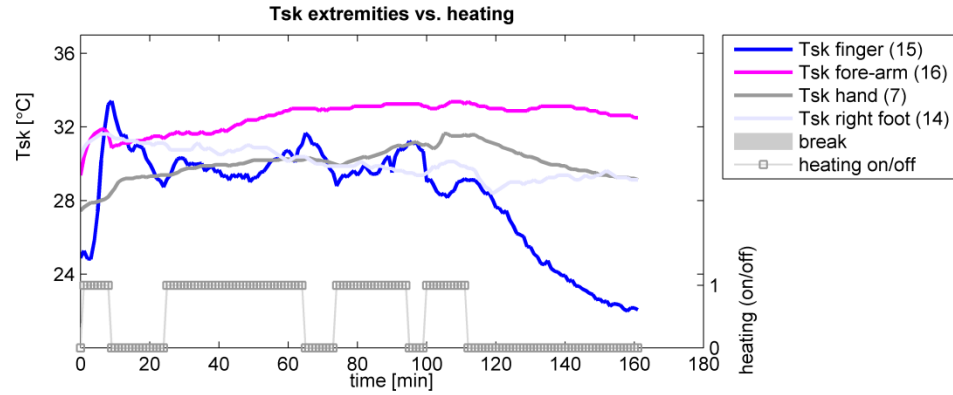
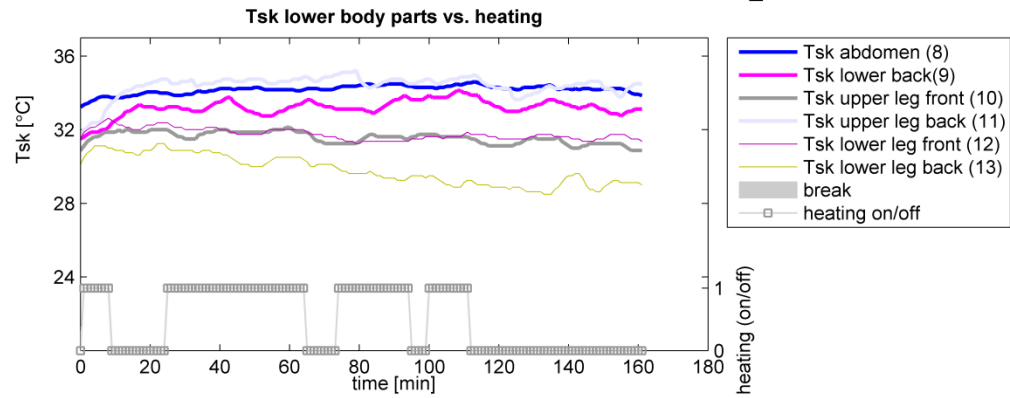
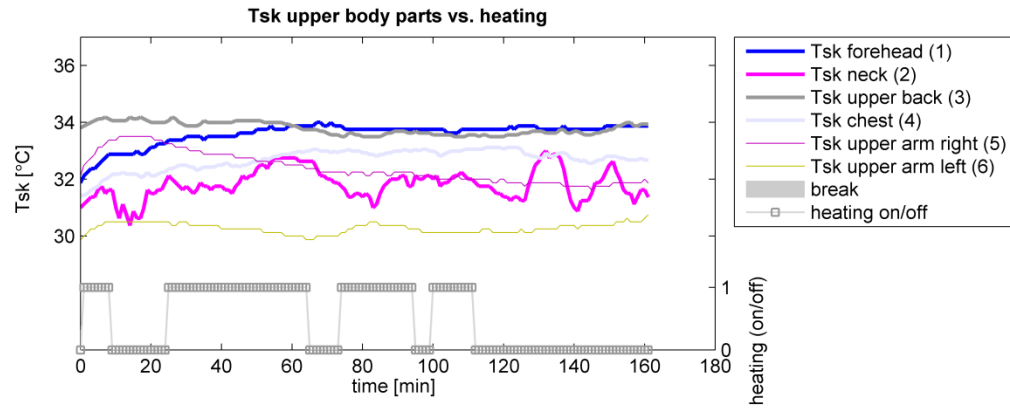
	T_a [°C]	T_r [°C]	V_a [ms ⁻¹]	RH [0-1]	PMV [-]	$T_{sk,mean}$ [°C]
Mean±SD	19.6±0.2	19.7±0.3	0.07±0.02	0.47±0.03	-0.71±0.05	31.8±0.3



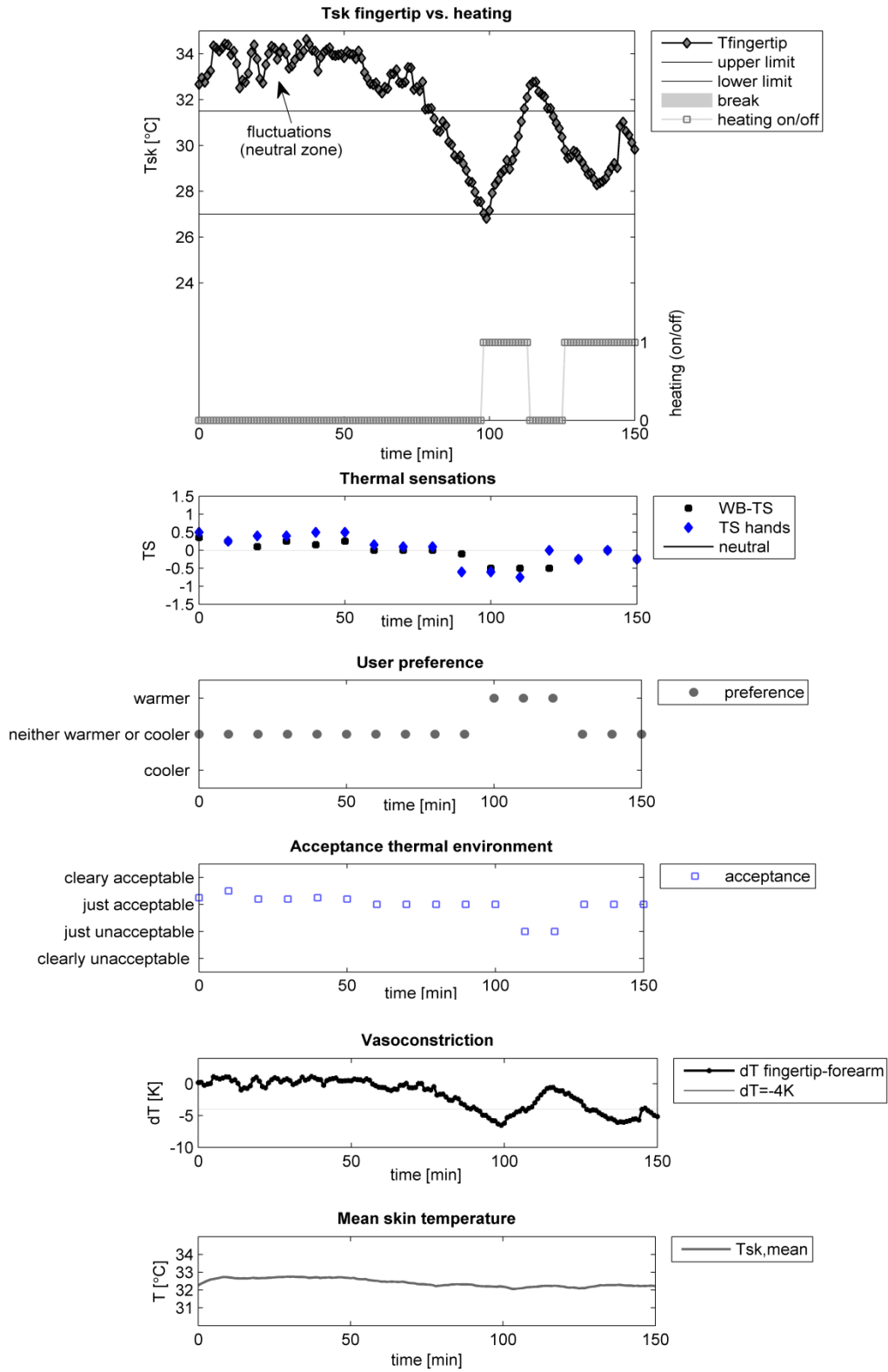
Session #6: 13-02-2012



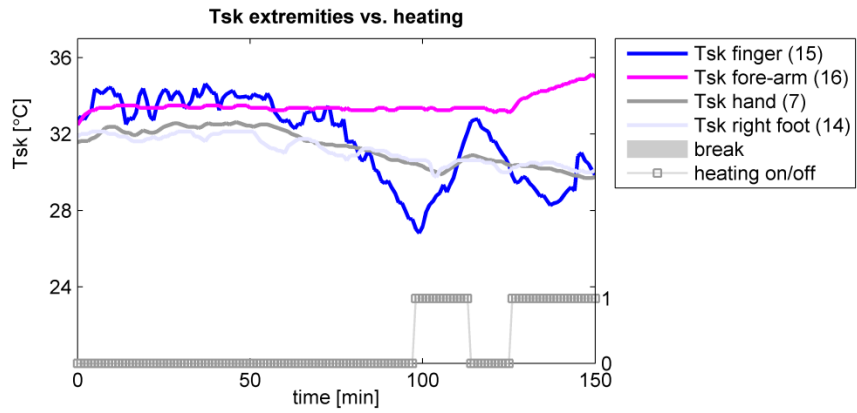
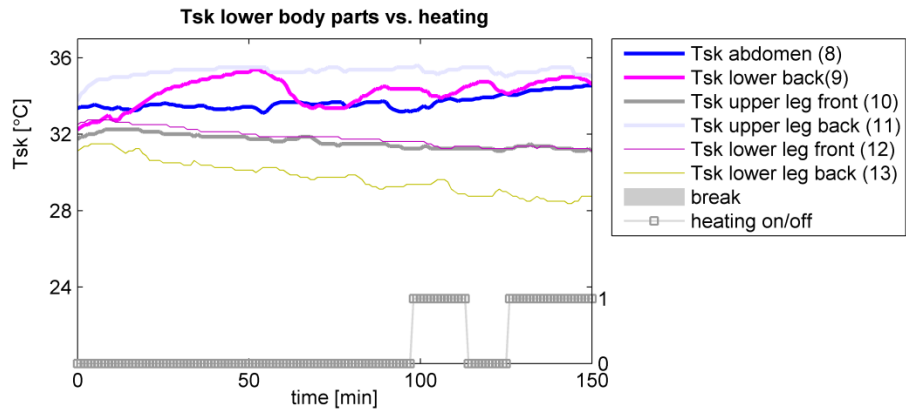
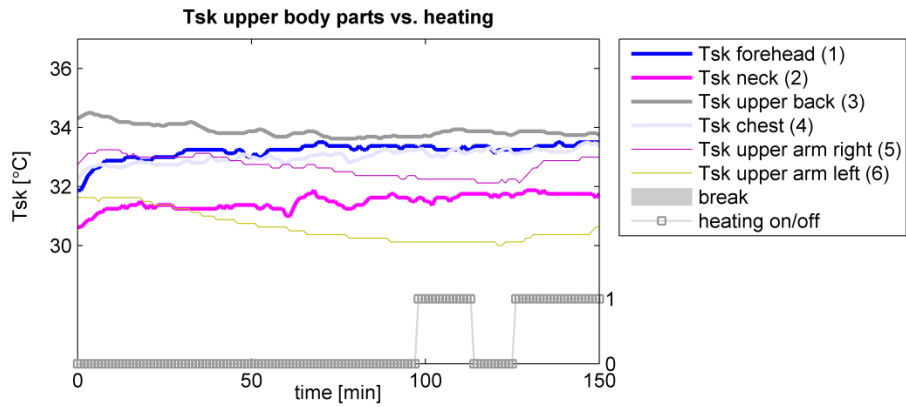
	T_a [°C]	T_r [°C]	V_a [ms ⁻¹]	RH [0-1]	PMV [-]	$T_{sk,mean}$ [°C]
Mean±SD	19.8±0.1	20.1±0.1	0.07±0.04	0.53±0.02	-0.61±0.08	32.2±0.2



Session #7: 14-02-2012



	T_a [°C]	T_r [°C]	V_a [ms ⁻¹]	RH [0-1]	PMV [-]	$T_{sk,mean}$ [°C]
Mean±SD	20.1±0.2	20.4±0.2	0.08±0.05	0.57±0.01	-0.54±0.10	32.4±0.2

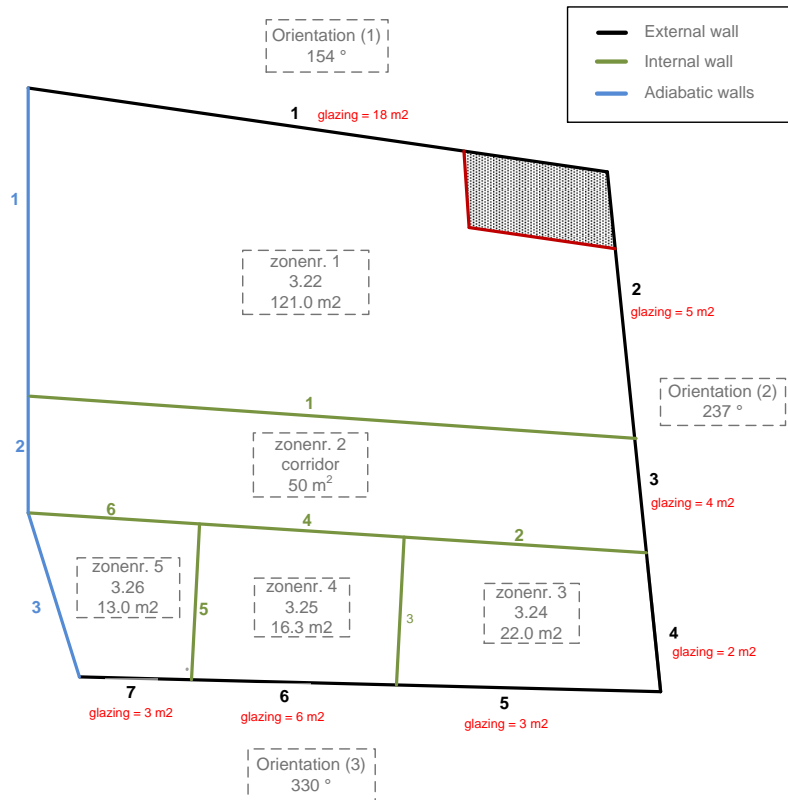


Appendix J: Simulation model Matlab/Simulink

J.1 HAMBBase floor plan

The floor plan of the Royal Haskoning office building used for HAMBBase simulation is shown below:

HAMBBase input floor plan



```

% -----
% PART 2 : THE BUILDING
% -----

% ZONES NUMBERS [-] & VOLUMES [m3]
%
% FORMAT BAS.Vol{zonenumber}=volume (m3);
BAS.Vol{1}= 411;      % room 3.22 / open office
BAS.Vol{2}= 170;     % corridor
BAS.Vol{3}= 75;      % room 3.24 / meeting room
BAS.Vol{4}= 55;      % room 3.25 / cell office
BAS.Vol{5}= 44;      % room 3.26 / cell office

% ** CONSTRUCTION COMPONENTS DATA **
%
% BAS.Con{conID}=[Ri, dl,matID,... , dn,matID, Re, ab, eb].
BAS.Con{1} = [0.13, 0.214,235, 0.150,409, 0.050,003, 0.100,234, 0.04, 0.9, 0.9];
BAS.Con{2} = [0.13, 0.013,381, 0.05,409, 0.013,381, 0.13, 0.5, 0.9];
BAS.Con{7} = [0.13, 0.200,312, 0.080,456, 0.050,312, 1, 0.9, 0.9];

```

```

% 1: limestone,insulation,air gap,brick (external wall)
% 2: plaster,insulation,plaster (internal wall)
% 7: floor construction

% ** GLAZING SYSTEMS DATA**
%
%BAS.Glas{glaID}=[Uglas,    CFr,        ZTA,        ZTAw,        CFrw,    Uglasw]
BAS.Glas{1}= [1.2,        0.03,        0.3,        0.3,        0.03,    1.2  ];

% ** ORIENTATIONS **
%
%BAS.Or{orID}=[beta,    gamma];

BAS.Or{1}= [90.0,        154.0  ];
BAS.Or{2}= [90.0,        237.0  ];
BAS.Or{3}= [90.0,        330.0  ];

% I. EXTERNAL WALLS
%BAS.wallex{exID}= [zonenr, surf, conID,    orID,    bridge]
BAS.wallex{1} = [1,    54,    1,    1,    0];
BAS.wallex{2} = [1,    24,    1,    2,    0];
BAS.wallex{3} = [2,    13,    1,    2,    0];
BAS.wallex{4} = [3,    13,    1,    2,    0];
BAS.wallex{5} = [3,    22,    1,    3,    0];
BAS.wallex{6} = [4,    18,    1,    3,    0];
BAS.wallex{7} = [5,    10,    1,    3,    0];

% II. WINDOWS IN EXTERNAL WALLS
%
%BAS.window{winID}= [exID,    surf, glaID,    shaID]
BAS.window{1} = [1,    18,    1,    0];
BAS.window{2} = [2,    5,    1,    0];
BAS.window{3} = [3,    4,    1,    0];
BAS.window{4} = [4,    2,    1,    0];
BAS.window{5} = [5,    3,    1,    0];
BAS.window{6} = [6,    6,    1,    0];
BAS.window{7} = [7,    3,    1,    0];

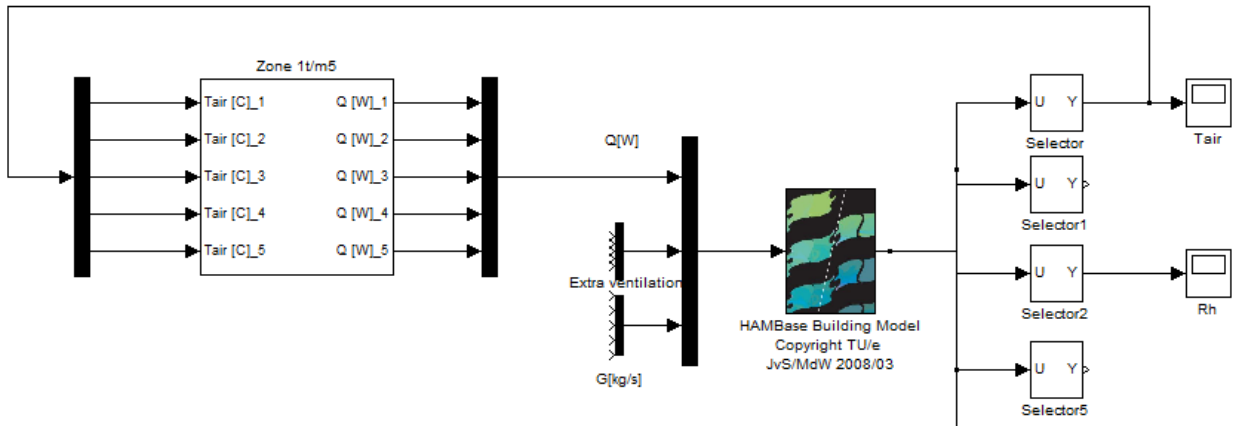
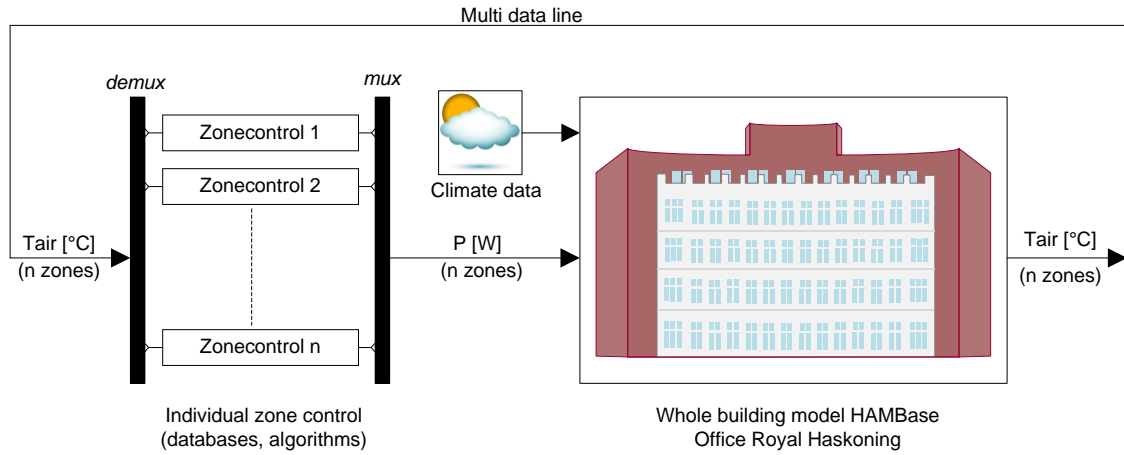
% III. CONSTANT TEMPERATURE WALLS
%
%BAS.walli0{i0ID}= [zonenr, surf, conID,    temp,    bridge]
BAS.walli0{1} = [1,    242,    7,    20.0,    0];
BAS.walli0{2} = [2,    100,    7,    20.0,    0];
BAS.walli0{3} = [3,    44,    7,    20.0,    0];
BAS.walli0{4} = [4,    32,    7,    20.0,    0];
BAS.walli0{5} = [5,    26,    7,    20.0,    0];

% IV ADIABATIC EXTERNAL WALLS
%
%BAS.wallia{iaID}= [zonenr, surf, conID]
BAS.wallia{1} = [1,    30,    2  ];
BAS.wallia{2} = [2,    10,    2  ];
BAS.wallia{3} = [3,    15,    2  ];

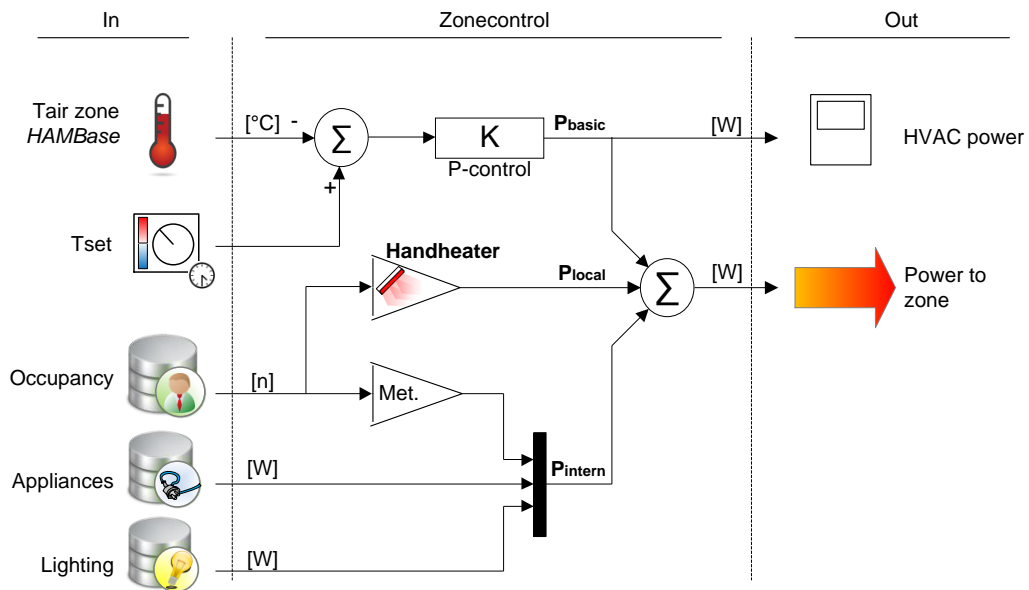
% V. INTERNAL WALLS BETWEEN AND IN ZONES
%
%BAS.wallin{inID}= [zonenr1,    zonenr2,    surf,    conID  ]
BAS.wallin{1} = [1,    2,    44,    2  ];
BAS.wallin{2} = [2,    3,    18,    2  ];
BAS.wallin{3} = [3,    4,    10,    2  ];
BAS.wallin{4} = [2,    4,    15,    2  ];
BAS.wallin{5} = [4,    5,    10,    2  ];
BAS.wallin{6} = [2,    5,    14,    2  ];

```

J.2 Simulink model
Whole building model



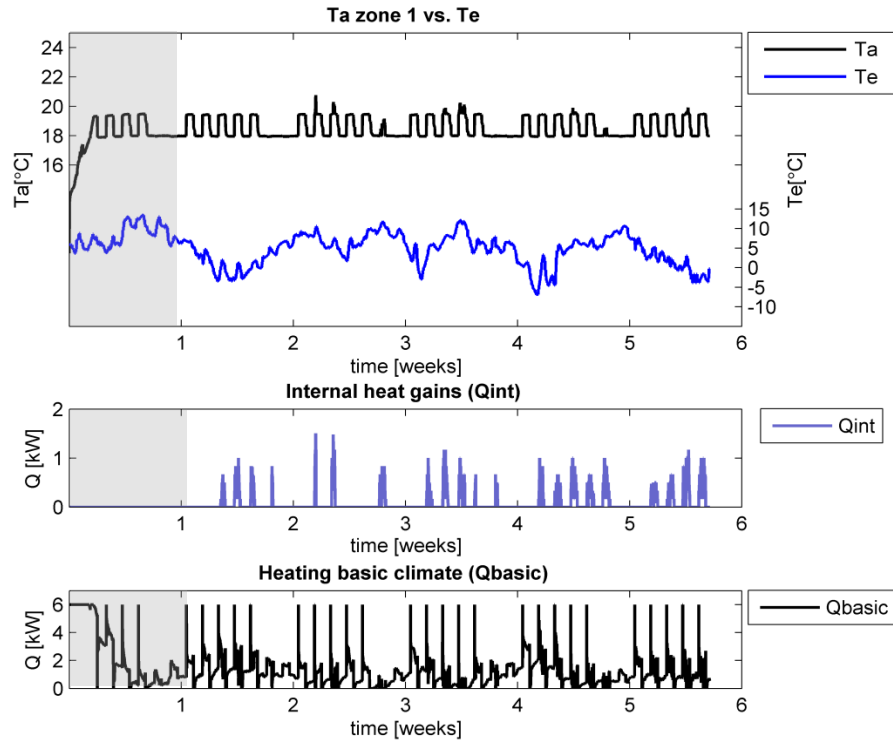
Zone model



J.3 Simulation results

Two examples of the simulation output are included for the 6-week winter period.

Indoor air temperature of 19.5°C



Indoor air temperature of 22°C

